THE UNIVERSITY OF CALGARY

cDNA Cloning, Protein Expression, Tissue Specific Expression Pattern and Functional Characterization of Nebulin and Nebulette, Two Homologous Striated Muscle Proteins

by

Ozgur Ogut

A THESIS
SUBMITTED TO THE FACULTY OF GRADUATE STUDIES
IN PARTIAL FULFILMENT OF THE REQUIREMENTS FOR THE
DEGREE OF MASTER OF SCIENCE

DEPARTMENT OF MEDICAL BIOCHEMISTRY

CALGARY, ALBERTA
AUGUST, 1997

ABSTRACT

Nebulin and nebulette are homologous proteins expressed in skeletal and cardiac muscles, respectively. Complementary DNA encoding nebulin or nebulette demonstrated that both proteins are composed of conserved motifs. Nebulin exons were found to encode multiples of the conserved motifs, suggesting the minimum functional unit of nebulin. Nebulette protein was found to be expressed as two isoforms throughout development, with different expression proportions in the left and right ventricles of the bovine heart. The nebulette protein bound F-actin, similar to nebulin. Although cloned nebulin and nebulette proteins inhibited the activity of unregulated acto-myosin S1 ATPase, a Ca^{2+} regulated acto-myosin system reconstituted in the presence or absence of the cloned nebulin or nebulette proteins showed no significant inhibition of the acto-myosin S1 ATPase, indicating that the interaction of nebulin-like proteins with the thin filament can be regulated by Ca^{2+} - troponin - tropomyosin, the major regulatory apparatus of striated muscles.

TABLE OF CONTENTS

LIST OF TABLES

LIST OF FIGURES

LIST OF ABBREVIATIONS

ABTS	2,2'-azinobis-(3-ethylbenzthiazolinesulfonic acid)
ATPase buffer	6.5 mM KCl, 20 mM imidazole, pH 7, 3.5 mM $MgCl_2$, 0.5 mM EGTA, 0.01% NaN_3, 1 mM dithiothreitol
BCIP	5-bromo-4-chloro-3-indolylphosphate
BSA	Bovine serum albumin
Buffer A	0.1 M KCl, 10 mM Tris-HCl, pH 7.5, 3 mM $MgCl_2$
Buffer B	Buffer A plus 1% BSA
Buffer P	Buffer A plus 0.1% BSA and 0.05% Tween-20
Buffer T	Buffer A plus 0.05% Tween-20
DEPC	Diethylpyrocarbonate
DMEM	Dulbecco's modified Eagle's medium
DMSO	Dimethylsulfoxide
ELISA	Enzyme-linked immunosorbant assay
FCS	Fetal calf serum
GFP	Green Fluorescent Protein
HAT	0.1 mM hypoxanthine, 0.4 mM aminopterin, 16mM thymidine
HT	0.1 mM hypoxanthine, 16 mM thymidine
IPTG	Isopropyl-1-thio-b-D-galactopyranoside
LB	Luria-Bertani medium (per litre: 10 g tryptone,
5 g	yeast extract, 10g NaCl)
LB-agar	LB + 15 g/L agar
mAb	Monoclonal antibody

MOPS	MOPS buffer (10X: 0.4 M MOPS, pH 7.0, 0.1
M	NaOAc, pH 4.0, 10 mM EDTA)
NBT	Nitro blue tetrazolium
pBL SK	pBluescript SK phagemid
PBS	Phosphate-buffered saline (137 mM NaCl,
2.7mM	KH_2PO_4, 8.0 mM Na_2HPO_4, pH 7.4)
PBS-B	PBS plus 1% BSA
PBS-P	PBS plus 0.1% BSA and 0.05% Tween-20
PBS-T	PBS plus 0.05% Tween-20
PCR	Polymerase chain reaction
PFU	Plaque forming units
RT-PCR	Reverse transcriptase coupled polymerase
chain	reaction
SDS-PAGE	Sodium dodecyl sulfate - polyacrylamide gel electrophoresis
SM	Suspension medium (0.1 M NaCl, 8 mM
$MgSO_4$,	50 mM Tris-HCl, pH 7.5, 0.01% gelatin)
TAE	Tris-acetate-EDTA buffer (1x: 0.04 M Tris-acetate, 1 mM EDTA)
TBE	Tris-borate-EDTA buffer (1x TBE: 90 mM
Tris-	borate, 2 mM EDTA)
TBS	Tris-buffered saline (150 mM NaCl, 50 mM
Tris-	HCl, pH 7.5)
TE	Tris-EDTA buffer (10 mM Tris-HCl, pH 8.0, 1mM EDTA)
X-Gal	5-bromo-4-chloro-3-indolyl-b-D-galactoside

CHAPTER ONE:
GENERAL INTRODUCTION

The organization and role of the contractile elements of vertebrate muscle has been the focus of substantial research. Three types of muscle, skeletal, cardiac, and smooth, are involved in both voluntary and involuntary tasks of the body, ranging from day to day actions as walking to the continuous beating of the heart and regulation of the tone of vascular tissue controlling blood flow through vessels. Studies characterizing the organization and function of the proteins which comprise and control muscle contraction are significant in understanding the pathology of human diseases ranging from muscular dystrophy to hypertension and hypertrophic cardiomyopathy. The regulation of muscle contraction is controlled first and foremost by calcium, a messenger used to mediate neural and hormonal signals into contraction of muscle.

A. Molecular Structure of Striated Muscle

A closer look at the myofibrils of the striated skeletal and cardiac muscles by light microscopy reveals that they are composed of regularly repeating units termed sarcomeres, which appear to be composed of alternating light and dark bands. The light band is the I band, as it is isotropic to polarized light, whereas the dark band is the A band, anisotropic to polarized light. The sarcomere is defined by the Z lines, a matrix which forms the border between adjacent sarcomeres (Figure 1.1). Actin is the major constituent of the thin filament, which is anchored to the Z lines and extends towards the M line, which defines the middle of the sarcomere. The I band is the exposed region of the thin filaments and is defined as the distance between the tips of two thick filaments on opposite sides of the Z line. The myosin thick filament is positioned in between two successive actin filaments, and consequently in the center of the sarcomere, forming the A band.

Generally, the overall morphology of the striated muscle sarcomeres are similar. Both cardiac and skeletal muscles show uniform length thick filaments, but only skeletal muscle shows uniform length thin filaments, whereas thin filaments lengths in cardiac muscle may vary (Robinson and Winegrad, 1979), even within single sarcomeres. As measured by electron microscopy, the thick filament length in skeletal and cardiac muscle sarcomeres is relatively consistent at 1.6 μm (Page and Huxley, 1963). In cardiac muscle sarcomeres, the thin filament length may vary from 0.6 to 1.1 μm (Robinson and Winegrad, 1979). Although the lengths of the thin and thick filaments do not vary with excitation of the muscle, the sarcomere length does as a result of thin and thick filament overlap. Both cardiac and skeletal muscle sarcomeres may be shortened to the point of overlap between successive thin filaments, and may be stretched to the point where thin and thick filaments no longer overlap, yet still regain integrity.

B. The Molecular Motors of Muscle Contraction

All three types of muscle achieve force generation and contraction through a conserved mechanism whereby thin and thick filaments in the muscle cell slide along one another. Myosin is the major component of the thick filament, and its head possesses ATPase activity, used to advantage in generating force for muscle contraction (Warrick and Spudich, 1987) during its interaction with the thin filament. The backbone of the thin filament is actin, a globular protein (G-actin) which polymerizes to become filamentous actin (F-actin). Two strands of F-actin wind in a helix, completing a revolution every 13 G-actins or roughly 70 nm. Active sites on actin are able to bind to and form cross-bridges with myosin heads; these actin sites are staggered due to the double helix form of F-actin, making one available every 2.7 nm. In the resting state of muscle, F-actins from successive Z lines overlap with myosin but barely overlap each other; in the contracted state, the actin filaments draw nearer and may overlap substantially. The overlap of the actin strand with the myosin strand allows both to slide along each other to regulate sarcomeric length through cross-bridge cycling (for review, see Leavis and Gergely, 1984; Huxley, 1990),

made possible through the energy provided by ATP hydrolysis by the myosin head (Figure 1.2). This globular head domain of myosin is able to bind ATP, resulting in a conformational change to cause a rapid dissociation of myosin from actin. The ATPase activity of the myosin head hydrolyzes the nucleotide into ADP and Pi, both of which remain tightly bound to myosin. The complex is in equilibrium with F-actin, eventually resulting in a slow transition to an activated, high affinity form of the acto-myosin complex where the myosin head contacts the available F-actin active sites; in this stage, the myosin is in a prestroke strained state. This triggers the release of Pi and a large conformational change in myosin pulls the F-actin strand towards the center of the sarcomere, shortening the sarcomere and giving rise to motion (Cooke *et al.*, 1982). The change in myosin conformation concurrently allows ADP to dissociate, allowing rapid binding of ATP and reinitiating the cross-bridge cycle (Spudich, 1994).

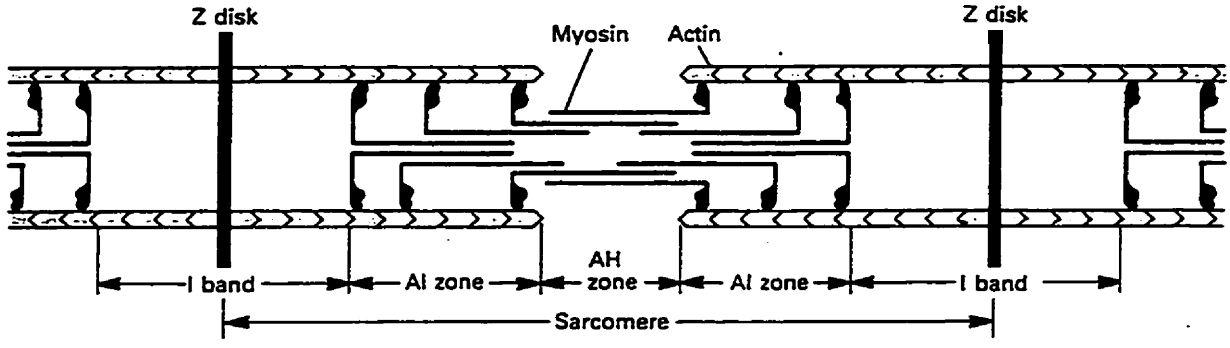

Figure 1.1. The arrangement of the striated muscle sarcomere.

The schematic of the striated muscle sarcomere demonstrates the position of the actin and myosin filaments within the sarcomere. Actin filaments are anchored at one end to the Z disk (or Z line), and in between are positioned myosin filaments. The sarcomere is defined as the length between successive Z disks. Myosin filaments cover the A band, which may overlap with the actin filaments (AI zone) or remain bare of actin filaments (AH zone). The stretch of bare actin filaments is called the I band (reprinted from Darnell *et al.*, 1986).

B.1. Myosin

Myosin is the major protein component of the muscle thick filament. Myosins are a superfamily of molecular motors which exist in muscle and non-muscle cells in conventional two-headed and unconventional single head forms (Goodson and Spudich, 1993). The myosin involved in muscle contraction is myosin II, a conventional two-headed member of the myosin superfamily, and will be the only one referred to in this dissertation. Myosin is a hexameric protein (Mr ~450 000) composed of two heavy chains, one pair of essential and one pair of regulatory light chains. The heavy chains are intertwined to form an elongated tail, a neck region and two heads. One essential and one regulatory light chain is associated non-covalently with each myosin head region, and another pair is associated with the neck region (Goldman, 1987). The light chains provide stability to the head/neck region, and have been shown to be necessary to achieve maximal speeds of shortening (Lowey *et al.*, 1993). The tail regions from separate myosins come together to form the body of the thick filament, whereas the neck region allows the head to extend and protrude towards the thin filament. All muscle types express different isomyosins which may differ in their myosin heavy chain components or in the isoforms of the regulatory or essential light chains expressed. The defining function of myosins are their ATPase activities, with skeletal muscle myosin ATPases operating at faster rates than the smooth and cardiac muscle myosin ATPases. X-ray crystallography analysis of the head of myosin, termed the subdomain 1 or S1 region, has shown it to form a major contact with subdomain 1 of actin (Rayment *et al.*, 1993), providing direct evidence for the cross-bridge cycling theory.

The majority of current evidence supports a change in the myosin head angle to produce the relative displacement and the force during contraction (Huxley, 1969). It has been observed that the hinge region of myosin is able to undergo a helix-coil transition, possibly collapsing in length and therefore providing another mechanism to generate displacement and force (Harrington and Rodgers, 1984).

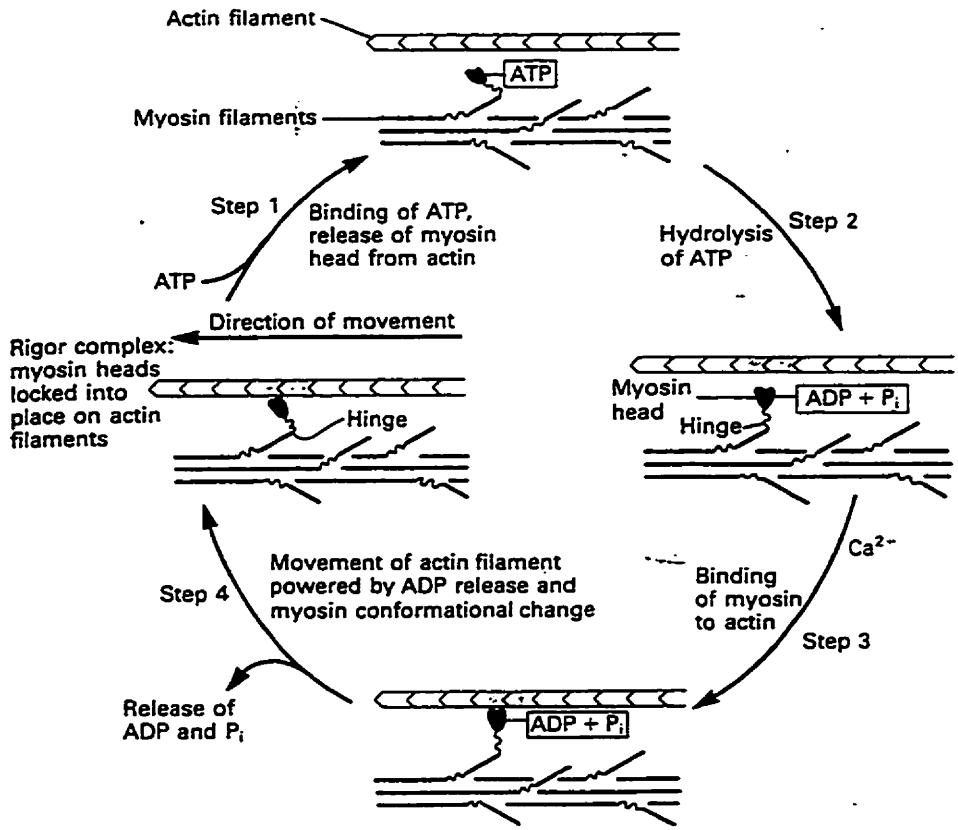

Figure 1.2. The ATPase cycle of myosin during contraction.

The binding of ATP to the myosin head triggers its release from a binding site on the actin filament (Step 1). The hydrolysis of ATP into ADP and Pi by the myosin ATPase results in a movement in the myosin hinge (Step 2) and promotes the favorable interaction between the myosin head and the actin filament. The release of the hydrolyzed nucleotide triggers a conformational change in the myosin hinge, which forces the actin filament towards the center of the sarcomere (Step 4). This rigor complex is released when the myosin head binds ATP, reinitiating the cycle (reprinted from Darnell *et al.*, 1986).

B.2. Actin

The muscle thin filament is formed by an actin backbone. Actins are a family of highly conserved proteins found in vertebrates and invertebrates. Actins serve crucial functions in cell motility, cell trafficking and determination of cytoskeletal shape. Two α-actin genes are responsible for actin expression in skeletal and cardiac muscle (Gunning *et al.*, 1983). Actin exists in a globular, monomeric form (G-actin) as well as a filamentous, helical form (F-actin). The polymerization of G-actin into F-actin is induced by divalent cation, with G-actin having primarily an ATP- Ca^{2+} complex associated with it, whereas F-actin has an ADP- Mg^{2+} complex with nucleotide exchange roughly 1000-fold faster in G-actin as compared to F-actin (Pollard *et al.*, 1992). X-ray crystallography of actin-DNase I co-crystals has shown actin to be a globular protein formed of 4 subdomains (Kabsch *et al.*, 1990; Figure 1.3). Subdomains 1 and 2, the small domain, are connected to subdomains 3 and 4, the large domain, by a hinge connecting subdomains 1 and 3. This results in a central cleft separating the large domain from the small domain. The central cleft is believed to be a nucleotide / divalent cation binding area (Szent-Gyorgyi and Prior, 1966), where a bound nucleotide or cation may stabilize the actin monomer by making contacts with all four subdomains. In G-actin, nucleotide exchange is rapid whereas the Mg^{2+}-induced polymerization of G-actin into F-actin results in an actin strand slow in nucleotide exchange (Barany *et al.*, 1966). In F-actin, it is believed that the actin monomers are oriented with the large domain (subdomains 3 and 4) close to the intertwined filament axis, whereas the small domain (subdomains 1 and 2) is more distant from the filament axis (Holmes *et al.*, 1990). Contacts do exist between one actin monomer and four adjacent ones in F-actin (Holmes *et al.*, 1990), supporting the possibility of cooperative interactions within F-actin. Data has shown that the tropomyosin - troponin complex of striated muscles may decrease the flexibility of the actin monomers, therefore increasing stability (Oosawa, 1983) while reducing the rate of release of actin-bound nucleotide. On the other hand, myosin, which binds primarily at subdomain 1, increases F-actin flexibility, possibly opening the actin cleft and facilitating release of actin-bound ADP (Oosawa, 1983; Szent-Gyorgyi and Prior, 1966). Although the myosin head forms a major contact with this part of actin, a part of the

cross-bridge cycle may have myosin attached in between two adjacent actin monomers (Milligan *et al.*, 1990).

C. Regulation of Contraction in Striated Muscle

The availability of F-actin active sites is the major determinant in the contraction of the sarcomere. In striated muscle, the actin filament is anchored at the Z line, and is decorated with tropomyosin and the troponin complex (Figure 1.4). Tropomyosin is a coiled-coil dimer which wraps around the F-actin filament in a head-to-tail fashion, believed to occupy the active sites of the F-actin strand during the resting state of muscle. Positioned on tropomyosin is the troponin complex, which is composed of three subunits: troponin I, the inhibitory subunit, troponin C, the Ca^{2+}-binding subunit and troponin T, the tropomyosin-binding subunit (Zot and Potter, 1987). In the presence of low levels of calcium (< 0.1 μM), the troponin complex, in association with tropomyosin, inhibits an otherwise favorable interaction between the myosin heads and the active sites of actin. During the active state, an increase in Ca^{2+} (> 0.7 μM; Greaser and Gergely, 1971) results in Ca^{2+} binding to troponin C. This is believed to induce a series of conformational transitions, eventually relieving troponin I inhibition as well as shifting thin filament associated tropomyosin from its steric block of the F-actin active sites. In striated muscles, the regulation of contraction is thin filament linked as the Ca^{2+} signal is mediated by the thin filament associated troponin complex (for review, see Zot and Potter, 1987). Other models for contraction have suggested that the interaction among proteins in the contractile apparatus is not a simple on-off switch, but instead, Ca^{2+}-troponin-tropomyosin, F-actin-myosin cross-bridge formation, and acto-myosin ATPase activity affect one another to regulate the striated muscle contraction (reviewed by Payne and Rudnick, 1989).

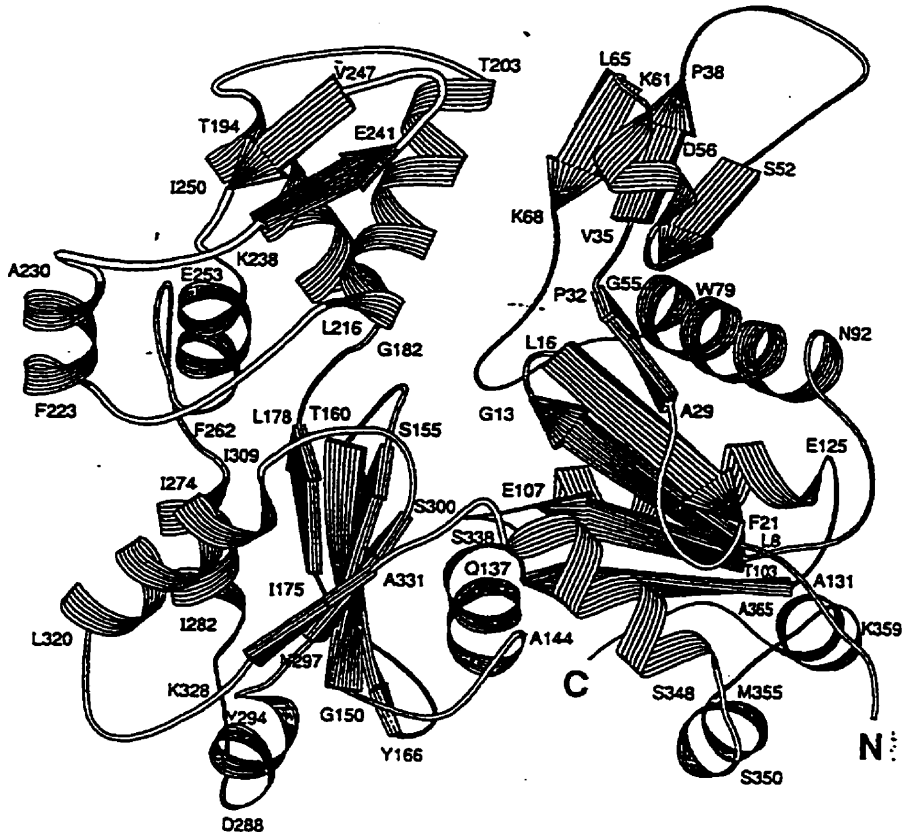

Figure 1.3. The structure of ATP-actin : Dnase I complex.

A diagram of the ATP-actin : Dnase I complex derived from x-ray crystallography data. The conserved actin structure demonstrates the hinge joining subdomain 1 (N-terminus) and subdomain 3 (bottom left). The hinge connects the small domain (subdomains 1 and 2; right hand side) to the large domain (subdomains 3 and 4; left hand side). The central space is the nucleotide binding cleft (reprinted from Kabsch *et al.*, 1990).

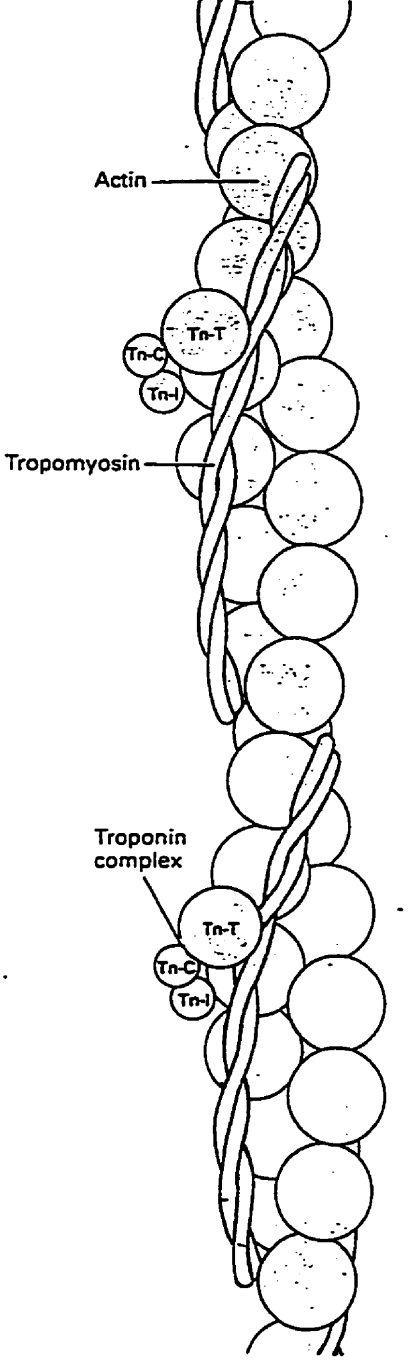

Figure 1.4. Tropomyosin and troponin decorate the actin filament.

The location of tropomyosin and the troponin complex is shown relative to the actin filament. Tropomyosin dimers are wrapped spirally around actin and occupy the actin active sites. An increase in Ca^{2+} will saturate binding sites on troponin C, eventually relieving troponin I and tropomyosin inhibition of the actin-activated myosin ATPase. Troponin T functions to secure the other two members of the troponin complex onto tropomyosin (reprinted from Darnell *et al.*, 1986).

C.1. The Thick Filament of Striated Muscle

Myosin is the major constituent of the thick filament. Different isomyosins are expressed in fast and slow skeletal muscles as well as cardiac muscles. Fast skeletal muscle myosins generally exhibit a higher maximum ATPase activity as compared to slow skeletal and cardiac myosins (Samaha *et al.*, 1970; Samuel *et al.*, 1981). Although phosphorylation of the regulatory light chains of myosins are essential for smooth muscle contraction, this is not the case for striated muscle. It has been proposed that phosphorylation of the regulatory light chain in skeletal muscle myosin by calmodulin activated myosin light chain kinase helps to increase or potentiate the force produced during isometric contraction (Sweeney *et al.*, 1993), but is not essential in force generation. In addition to myosin, other proteins contribute to the structure and function of the thick filament. C protein (140 kDa), H protein (74 kDa), M protein (165 kDa) and myomesin (185 kDa) are thick filament associated proteins expressed in various fibre types (Starr and Offer, 1983). These proteins are expressed in different patterns along the 43 nm transverse stripes of the thick filament (Bennet *et al.*, 1986). The specific function of these thick filament associated proteins remains under investigation. Although C protein and myomesin are expressed in cardiac muscle and all fibre types of skeletal muscle, H protein and M protein are absent from some skeletal muscle fibre types (Bahler *et al.*, 1985), suggesting that these proteins play modulatory roles in fine tuning contraction, but are not essential for the regulation or occurrence of contraction.

C.2. The Thin Filament Regulated Contraction of Striated Muscle

The troponin complex, along with tropomyosin, is the major regulatory factor for striated muscle contraction. The troponin complex is formed by three subunits: troponin C, the Ca^{2+} binding subunit, troponin I, the inhibitory subunit, and troponin T, the tropomyosin binding subunit. It is believed that the troponin complex is associated with tropomyosin, mediating the latter's effect on the exposure of the F-actin active sites.

Troponin C (Mr 19000) belongs to a family of Ca^{2+} binding proteins which feature EF hands, a distinct structure characterized by two perpendicular alpha helices separated by a short loop, which provides the Ca^{2+} binding pockets (Zot *et al.*, 1983; Herzberg *et al.*, 1986). Skeletal muscle troponin C has four Ca^{2+} binding sites, two each in the NH_2- and the COOH-terminus of the protein which remain separated by a central helix (Herzberg and James, 1988). The Ca^{2+} binding sites are numbered I and II in the NH_2-terminus and III and IV at the COOH-terminus. Sites I and II are low affinity Ca^{2+} binding sites (Ka 10^5 M^{-1}) whereas sites III and IV bind Ca^{2+} with high affinity (Ka 10^7 M^{-1}) as well as binding Mg^{2+} (Potter and Gergely, 1975). Binding of Ca^{2+} to sites I and II is cooperative (Pan and Solaro, 1987) and the Ca^{2+} affinity of sites I and II is consistent with their involvement in the regulatory role of troponin C in the troponin complex (Johnson *et al.*, 1994). Thin filament systems reconstituted with recombinant troponin C proteins mutant in Ca^{2+} binding sites I and II exhibit no contraction, even in the presence of Ca^{2+} (Sorenson *et al.*, 1995). Mutations in sites III and IV that abolish metal-binding do not affect the Ca^{2+} dependence of muscle contraction, although troponin I's interactions with the COOH-terminal region of troponin C appears to be weakened (Negele *et al.*, 1992), indicating the importance of the COOH-terminal region in anchoring troponin C to the troponin complex.

The binding of Ca^{2+} to sites I and II of troponin C facilitates the movement of central regions of troponin I away from actin (Tao *et al.*, 1990), as well as creating a more flexible troponin complex (Zhao *et al.*, 1995), which contributes to overall structural changes permitting acto-myosin interaction. The inhibitory and COOH-terminal regions of troponin I switch from binding F-actin and tropomyosin in the absence of Ca^{2+} to binding both the NH_2- and COOH-terminal domains of troponin C in the presence of Ca^{2+} (Farah *et al.*, 1994). On the other hand, interactions between the COOH-terminal region of troponin C and the NH_2-terminal region of troponin I appear to be Ca^{2+} insensitive (Sheng *et al.*, 1992). Calcium binding to sites I and II of troponin C has been postulated to expose a hydrophobic pocket at the NH_2-terminal region of the protein. In theory, this pocket could interact with troponin I or troponin T, signaling overall conformation changes of the

troponin complex in the presence of Ca^{2+}. In agreement with this model, troponin C mutants which inhibit this Ca^{2+} induced conformational change also abolish troponin C's regulatory activity as well as its interaction with troponin I (Grabarek *et al.*, 1990). A significant difference between skeletal and cardiac muscle troponin C is that the latter has several amino acid substitutions in Ca^{2+} binding site I, leaving it with only a single functional regulatory Ca^{2+} binding site (Krudy *et al.*, 1994). For this reason, Ca^{2+} activation of cardiac muscle is accompanied by a coupling free energy release smaller than that seen for troponin I / troponin C in skeletal muscle (Liao *et al.*, 1994), which may have implications for the speed and strength of contraction in cardiac muscle.

Troponin I, the inhibitory subunit of the troponin complex, is a 21 kDa protein that binds F-actin, tropomyosin, troponin T and troponin C (Zot and Potter, 1987). Troponin I is found to inhibit acto-myosin ATPase activity autonomously in a Ca^{2+} independent manner, an effect which is further potentiated by tropomyosin (Potter and Gergely, 1974). Domain mapping of the troponin I polypeptide has narrowed the inhibitory region to residues 96-116 in the rabbit isoform (Syska *et al.*, 1991). In this respect, troponin I has been dissected as a protein of three distinct domains: NH_2- and COOH-terminal domains as well as the inhibitory domain. In the absence of Ca^{2+}, the NH_2-terminal region of troponin I is in contact with the COOH-terminal region of troponin C and troponin T, lying anti-parallel to both proteins (Sheng *et al.*, 1992). The proximity of troponin I to F-actin is affected by the availability of Ca^{2+}, as activating Ca^{2+} concentrations result in a significant distance increase between troponin I and F-actin (Tao *et al.*, 1990). This Ca^{2+} dependent separation between troponin I and F-actin is initiated by troponin C as it receives the Ca^{2+} signal. As mentioned earlier, the preferred interaction of troponin I with troponin C in the presence of activating Ca^{2+} concentrations is consistent with the initiation of muscle contraction by Ca^{2+}, as F-actin active sites are freed for myosin head interaction.

Cardiac muscle troponin I has 32 additional amino acids at its NH_2-terminal, with two serine residues at positions 23 and 22 or 24, depending on the species (Mittmann *et al.*,

1990). Both serine residues may be phosphorylated, resulting in a decreased Ca^{2+} sensitivity in isolated cardiac myofibrils (Garvey *et al.*, 1988). In reconstituted troponin complexes, the phosphorylation of cardiac troponin I increases the rate of Ca^{2+} dissociation from troponin C, suggesting that phosphorylation of cardiac troponin I may play a role in increasing the rate of cardiac muscle relaxation (Robertson *et al.*, 1982; Zhang *et al.*, 1995a). Because cardiac troponin I remains phosphorylated even at the return of muscle to pre-contractile basal levels (Talosi *et al.*, 1993), the significance of this phosphorylation has not been concluded. Recent studies indicate that of two phosphorylation sites, one is constitutively phosphorylated whereas phosphorylation of the other site may be the functionally important process (Zhang *et al.*, 1995b).

Although the release of troponin I inhibition of the acto-myosin ATPase is accounted for by its Ca^{2+} sensitive interactions with troponin C, it cannot account for the release of tropomyosin inhibition of the actin-activated myosin ATPase. It is believed that troponin T, the tropomyosin-binding subunit of the troponin complex (Leavis and Gergely, 1984), serves to mediate the Ca^{2+} signal to relieve tropomyosin inhibition. Troponin Ts are encoded by three genes expressed in cardiac, fast and slow skeletal muscles. Muscle type specific or developmentally regulated troponin T isoforms are expressed from each gene through alternative mRNA splicing (Cooper and Ordahl, 1985; Breitbart and Nadal-Ginard, 1986; Jin *et al.*, 1992). In fast skeletal muscle troponin T, alternative mRNA splicing involving a pair of mutually exclusive COOH-terminal exons (16/17) and seven (Breitbart and Nadal-Ginard, 1986; Smillie *et al.*, 1988; Briggs and Schachat, 1993) or possibly more (Schachat *et al.*, 1995) exons encoding a variable NH_2-terminal region produces a large number of protein isoforms. Previous work on rabbit fast skeletal muscle troponin T had dissected the protein into two major functional domains. The COOH-terminal chymotryptic fragment T2 (residues 159-259) binds to the central region of tropomyosin (Ohtsuki, 1979; Morris and Lehrer, 1984) as well as interacting with F-actin, troponin I and troponin C (Pearlstone and Smillie, 1978, 1980, 1982; Heeley and Smillie, 1988; Schaertl *et al.*, 1995). The NH_2-terminal chymotryptic fragment T1 (residues 1-158) interacts with the carboxy

terminus of tropomyosin, extending to include the amino terminus of the adjacent tropomyosin molecule in the head to tail overlap of tropomyosin along the thin filament (Pato *et al.*, 1981; Brisson *et al.*, 1986; White *et al.*, 1987). The central region of troponin T (residues 70-150) has been shown to contribute to the tight association of the troponin complex to tropomyosin (Fisher *et al.*, 1995). In contrast, the variable NH_2-terminal region of troponin T has not been directly associated with a defined function (Pearlstone and Smillie, 1982). Although a troponin T isoform switch, primarily due to alternative splicing of this NH_2-terminal region, is well regulated during avian and mammalian heart development (Cooper and Ordahl, 1985; Jin and Lin, 1988; Jin *et al.*, 1990), deletion of the first 45 NH_2-terminal residues from rabbit fast skeletal muscle troponin T was shown not to affect the cooperative response of regulated acto-myosin ATPase to Ca^{2+} (Pan *et al.*, 1991). On the other hand, differences in the Ca^{2+} sensitivity of acto-myosin ATPase have been observed in reconstituted systems containing two bovine cardiac troponin T isoforms differing in the NH_2-terminal variable region (Tobacman and Lee, 1987). Recent evidence has demonstrated that differences in the primary structure of the variable NH_2-terminus of troponin T may reconfigure the overall conformation of the protein (Ogut and Jin, 1996). Interestingly, this variable NH_2-terminus is in contact with two adjacent tropomyosin dimers, allowing this region of the protein to play a significant role in the release of tropomyosin inhibition under activating Ca^{2+} concentrations. Although the functional significance of troponin T isoform diversity is not fully understood, certain pathological conditions have demonstrated a concurrent change in troponin T isoform expression (Gulati *et al.*, 1994; Akella *et al.*, 1995; Anderson *et al.*, 1995). Furthermore, a relationship between cardiac troponin T mutation and human familial cardiomyopathies has been reported (Thierfelder *et al.*, 1994; Watkins *et al.*, 1995).

The troponin complex, in a 1:7 molar ratio with actin, does not physically contact each of the seven actin monomers under its regulatory control. For this reason, the importance of troponin T and tropomyosin in the regulation of the thin filament structure becomes evident. Due to troponin T's direct interactions with tropomyosin, it is believed to

mediate or modify tropomyosin's binding to F-actin. Further, the large isoform diversity of troponin T suggests that it may even modify the Ca^{2+} sensitivity or cooperativity of the thin filament. The Ca^{2+} dependent control of acto-myosin ATPase of an F-actin filament decorated by tropomyosin, troponin C and troponin I is only observed at troponin I : actin ratios greater than the physiological ratios (Farah *et al.*, 1994). In the absence of troponin T, troponin C can remove troponin I from its F-actin - tropomyosin association independent of Ca^{2+}. Under these conditions, the F-actin / tropomyosin / troponin I complex is stabilized only by troponin T (Potter and Gergely, 1974). In agreement, the addition of troponin T provides a more effective inhibition of the acto-myosin ATPase in the absence of Ca^{2+}; in the presence of activating Ca^{2+} concentrations, the activity in the presence of troponin T is increased to levels greater than observed for F-actin / tropomyosin / myosin alone (Greaser and Gergely, 1971; Farah *et al.*, 1994). These reasons support troponin T's role as an intermediary in transmitting the inhibitory effect initiated by troponin I / troponin C interactions in the absence of Ca^{2+} to tropomyosin, which in turn spreads the inhibitory effect to the seven actin monomers. In this case, the presence of Ca^{2+} and the consequent removal of the inhibitory effect placed on the seven actin monomers is also mediated indirectly by troponin T and directly by tropomyosin. In support of troponin T's function, the COOH-terminal region of troponin T which interacts with troponin I / troponin C, as well as forming the primary, high affinity contact with tropomyosin, is well conserved in primary structure among isoforms and species, indicating a conserved, important basic function. On the other hand, the NH_2-terminal region of troponin T, which has very high primary structure diversity, is implicated in lower affinity interactions with two adjacent tropomyosin molecules (Pearlstone and Smillie, 1982). This versatility in the NH_2-terminal of troponin T isoforms may result in subtle changes in its three dimensional structure, effecting different responses to Ca^{2+} through its interaction with tropomyosin, consequently affecting the Ca^{2+} sensitivity or cooperativity of the thin filament.

Although the Ca^{2+} dependence of contraction in striated muscle is regulated by troponin, tropomyosin remains as the principal inhibitory factor of the acto-myosin

ATPase, and is therefore the species directly regulated by troponin. Tropomyosins form a diverse family of genes expressed in all three types of muscles, as well as the brain and non-muscle cells (Goodwin *et al.*, 1990; Forry-Schaudies *et al.*, 1990; Wieczorek *et al.*, 1988). Although the significance of tropomyosin isoform diversity is not understood, the number of isoforms is large, and the generation of these isoforms from the tropomyosin genes is unique. Unlike troponin T which shows isoform diversity through alternative splicing of genes, tropomyosin isoforms are generated by alternative splicing of a gene, as well as alternate promoters in the gene which are responsible for isoform generation (Hanke and Storti, 1988). For example, alternative splicing and the use of alternative promoters in the α-tropomyosin gene can encode for at least nine tropomyosin isoforms (Wieczorek *et al.*, 1988; Lees-Miller *et al.*, 1990). In striated muscles, two genes, α and β, encode tropomyosin isoforms. Products of the α-tropomyosin gene are prominent in cardiac muscle whereas β-tropomyosin isoforms are the major isoforms expressed in slow skeletal muscles. Both α- and β-tropomyosin isoforms are expressed in fast skeletal muscles at varying ratios depending on the species (Cummins and Perry, 1974). Tropomyosin is an elongated protein which natively forms coiled-coil dimers which may be homogeneous or heterogeneous in the tropomyosin isoforms associated. These coiled structures present a repeated pattern of seven amino acids with hydrophobic residues at the first and fourth positions, a feature highly conserved in all tropomyosins (Smillie, 1979; Heeley *et al.*, 1987). Monomer Mr for muscle specific tropomyosins vary between 33000 and 38000. At the level of the thin filament, tropomyosin dimers are wrapped spirally around F-actin to occupy 7 active sites during the resting state, but not during the active state (Heeley *et al.*, 1987). Adjacent tropomyosins on the thin filament are in a head-to-tail overlap, with this region of the dimers spanned by the NH_2-terminus of troponin T. Tropomyosin's position on the actin filament, in the absence of Ca^{2+}, inhibits a step in the definitive acto-myosin interaction. An increase in the availability of Ca^{2+} and its binding to troponin C results in changes in conformations along the troponin complex, resulting in an eventual shift of the position of tropomyosin, removing its steric inhibition of the active actin sites. Evidence is accumulating whereby the inhibition brought forth by tropomyosin may occur at the F-actin

binding step and/or at a step subsequent to the actin binding, possibly a kinetic step such as the release of phosphate after ATP hydrolysis by myosin (Chavolich and Eisenberg, 1982; Chavolich, 1992). Such findings indicate that the steric blocking model for striated muscle contraction may be a simplified case and that complex and cooperative interactions between the troponin complex, tropomyosin, F-actin and myosin work together to define muscle contraction.

D. The Third and Fourth Filaments of Striated Muscles

Although many of the events responsible for regulating sarcomere length have been studied in detail, the two filament model for muscle contraction can not account for all observed mechanical characteristics of muscle. Muscles exhibit passive elasticity, producing forces that resist stretch independently of ATP hydrolysis or contact between the thin and thick filaments. In fact, sarcomeres may be stretched beyond the point of thin - thick filament overlap yet still retain and regain integrity. Such observations, as well as the advancement of polyacrylamide gel electrophoresis techniques, led to further investigations and the discovery of the filamentous proteins titin and nebulin, which may further function in the organization of contractile proteins along the thick and thin filaments.

D.1. Titin

The ability of the sarcomere to regain integrity after being stretched beyond acto-myosin overlap is a reason why the two filament model of muscle contraction was not comprehensive. When striated muscle myofibrils are solubilized in hot sodium dodecyl sulfate solution, a protein of extremely high Mr called titin is visualized on high porosity polyacrylamide gels (Wang *et al.*, 1979). Titin (or connectin) has been shown to span the length of a half sarcomere from the Z line to the M line (Furst *et al.*, 1988). Initial experiments characterizing the sequence of titin cDNA revealed a protein consisting mainly of two classes of 100 residue motifs (Labeit *et al.*, 1990). These class I and II motifs have been identified as members of the fibronectin and immunoglobulin superfamilies, respectively (Benian *et al.*, 1989). In the A band region of titin, the motifs are arranged in

super-repeats of I-I-II-I-I-I-II-I-I-I-II (Labeit *et al.*, 1990), potentially following the 43 nm cross-bridge repeat of the thick filament (Labeit *et al.*, 1992). The I-band section of titin makes extensible and elastic connections between the ends of the thick filaments and the Z line (Furst *et al.*, 1988; Whiting *et al.*, 1989). This I-band region of titin is composed of long stretches of class II motifs and may work to center the thick filaments in the sarcomere while providing passive tension for striated muscle upon stretch (Horowitz *et al.*, 1989; Granzier and Irving, 1995). It has been proposed that reversible folding of the class II motifs (Soteriou *et al.*, 1993a) or the likely extensibility of the PEVK domain (Labeit and Kolmerer, 1995b) may contribute to the elasticity in this region.

The determination of the complete cDNA nucleotide sequence of titin has shown an 82 kb transcript in cardiac muscle, encoding a protein of 3 MDa. In fast and slow skeletal muscles, expression of exons encoding additional class II motifs in the I band region, as well as a larger proline, glutamic acid, valine and lysine rich (PEVK) domain increases the size of the transcript to 101 kb and the protein encoded to 3.7 MDa (Labeit and Kolmerer, 1995b; Figure 1.5). The protein has also been shown to contain tandemly arranged serine-proline repeats at the NH_2- and COOH-terminus which are phosphorylatable and have been postulated as possible factors controlling the integration of titin into the framework of the sarcomere (Gautel *et al.*, 1993; Labeit and Kolmerer, 1995b). Studies of the properties of the titin protein have shown it to interact with other proteins in the striated muscle sarcomere. Proteolytic fragments as well as cloned titin proteins from the A band have shown it to interact with myosin (Soteriou *et al.*, 1993b; Jin, 1995), particularly light meromyosin (Labeit *et al.*, 1992), as well as with C-protein (Labeit *et al.*, 1992; Soteriou *et al.*, 1993b). Moreover, single class I and class II motifs have been shown to bind F-actin (Jin, 1995), with a linked class I-II protein showing higher affinity binding to F-actin.

Recent focus on the elastic property of titin has introduced a wealth of information regarding the extensibility of the protein and its contribution to the integrity of the sarcomere. Recent experiments measuring forces generated by titin molecules in atomic

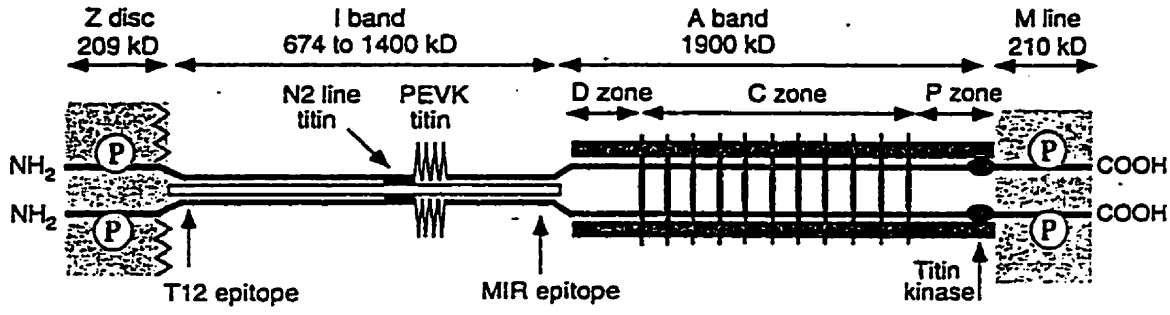

Figure 1.5. The arrangement of titin and its domains within the sarcomere.

The position of the giant protein titin within the sarcomere is shown. A single titin polypeptide spans from the Z disc to the M line and forms contact with both actin (I band region) and myosin (A band region) filaments. The unique NH_2- and COOH-termini of the protein are believed to arrange its integration into the sarcomere. The extensible region of titin follows the N2 line and is depicted as a zig-zag pattern (reprinted from Labeit and Kolmerer, 1995b).

force microscopy as well as by optically trapped titin molecules has led to advancements in understanding the mechanics of titin elasticity, more specifically with respect to the folding and unfolding of the immunoglobulin-like class II motifs to generate extensibility (Rief *et al.*, 1997; Kellermayer *et al.*, 1997). The advancement and refinement of these techniques will contribute significantly to the study of titin mechanics.

D.2. Nebulin

Nebulin is a giant protein present in only the skeletal muscle sarcomeres of vertebrates (Hu *et al.*, 1986). One of the last proteins to appear during embryonic development (Furst *et al.*, 1989), nebulin accounts for ~4% of total myofibrillar proteins (Wang and Williamson, 1980), varying in mass from 600 kDa to 900 kDa (Locker and Wild, 1986), possibly depending on and reflecting the length of the sarcomeric thin filament. Nebulin filaments are anchored to the Z-line through the protein's COOH-terminal domain, marked by a distinct Src homology 3 (SH3) region. Nebulin runs in parallel with titin along the thin filament, with the NH_2-terminus of the protein situated near the tip of the actin filaments (Labeit and Kolmerer, 1995a). A survey of various nebulin monoclonal antibody (mAb) epitopes by immunoelectron microscopy has shown them to be fixed at all lengths of the sarcomere, indicating that nebulin is an inelastic polypeptide within this framework (Wang and Wright, 1988). This is in contrast to titin, which shows elastic character in a domain located close to the A band / I band junction in striated muscle sarcomeres (Trombitas *et al.*, 1995). For acto-myosin preparations, methods have been developed in which nebulin has also been recovered (Meng *et al.*, 1995), suggesting further that this basic protein makes intimate contact with the thin filament.

Nebulin's limited solubility and tendency to aggregate in physiological buffers (Wang, 1982) creates difficulties in purifying the protein in its native form for structure and function studies. The full length cDNA for adult human nebulin has been documented (Labeit and Kolmerer, 1995a), revealing a protein consisting of repeats of conserved ~35

residue motifs, marked by a conserved SxxxY pentapeptide as well as evenly spaced proline residues (Figure 1.6). It has been proposed that seven ~35 residue motifs form a super-repeat, of which 22 span the length of the polypeptide. Although the conserved ~35 residue motifs are homologous to each other, the 22 super-repeats show greater sequence homology to each other than do the single motifs (Labeit and Kolmerer, 1995a). It has been speculated that a seven motif super-repeat spans the length of the vertebrate 38.5 nm thin filament repeat which consists of the troponin complex, tropomyosin and actin in a 1:1:7 stoichiometric ratio (for a review, see Squire, 1981). With the publication of nebulin cDNA, specific expression of these nebulin motifs, whether by a prokaryotic expression system or synthetic peptide synthesis, has been possible. Bacterially expressed multiples of the ~35 residue nebulin motifs have been shown to specifically bind F-actin in a solid phase binding assay, showing greater avidity as the number of motifs expressed increases (Jin and Wang, 1991a,b). These results initially described nebulin's interaction with the thin filament, implying that the complete nebulin protein would have a very high binding avidity to actin. In the same study, it was shown that the expressed nebulin proteins had no specific binding to troponin or tropomyosin but were able to bind myosin. Studies by Pfuhl and coworkers (1994) using synthetically synthesized peptides have shown that nebulin motifs have a helical structure. By theoretical modeling, the alpha helical propensity of motifs near the COOH-terminus was predicted to be higher than those in the NH_2-terminus (Pfuhl *et al.*, 1996). More specifically, the 35 amino acid motifs were shown to exhibit a tendency to form transient helices. These structures were found to be stabilized by a negatively charged environment, one which the F-actin thin filament may provide. This work also suggested that nebulin motifs near the COOH-terminus of the protein were able to bind actin with greater affinity than those near the NH_2-terminus. Investigations confirming the position of nebulin in the sarcomere, as well as its F-actin binding, led to the proposal that nebulin was an actin ruler in the skeletal muscle sarcomere (reviewed by Trinick, 1992). In this context, nebulin could act as a scaffold used by actin during its assembly in development. Nonetheless, studies of muscle protein expression through development have not documented a nebulin dependence of actin filament formation. In fact, striated myofibrils

have been shown to be either heterogeneous with respect to the timing of expression of muscle proteins (Lin *et al.*, 1994), or show an onset of expression in the order of desmin, titin, actin, myosin heavy chain and later on the expression of nebulin (Furst *et al.*, 1989). These data do not support nebulin's role as a guiding factor in actin thin filament formation.

Binding experiments using prokaryotically expressed nebulin fragments have shown their specific interaction with F-actin (Jin and Wang, 1991a,b). Nebulin's interaction with other proteins of the thin filament, particularly troponin and tropomyosin, remains under question. Reports have indicated no interaction (Jin and Wang, 1991b) or a strong interaction (Wang *et al.*, 1996) between nebulin motifs and these proteins. Overlay experiments using nebulin transferred to nitrocellulose membrane have shown that ^{125}I iodinated α-actinin is able to interact with nebulin, possibly providing a preliminary indication of the anchoring of the nebulin COOH-terminus in the Z line (Nave *et al.*, 1990). In this experimental system, nebulin was the only protein shown to bind α-actinin, as total muscle homogenates from skeletal and cardiac muscles showed no other interacting proteins. This does place the experimental system into question since other proteins, such as actin, are known to be associated with α-actinin in the Z line.

There is some evidence that nebulin may contribute to the regulation of skeletal muscle contraction. *In vitro* motility assays showed that cloned nebulin motifs from the NH_2-terminal region of the intact protein were able to inhibit the sliding of actin over myosin, with this inhibition released by Ca^{2+}-calmodulin (Root and Wang, 1994). This may provide initial evidence of a regulatory role for nebulin in the skeletal muscle sarcomere. In this respect, the position of nebulin's interaction with F-actin becomes important. Recent experiments using a two motif nebulin fragment have shown it to cross-link to the NH_2-terminus of actin at subdomain 1, providing a possible localization of nebulin's association with the F-actin strand (Shih *et al.*, 1997).

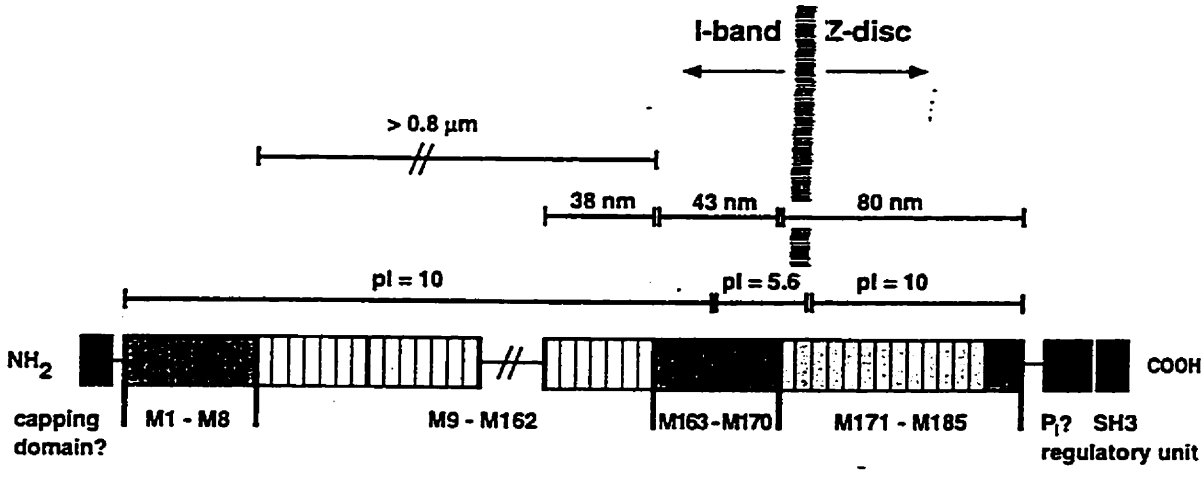

Figure 1.6. The nebulin polypeptide within the skeletal muscle sarcomere.

A model for the layout of nebulin within the skeletal muscle sarcomere shows the COOH-terminus of the protein oriented towards the Z disc. The blocks (M1-185) represent repeats of the ~35 amino acid motif. Unique sequences at both the NH_2- and COOH-termini of the protein complete the primary structure make-up. Lengths denoted are based on the assumption that one motif spans 5.5 nm. The pI values are those predicted from the primary structure (reprinted from Labeit and Kolmerer, 1995a)

Nonetheless, a nebulin-sized counterpart in cardiac muscle had not been identified, questioning the importance of the role of nebulin in the function of the vertebrate skeletal muscle sarcomere. Recently, Moncman and Wang (1995) have identified a nebulin-like protein in chicken cardiac muscle extracts. By immunoprecipitation with nebulin monoclonal antibodies specific for epitopes near the COOH-terminal of the protein, the researchers were able to identify a ~107 kDa protein from cardiac muscle of various species. By immunological screening of a chicken cardiac muscle expression cDNA library, three overlapping cDNA clones were isolated. Translation of the consensus of these three cDNAs showed a partial protein composed of nebulin-like ~35 amino acid motifs. Interestingly, Northern blot hybridization showed the cardiac muscle-specific nebulette transcript to be ~8 kb, implying a substantial untranslated region. Studies by immunofluorescence microscopy have shown the COOH-terminus of the protein to be situated in the I-Z-I region of cardiac myofibrils. Therefore, the cardiac muscle nebulette is a protein homologous, and possibly analogous, to skeletal muscle nebulin, indicating a family of nebulin-like proteins involved in the organization and/or regulation of contraction of striated muscle sarcomeres.

E. Hypothesis

The majority of current research has focused on nebulin's interaction with F-actin, with studies proposing that nebulin works as a template for F-actin and thin filament assembly. The discovery of the smaller, homologous cardiac nebulette protein has resulted in the need to reassess the role of nebulin and nebulin-like proteins in the sarcomere. The proposal that nebulin directs the formation of the thin filament is not consistent with the cardiac muscle nebulette protein, as its smaller size means that it cannot span the entire length of cardiac muscle thin filaments, and therefore cannot direct their assembly. Furthermore, studies of the appearance of muscle-specific proteins through development have not demonstrated a nebulin-dependent actin filament formation. Therefore, nebulin, and its homologous partner nebulette, must perform functions other than as an actin ruler.

Initial studies with cloned nebulin proteins have shown that they have the ability to inhibit the unregulated acto-myosin S1 ATPase activity. This provides a new avenue for research into the function of nebulin, providing the possibility that it may participate in the regulation of muscle contraction. Its ability to inhibit the acto-myosin S1 ATPase means that nebulin's interaction with the thin filament, and its position in the presence and absence of Ca^{2+}, should be regulated. Apart from a limited cDNA sequence and immunofluorescence localization, no information is available regarding nebulette, the nebulin-like protein in cardiac muscle. To further clarify the function of nebulin-like proteins, a comparison of nebulin and nebulette is advantageous, as common properties between the two proteins are useful indications in proposing a model for their roles in the skeletal and cardiac muscle sarcomeres.

The large size and relative insolubility of nebulin creates difficulties in studying the structure and function of the full length protein. Therefore, studies characterizing nebulin must take advantage of nebulin fragments, extrapolating the results for the intact protein. In characterizing fragments of such a large protein, the functional unit of nebulin is important to consider. Since gene expression controls protein expression, the exon organization of the nebulin gene is expected to reflect the functional organization of the encoded protein, representing logical dissection points for the polypeptide. Therefore, the genomic organization of a limited stretch of the nebulin gene will be examined in an attempt to identify the functional unit of nebulin. Nebulin fragments engineered based on this criterion will be characterized, with the goal of applying the data for the intact protein. In addition, this research will also address the relationship between nebulin and nebulette, two proteins which may form a family of related striated muscle proteins. Through initial characterization of a cloned nebulette protein, functional similarities between nebulin and nebulette will be addressed. Furthermore, their expression regulation and their possible effects on acto-myosin ATPase activity will be monitored. Due to the high avidity interaction between nebulin and the F-actin thin filament and the high homology between nebulin and nebulette, it is proposed that nebulin, and nebulin-like proteins such as

nebulette, participate in the regulation of contraction of striated muscle sarcomeres. The large size difference between skeletal muscle nebulin and cardiac muscle nebulette is expected to reflect differences between the skeletal and cardiac muscle sarcomeres, providing a starting point, along with their functional comparison, in proposing a role for nebulin and nebulin-like proteins in sarcomeres.

F. Objectives

The following objectives are outlined for this research project:

1) Complementary DNA encoding nebulin and nebulette will be cloned, providing genetic materials for isolation of genomic DNA as well as prokaryotic and eukaryotic expression of cloned proteins.

2) Nebulin genomic DNA will be isolated in an attempt to identify nebulin exons and provide a logical dissection point for the repeating organization of nebulin-like proteins.

3) Cloned complementary DNA will be used to express nebulin or nebulette proteins in bacteria. Effective purification of the cloned proteins will provide material for further characterization.

4) An antiserum specific for nebulette will be generated in mouse, providing a tool to detect nebulette expression in various species and throughout development.

5) Through solid phase binding assays and acto-myosin ATPase assays, the contribution of the cloned nebulin and nebulette proteins to the structure and function of the striated muscle thin filament will be explored.

CHAPTER TWO:
CLONING AND CHARACTERIZATION OF NEBULIN AND NEBULETTE cDNA

INTRODUCTION

Complementary DNA for proteins allows flexibility in manipulation by genetic engineering approaches to characterize proteins, as well as providing information regarding the primary structure of a protein, and its relation to other proteins. The complete primary structure of the mRNA transcript of human skeletal muscle nebulin has been documented, showing the protein to be composed almost exclusively of well conserved ~35 amino acid repeat motifs along its entire length (Labeit and Kolmerer, 1995a). Small unique domains at both the NH_2- (5' end of mRNA transcript) and COOH-terminal (3' end of mRNA transcript) of the protein complete its primary structure make-up. Seven of the ~35 amino acid motifs form a super-repeat, of which 22 comprise nebulin. Assuming that a single module spans 5.5 nm, a super-repeat is expected to span the 38.5 nm thin filament troponin / tropomyosin / 7 actin periodicity (Labeit and Kolmerer, 1995a; Wang *et al.*, 1996).

Nebulin cDNA cloned from mouse is advantageous because the host is ideal for advanced mammalian genetic manipulations. To date, only a limited (1272 bp; Muller-Seitz *et al.*, 1993) sequence of the mouse nebulin mRNA transcript is available. This available sequence was used to advantage in designing synthetic oligonucleotide primers to facilitate cloning of mouse nebulin cDNA. In addition, a 38 base oligonucleotide primer complementary to a well conserved region near the 3' end of the human nebulin cDNA transcript was designed to clone 3' nebulin cDNA encoding the COOH-terminus of the protein. A 129 mouse neonatal skeletal muscle cDNA library was constructed to facilitate cloning of multiple nebulin cDNAs. Nebulette, the small, nebulin-like protein in cardiac muscle (Moncman and Wang, 1995), has also been shown to be predominantly composed of well conserved ~35 amino acid repeats as those found in skeletal muscle nebulin. To date, only a partial cDNA from chicken nebulette is available. Using reverse transcriptase

coupled polymerase chain reaction, chicken nebulette cDNA was cloned, providing a genetic coding template for protein expression.

Recombinant DNA technologies were used to clone the representative nebulin and nebulette cDNA. The results indicate that nebulin transcripts are well conserved among mammalian species and that nebulin and nebulette share significant homology.

MATERIALS AND METHODS

A. Construction of a 129 Mouse Neonatal Skeletal Muscle cDNA Library

To isolate nebulin cDNA, a 129 mouse neonatal skeletal muscle cDNA library was constructed using the Stratagene ZAP cDNA synthesis kit. Using fresh, neonatal 129 mouse skeletal muscle, total RNA was extracted by the TRIzol reagent (Gibco BRL) as described by the manufacturer's protocol. The TRIzol reagent is a denaturing, acid/phenol extraction buffer designed to separate RNA from DNA and cellular proteins. Total RNA precipitated by isopropanol was resuspended in 0.1% diethylpyrocarbonate (DEPC)-treated H_2O and analyzed by agarose gel electrophoresis for integrity and approximate concentration. A 5 μL aliquot of the extracted total RNA was added to 1 μL of 6x agarose gel sample buffer (6x agarose gel sample buffer: 40% sucrose, 0.25% bromophenol blue, 0.25% xylene cyanol; solution made in 10 mM Tris-HCl, pH 8.0, 1 mM EDTA) and analyzed by 0.7% agarose gel electrophoresis at a potential difference of 5 mV/cm using a Tris-borate-EDTA (1x TBE: 90 mM Tris-borate, 2 mM EDTA) running buffer. Integrity of the RNA was determined by the presence and sharpness of the abundant 18S and 6S ribosomal RNA bands. Poly-A RNA was selectively separated from the total RNA mixture by biotinylated oligo-dT capture using the Poly-ATract system (Promega). First strand cDNA was made from 5 μg of poly A mRNA using a mixture of oligo-dT primers as well as random hexamers priming reverse transcriptase (50 units) first strand DNA synthesis at 37 °C for 1.5 hours. The complementary DNA strand was synthesized by DNA polymerase I (100

units) at 15 °C for 2 hours. RNase H (4.5 units) was included in this mixture to degrade the remaining RNA template while facilitating complementary DNA strand synthesis. The double stranded cDNA mixture was extracted with an equal volume of phenol:chloroform and then with chloroform to remove the enzymes from the mixture. The cDNA was precipitated at -20 °C overnight by adding 1/10 volume of 3 M NaOAc, pH 5.2, and 2.5 volumes of 100% ethanol. Following centrifugation (15000g/60min), the precipitated cDNA was blunt ended using the Klenow fragment of DNA polymerase I (2 units) by incubating at 37 °C for 30 minutes. This mixture was extracted with phenol:chloroform and chloroform and precipitated at -20 °C for 3 hours as described earlier. Following centrifugation, EcoRI adapters (Stratagene) were ligated to the cDNA by incubation with 4 U of T4 DNA ligase overnight at 8 °C. The cDNA was then size fractionated using a 3 cm x 0.3 cm Sephacryl S400 column (Stratagene) and fractions were analyzed by 0.8% agarose gel electrophoresis. Size fractions containing cDNAs greater than 0.8 kb were pooled and 1 μg of the cDNA was ligated with 1 μg of Uni-Zap XR II phage arms overnight at 8 °C by 3 U of T4 DNA ligase. The ligated, reconstituted phage DNA were packaged using the Gigapack Gold packaging extract kit (Stratagene), according to the manufacturer's protocol. The packaged phage were allowed to infect 1.2 mL of $O.D._{600} = 1$ *E. coli* XL1 Blue MRF' cells for 20 minutes at 37 °C, added to 100 mL of 37 °C top agar (for 1 L; 10 g tryptone, 5 g yeast extract, 5 g NaCl, 8 g agar), mixed, and plated out on 10 150 mm LB-agar (LB, per litre: 10 g tryptone, 5 g yeast extract, 10 g NaCl) plates. Following overnight incubation at 37 °C, the number of plaques on the bacterial lawn was estimated by sampling 1 cm^2 areas. The phage was recovered from the plates by soaking the top agar in suspension medium (SM buffer: 0.1 M NaCl, 8 mM $MgSO_4.7H_2O$, 50 mM Tris-HCl, pH 7.5, 0.01% gelatin) and scraping it into a sterile 500 mL bottle. Chloroform was added to 1% and the mixture shaken for 30 minutes to ensure suspension of the phage into the aqueous SM buffer as well as lysing the remaining bacterial host. The suspension was centrifuged (8000rpm/10min/JA10) and the high titre supernatant was recovered. For long term storage, dimethyl sulfoxide (DMSO) was added to 7.5% and the phage stock stored at -80 °C.

B. Isolation of Nebulin cDNA from the 129 Mouse Neonatal Skeletal Muscle cDNA Library

An oligonucleotide was designed to screen a 129 mouse neonatal skeletal muscle cDNA library for nebulin cDNA covering the 3' end of the full length transcript. The oligonucleotide spanned from bp 19125 to 19162 of human nebulin, overlapping a region of complete amino acid identity and 89% nucleotide identity (34 of 38) between the published human nebulin and chicken nebulette nucleotide sequences (N38 5'-TTCTCTTGATTNC(G/T)(A/G)TTGACTCT(A/G)TCAATCTCTGGAGT-3'). To accommodate the mismatches in nucleotide sequences, the oligonucleotide was designed with degenerate bases at positions where the nebulin and nebulette sequences were not identical.

B.1. Oligonucleotide Screening of the Mouse Skeletal Muscle cDNA Library

The N38 oligonucleotide (20 pmol) was end-labelled with ^{32}P by 10 units of T4 polynucleotide kinase using γ-^{32}P-ATP as an exchange substrate. Briefly, 20 pmol of the oligonucleotide primer was combined with an equimolar amount of γ-^{32}P-labelled ATP in a 50 µL solution containing 10 units of T4 polynucleotide kinase, 50 mM Tris-HCl, pH 7.6, 10 mM $MgCl_2$, 5 mM dithiothreitol, 0.1 mM spermidine, 0.1 mM EDTA, 0.2 mM ATP. The reaction was incubated at 37°C for 2 hours and the unincorporated γ-^{32}P-ATP was separated from the oligonucleotide primer using a 0.4 cm x 2 cm Biogel P2 gel filtration column (Bio-Rad). Following the reaction, the labelled oligonucleotide probe was used to screen filter replicas of the 129 mouse neonatal skeletal muscle library. Briefly, an aliquot of phage equivalent to ~1.5 times the original library size (315 000 plaque forming units (PFU) x 1.5) was incubated at 37°C for 20 minutes with 1.2 mL of $O.D._{600}$ = 0.7 *E. coli* XL-1 Blue MRF' bacteria for infection. The suspension was then mixed into 120 mL of 37°C top agar and the suspension was plated equally onto 12 150 mm LB-agar plates. Following 8 hours of growth at 37°C, membrane replicas of the plates were made by

placing 150 mm nylon filters onto the top agar surface for 5 minutes to allow transfer of the phages. The filters were then denatured by placing on filter paper soaked in 0.5 M NaOH / 1.5 M NaCl for 2 minutes, renatured with 0.5 M Tris-HCl, pH 8.0 / 1.5 M NaCl for 2 minutes, rinsed in 6x SSPE (20x SSPE: 3 M NaCl, 0.2 M NaH_2PO_4, 20 mM EDTA, final pH = 7.4) and baked dry. The filters were sealed in a bag containing 100 mL of prehybridization solution (5x SSPE, 5x Denhardt's solution, 1% SDS, 100 mg/mL denatured salmon sperm DNA) and incubated at 50°C for 6 hours, after which time the radiolabelled oligonucleotide probe was added to the immersed filters. The filters were hybridized with the probe at 55°C for 12 hours and then at 37°C for 12 hours. Following the hybridization period, the filters were washed successively at room temperature with 2x SSPE, 1x SSPE, 0.5x SSPE and 0.2x SSPE and monitored with a hand-held Geiger counter. The filters were exposed to X-ray film overnight (X-Omat AR, Kodak) to reveal hybridization signals. For putative positive signals, a small circular agar window was recovered from the original plate corresponding to the area of the signal. The agar circle was resuspended in 500 µL of SM buffer containing 5 µL of chloroform, vortexed, and stored overnight at 4°C for elution of the phage into the aqueous medium. The following day, the eluted phages were plated on separate 50 mm LB-agar plates in two different densities. Briefly, 0.5 µL of the phage suspension was mixed with 100 µL of $O.D._{600} = 0.6$ *E. coli* XL-1 Blue MRF' and incubated at 37°C for 20 minutes. To the tube containing the infected bacteria, 3 mL of 37°C top agar were added and this suspension spread on one half of the 50 mm LB-agar plate, providing an area highly dense in phage plaques. To the same tube, 2 mL of 40°C top agar containing 30 µL of $O.D._{600} = 0.6$ *E. coli* XL-1 Blue MRF' bacteria were added, mixed, and plated onto the other half of the 50 mm LB-agar plate, providing a low density plaque area. The plates were incubated at 37°C for 8 hours and used to make nylon filter replicas for another round of hybridization screening using the same radioactive probe. The hybridization screening was repeated until a pure population of the positive phage was isolated.

B.2. Autoexcision Subcloning of the cDNA Inserts of Positive λZAPII Phage Clones

To recover the cDNA inserts of the positive Zap XR II phages, autoexecision was performed as described (Short *et al.*, 1988). Briefly, 80 μL of O.D.$_{600}$ = 0.7 *E. coli* XL-1 Blue MRF' bacteria were mixed with 3.6 x 10^5 plaque forming units (PFU) of pure phage stock and 2.5 x 10^6 PFU of EXassist helper phage and incubated at 37°C for 20 minutes. After addition of 0.8 mL of SOC medium (SOC, per litre: 20 g tryptone, 5 g yeast extract, 0.5 g NaCl, 3.6 g glucose), the suspension was mixed at 37°C for 6 hours, followed by heating to 70°C for 20 minutes. The tubes were centrifuged (12000g/4°C/10 min) to pellet the bacterial debris and 50 μL of the supernatant containing the phagemid were added to 100 μL of O.D.$_{600}$ = 0.6 *E. coli* JM109 bacteria. This mixture was incubated at 37°C for 20 minutes, streaked out onto LB-agar plates and incubated at 37°C overnight. Five colonies from each plate were checked for plasmid insert size by polymerase chain reaction (PCR) using 1 unit of *Taq* polymerase and excess deoxynucleotides (0.1 mM final concentration each of dATP, dCTP, dGTP and dTTP) in a 50 μL reaction volume containing 20 mM Tris-HCl, pH 8.3, 50 mM KCl and 2 mM $MgCl_2$. The PCR program was 35 cycles of 94°C - 1 min, 55°C - 1 min, 72°C - 3 min. To ensure that the autoexcised plasmids contained the N38 oligonucleotide probe positive insert, serial dilutions (10 ng, 1 ng, 0.1 ng) of each prepared plasmid, along with dilutions of a negative control pBluescript SK (pBL SK; Stratagene) vector, were spotted onto nylon membrane, denatured, renatured and baked as before. The plasmids were screened using the radiolabelled N38 primer, as described earlier, to ensure no artifacts were amplified during the autoexcision process.

C. PCR Cloning of Mouse Nebulin cDNA

To clone a representative nebulin cDNA closer to the 5' end of the transcript, a Genbank sequence (1272 bp) of nebulin cDNA from Balb/C strain mouse (Muller-Seitz *et al.*, 1993) was used to design two synthetic oligonucleotide primers to amplify nebulin

cDNA from 129 mouse cDNA. The upstream primer was designed to introduce a 5' NdeI restriction enzyme site to facilitate cloning of the insert as well as in-frame expression of the encoded protein into an expression vector. An in-frame translation stop codon (TAG) was designed into the downstream primer to stop translation. A mouse cDNA was cloned to take advantage of *in vivo* genetic manipulation methods that have been well developed for the murine host system. Using 10 pmol each of two synthetic oligonucleotide primers (Neb-F: 5'-TCTCCAGAGTAAACCAGATCCATATGAGTG-3' ; Neb-R: 5'-CGGCATACTATGCCTTATACTGATTATCAC-3') and 50 ng of available neonatal 129 mouse gastrocnemius muscle cDNA as template, PCR was done using a program of 30 cycles of 94 °C - 1 min., 51 °C - 1 min., 72 °C - 2 min. Following PCR, a 5 μL aliquot of the reaction was analyzed by 0.7% agarose gel electrophoresis at a potential difference of 5 mV/cm using TBE running buffer.

In order to clone the amplified PCR product into a vector, the PCR reaction containing the target DNA fragment was extracted with an equal volume of phenol:chloroform and precipitated by the addition of 0.5 volume 10 M ammonium acetate, pH 7.4, and 2.5 volumes of 100% ethanol. Following incubation at -70 °C for 20 minutes, the tube was centrifuged (12000g/20min/4 °C) and the precipitated DNA was resuspended to a concentration of 50 ng/μL using 10 mM Tris-HCl, pH 8, 1 mM EDTA (TE) buffer. A ligation reaction using 100 ng of the DNA fragment, 70 ng of SmaI digested pBL SK plasmid DNA and 1 unit of T4 DNA ligase was incubated at room temperature overnight. After overnight ligation, the mixture was incubated on ice for 40 minutes with 120 μL of competent *E. coli* JM109 cells, followed by incubation at 42 °C for two minutes. To allow an initial outgrowth of transformed bacteria, 400 μL of SOC medium were added and the mixture was further incubated for 40 minutes at 37 °C with shaking. For color selection of recombinant bacterial colonies through α-complementation (Messing *et al.*, 1977; Vieira and Messing, 1982), isopropyl-1-thio-β-D-galactopyranoside (IPTG) was added to 1 mM along with 1 mg of 5-bromo-4-chloro-3-indolyl-β-D-galactoside (X-Gal). The mixture was

mixed and plated out on LB-agar plates containing 100 μg/mL ampicillin and incubated overnight at 37 ° C.

To identify recombinant bacterial colonies harboring the DNA insert of interest, white colonies were identified on the plate and used directly for PCR by resuspending individual colonies in a PCR mix while simultaneously seeding the colony onto an LB-ampicillin plate. PCR was done using two conserved primers flanking the multiple cloning site of the pBL-SK plasmid. Following PCR (94 ° C - 40 s; 55 ° C - 40 s; 72 ° C - 1 min. for 25 cycles), aliquots from the individual tubes were analyzed by agarose gel electrophoresis to identify colonies harboring pBL-SK plasmids bearing inserts. A positive colony showing an amplified product in the expected size range (487 bp) was then used to inoculate a 20 mL overnight culture of LB broth containing 100 μg/mL ampicillin. The bacteria were harvested from the saturated culture and the recombinant plasmid was recovered using an ion-exchange based preparation method (QiaGen). The insert bearing plasmid was sequenced by the dideoxy chain termination method (Sanger *et al.*, 1977) using a T7 DNA polymerase-based sequencing kit (Pharmacia Inc.). The sequencing reactions were resolved by a 7 M urea / 6% polyacrylamide gel run at 65 W using 0.5x TBE running buffer. The sequencing gel was fixed in 7% acetic acid / 7% methanol, dried onto filter paper at 80 ° C using a Bio-Rad gel dryer, and exposed to x-ray film overnight. The sequences of the clones were compared to the available mouse nebulin cDNA sequence to ensure accurate cloning.

D. RT-PCR Cloning of Rat and Chicken Nebulin cDNA

To clone nebulin cDNA from other species, the Neb-F and Neb-R primers were used for reverse transcriptase coupled PCR (RT-PCR). Briefly, total RNA was isolated from the gastrocnemius muscle of a Sprague-Dawley rat and from the pectoralis major muscle of a Broiler chicken, using the TRIzol reagent (Gibco BRL) according to the manufacturer's protocol. Total RNA precipitated by isopropanol was resuspended in DEPC-

treated H_2O and analyzed by agarose gel electrophoresis for integrity and approximate concentration. Integrity of the RNA was determined by the presence and sharpness of the abundant 18S and 6S ribosomal RNA bands.

To perform the first strand cDNA synthesis, 20 pmol of Neb-R primer was used with 5 μg of total RNA as the template in a 50 μL reaction containing 1 mM deoxynucleotides, 50 mM Tris-HCl, pH 8.3, 75 mM KCl, 3 mM $MgCl_2$ and 10 mM dithiothreitol (DTT). After heating the mixture to 75°C to denature RNA secondary structure, 40 units of Moloney murine leukemia virus reverse transcriptase (Pharmacia Inc.) were added and the first strand cDNA synthesis was carried out overnight at 37°C. To amplify using the synthesized first strand cDNA, 10 μL of the RT-PCR reaction was used as template in a PCR cycle (94°C-1 min.; 49°C - 1 min.; 72°C - 2 min. for 30 cycles) using Neb-F and Neb-R primers to amplify nebulin cDNA. A lower annealing temperature was used in this PCR cycle to accommodate possible mismatches between the rat and chicken nebulin cDNAs and the mouse nebulin based Neb-F primer. Aliquots of the PCR were resolved by 0.7% agarose gel electrophoresis to visualize amplified bands, which were cloned into the EcoRV site of pBL-SK, as described before. The sequences of the rat and chicken cDNA insert were sequenced to confirm the accurate cloning of nebulin cDNA.

E. RT-PCR Cloning of Chicken Nebulette cDNA

To clone chicken nebulette cDNA, 5 μg of Leghorn chicken heart RNA was used as template in an RT-PCR reaction using 20 pmol each of two synthetic oligonucleotides (CCN-F, 5'-AGCACTCATATGAACATC-3'; CCN-R2, 5'-CCTTTGAATTCTCAAAATCTTAATGGTA-3') which encoded NdeI and EcoRI restriction endonuclease sites, respectively. RT-PCR was done as described earlier, with a PCR program of 35 cycles at 94°C - 1 min, 48°C - 1 min, 72°C - 3 min. An aliquot of the PCR reactions was analyzed by agarose gel electrophoresis to confirm a PCR product at the expected size of 535 bp. The amplified DNA was resolved by a 0.7% agarose gel run with

Tris-acetate-EDTA buffer (1X TAE: 0.04 M Tris-acetate, 1 mM EDTA). The DNA band of interest was excised from the agarose gel and recovered using the Prep-a-Gene silica based DNA recovery kit (Bio-Rad). The recovered DNA was digested with NdeI and EcoRI restriction endonucleases and ligated to similarly digested pAED4 expression vector DNA to create the CCN-C5 nebulette expression vector. The insert sequence and frame of translation was confirmed by dideoxy chain termination sequencing.

F. Construction of Prokaryotic Expression Vectors Encoding Nebulin

The pBL cloning vectors containing the cloned mouse nebulin MSN-N4 and chicken CSN-N4 cDNAs were digested with NdeI and EcoRI to yield the full length fragment. The digestion products were separated by electrophoresis in a 0.7% agarose gel run with TAE buffer and the DNA band of interest was recovered using the Prep-a-Gene DNA recovery kit. The recovered fragment was mixed with NdeI/EcoRI digested pAED4 expression vector DNA along with 1 unit of T4 DNA ligase. Following overnight incubation at 14°C, the ligation mixture was used to transform *E. coli* JM109 competent cells, which were then plated onto LB-agar-ampicillin plates and incubated at 37°C overnight. Colonies were picked from the plate and tested by PCR using conserved vector primers, as before, to confirm ligation of the nebulin cDNA insert. The ligated vector was sequenced, as described earlier, to confirm in-frame cloning of the nebulin cDNA constructs.

G. Construction of a Eukaryotic Vector for Transfection and Expression of Nebulin

The mouse nebulin sk9-3 3' cDNA was used as a template for *in vivo* expression of a nebulin COOH-terminal protein fragment in the mouse myoblast cell line C2C12 (ATCC # CRL 1772). Using a Green Fluorescent Protein (GFP; Chalfie, 1994) NH_2-terminal fusion vector (Clontech), the mouse nebulin sk9-3 cDNA insert was cloned downstream of the GFP cassette. The mouse nebulin cDNA clone sk9-3 covers 2.5 kb of the 3' end of the

nebulin transcript (Table 2.1), predicted to encode an ~80 kDa COOH-terminal fragment of the nebulin polypeptide. The cDNA clone sk9-3 was digested with SacI and XhoI, the insert recovered by the Prep-a-Gene matrix (Bio-Rad) and ligated to similarly digested GFP fusion vector using T4 DNA ligase as described previously. This ensured in frame translation of the cDNA insert corresponding to the reading frame of the GFP cassette. The endogenous stop codon of the mouse nebulin cDNA insert ensured proper termination of translation. For high level expression of the GFP-nebulin fusion protein, a 2.5 kb fragment of the slow troponin T promoter region (Jin *et al.*, 1997) was used. This promoter provides a differentiation dependent expression with a ~2 fold increased expression level versus the commonly used cytomegalovirus promoter (Jin *et al.*, 1997). Further, the pcDNA 3.1 vector encodes the bovine growth hormone poly A adenylation signals (Goodwin and Rottman, 1992) for proper processing of the mRNA. The fused GFP-nebulin cDNA was recovered from the GFP fusion vector by digestion with HinDIII, and ligated downstream of the 2.5 kb region of the slow troponin T promoter and upstream of the bovine growth hormone poly A adenylation signal in a recombinant, neomycin resistant pcDNA 3.1 vector (Jin *et al.*, 1997). Partial dideoxy chain termination sequencing and restriction endonuclease mapping confirmed the orientation and ligation of the promoter and cDNA sequences.

RESULTS

A. Mouse Nebulin cDNA Cloned from Neonatal Mouse Skeletal Muscle cDNA

The gene specific Neb-F and Neb-R primers were used to specifically amplify mouse nebulin cDNA from a size fractionated aliquot of 129 mouse neonatal cDNA. A specific PCR product was amplified from cDNA, consistent with the expected size of 477 bp according to the available mouse cDNA sequence (Fig. 2.1). This PCR product was cloned into the SmaI site of pBL SK and sequenced in full to ensure accurate cloning without mutations. The open reading frame of the cDNA theoretically encodes a 150 amino

acid protein with an Mr of 17268 and a pI of 9.195. The amino acid sequence of the encoded protein is shown in Fig. 2.2A.

B. Cloned Rat and Chicken Nebulin cDNAs

Using reverse transcription and low stringency PCR, nebulin cDNA were cloned from Sprague Dawley rat and Broiler chicken using the mouse nebulin cDNA specific Neb-F and Neb-R primers. The size of the RT-PCR amplified products were consistent with that amplified from 129 mouse cDNA (Fig. 2.1). After cloning the PCR products into the EcoRV site of pBL SK, the inserts were sequenced to verify that they were nebulin cDNA. The rat nebulin cDNA was found to be 477 bp, encoding a 150 amino acid protein with a theoretical Mr of 17118 and a pI of 9.288. By sequence comparison, the protein encoded by the rat cDNA was found to be 95% identical to that encoded by the mouse cDNA. The primary structure of the chicken nebulin cDNA was significantly divergent from the mouse and rat cDNAs. Interestingly, the chicken cDNA encoded a 149 amino acid protein, with an Mr of 17251, but a significantly different pI of 8.309. The mouse, rat and chicken protein sequences encoded by the cloned cDNAs are shown aligned with the human nebulin sequence according to their highest identity. (Figure 2.2). Although the mouse and rat protein sequences encoded match best with a continuous stretch of human nebulin, the chicken protein sequence does not show a best match with a continuous stretch of human nebulin but shows best identity with two stretches of the human nebulin sequence 500 residues apart.

Figure 2.1. PCR amplification and cloning strategy for the mouse, rat and chicken nebulin cDNAs.

To clone nebulin cDNAs from various species, a single set of primers was used in direct PCR reactions on double stranded cDNA or reverse transcriptase generated single strand cDNA templates. Following amplification of the double stranded cDNA by PCR, the fragments (as seen in the inset of the 0.9% agarose gel) were precipitated by ethanol and ligated to digested pBluescript SK cloning vector. The cloned inserts were sequenced in full by dideoxy chain termination sequencing to verify the cloned cDNA inserts.

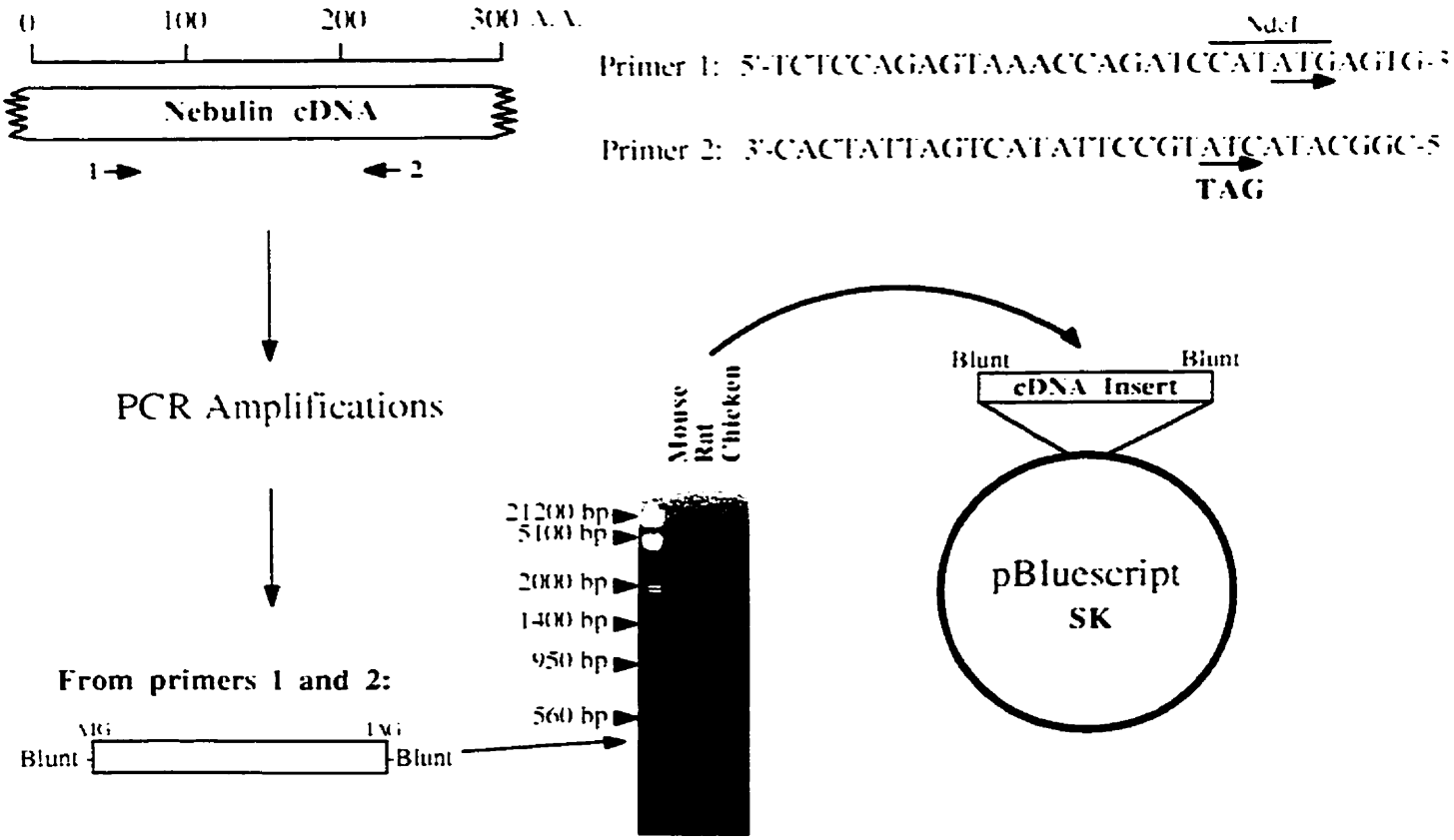
0
100
200
300 A.A.
Nebulin cDNA
1
2
NdeI
Primer 1: 5'-TCTCCAGAGTAAACCAGATCCATATGAGTG-3
Primer 2: 3'-CACTATTAGTCATATTCCGTATCATACGGC-5
TAG
PCR Amplifications
From primers 1 and 2:
Blunt
Blunt
Mouse
Rat
Chicken
21200 bp
5100 bp
2000 bp
1400 bp
950 bp
560 bp
Blunt
Blunt
cDNA Insert
pBluescript
SK

C. Mouse Nebulin cDNAs Cloned by Oligonucleotide Probe Screening of a Mouse Skeletal Muscle cDNA Library

A 129 mouse skeletal muscle cDNA library containing 315 000 original PFU was constructed in the Zap XR II phage. Skeletal muscle cDNA library screening using the N38 primer yielded 8 confirmed nebulin cDNA clones. Following autoexcision of the cDNA insert from the recombinant Zap XR II phage, partial sequencing of the 5' ends of the cDNA, combined with PCR sizing of the cDNA insert, provided the relationship of these nebulin cDNAs to the full length transcript. One cDNA clone, sk9-3, was confirmed to cover the 3' end of the nebulin transcript and contain the 3' untranslated region as well as the polyadenylation signal (Table 2.1; Fig. 2.3). This clone provides an excellent tool to further investigate the function and characteristics of the COOH-terminus of nebulin.

D. Cloned Chicken Nebulette cDNA

According to the published partial cDNA sequence of chicken nebulette, two oligonucleotide primers were synthesized for use in RT-PCR reactions to amplify chicken nebulette cDNA encoding a protein of theoretical Mr 19251. A 535 bp cDNA was amplified by RT-PCR, digested with NdeI / EcoRI restriction endonucleases and ligated to similarly digested pAED4 expression vector DNA. This expression construct was sequenced to confirm in-frame cloning of the nebulette cDNA to allow prokaryotic expression of the cloned message. The chicken nebulette cDNA is shown aligned near the 3' end of the human nebulin transcript (Fig. 2.3) where it shows greatest amino acid identity.

Figure 2.2. Amino acid comparisons of the cloned mouse MSN-N4, rat RSN-N4 and chicken CSN-N4 proteins with the human nebulin polypeptide.

Following dideoxy chain termination sequencing of the cloned mouse, rat and chicken nebulin cDNAs (Fig. 2.1), the theoretically encoded protein sequences were compared for homology to the complete human nebulin polypeptide (Labeit and Kolmerer, 1995a). A) The results indicate >90% identity at the amino acid level between the translated mouse and rat cDNAs with a continuous sequence of the human nebulin polypeptide. B) The chicken nebulin cDNA encoded a protein which showed highest identity with two discontinuous stretches of the human nebulin polypeptide, indicating a significantly different primary structure arrangement between chicken and human nebulins. Conserved residues are underlined, whereas non-conserved residues are in bold.

A

```
1                                                                   37
M S D K L Y K A G W E E E K T K G Y D L K P D A I A I K A A K A S R D I A      Mouse

M S D K L Y K A G W E E D K T K G Y D L K P D A I A I K A A K A S R D I A      Rat

M S D K L Y K A G W E E E K K K G Y D L R P D A I A I K A A R A S R D I A      Human
1779                                                                1815

  38                                                                   75
  S D Y K Y K Q A Y E Q S K G K H I G F R S L E D D P K L V H F M Q V A K I Q  Mouse

  S D Y K Y K K A Y E Q S K G K H I G F R S L E D D P K L V H F M Q V A K I Q  Rat

  S D Y K Y K K A Y E Q A K G K H I G F R S L E D D P K L V H F M Q V A K M Q  Human
  1816                                                              1853

  76                                                                  110
  S D R E Y K K G Y E K S K T S F H T P V D M F S V V A A K K S Q E V A        Mouse

  S D R E Y K K G Y D K S K T S F H T P V D M F S V V A A K K S Q E V A        Rat

  S D R E Y K K G Y E K S K T S F H T P V D M L S V V A A K K S Q E V A        Human
  1854                                                              1888

  111                                                                 147
  T N A N Y R N I I H T Y N M L P D A M S F E L A K N M M Q I Q S D N Q Y K  Mouse

  T N A N Y R N I I H T Y N M L P D A M S F E L A K N M M Q I Q S D N Q Y K  Rat

  T N A N Y R N V I H T Y N M L P D A M S F E L A K N M M Q I Q S D N Q Y K  Human
  1889                                                              1925
```

B

```
1                                                                   36
M S D K N Y K A D Y E E E K T K C Y F P Q T I T Q E Y E A I K K L E Q C      Chicken

N S D K S Y K A E Y E E D K G K C Y F P Q T I T Q E Y D A I K K L D Q C      Human
700                                                                 735

  37                                                                69
  K D H T Y K K H P D Q I K F T P V T D S P V Q K Q A E I N S K Q L          Chicken

  K D H T Y K V H P D K T K F T A V T D S P V L L Q A Q L N T K Q L          Human
  736                                                               768

  70                                                                  104
  S D K L Y R S S G E E V K H K Y T L P P D V P Q F I Q A R Y N A A N V      Chicken

  S D I L Y K A K G E D V K H K Y T M S P D L P Q F L Q A K C N A Y S I      Human
  1257                                                              1291

  105                                                                 140
  S D A Y Y K Q D Y H D L I A K G N N V S L D A I P I T R A K A S R N I A  Chicken

  S D V C Y K R D W H D L I R K G N N V L G D A I P I T A A K A S R N I A  Human
  1292                                                              1327

  141       146
  S D N Q Y K       Chicken

  S D Y K Y K       Human
  1328      1333
```

Clone Name	*cDNA Size*	*5' end of the cDNA*
sk1-1	2.0 kb	bp 18865
sk5-1	2.5 kb	bp 18323
sk8-1	2.8 kb	bp 18056
sk9-1	1.8 kb	bp 17946
sk9-3	2.5 kb	bp 18225
sk11-5	2.0 kb	bp 18810
sk12-2	2.1 kb	bp 17696
sk12-6	2.1 kb	bp 18613

Table 2.1. Isolated 129 mouse nebulin 3' cDNA.

By oligonucleotide screening of a 129 mouse neonatal skeletal muscle cDNA library, eight nebulin cDNAs were isolated. The cDNA sizes ranged from 1.8 to 2.8 kb, as determined by agarose gel electrophoresis of PCR amplified inserts. The location of the 5' end of the cDNA with respect to the complete human nebulin sequence (Labeit and Kolmerer, 1995a) is indicated.

Figure 2.3. Schematic representation of the cloned nebulin and nebulette cDNAs with respect to the human nebulin mRNA map.

The nebulin and nebulette cDNAs cloned in this study are depicted with their relation to the complete human nebulin transcript which encodes multiples of the ~35 amino acid motif (The regions encoding the unique NH_2- and COOH-termini of nebulin are shaded; Labeit and Kolmerer, 1995a). The MSN-N4 mouse nebulin and RSN-N4 rat nebulin cDNA encode a four unit polypeptide showing high identity with a segment near the NH_2-terminus of human nebulin. The chicken nebulin CSN-N4 cDNA shows best identity with nebulin sequences upstream of the MSN-N4 region. The chicken nebulette cDNA (CCN-C5) encodes a five unit protein with best identity to a stretch near the COOH-terminus of human nebulin. Large, overlapping mouse nebulin cDNA clones covering the 3' region of the transcript were also isolated.

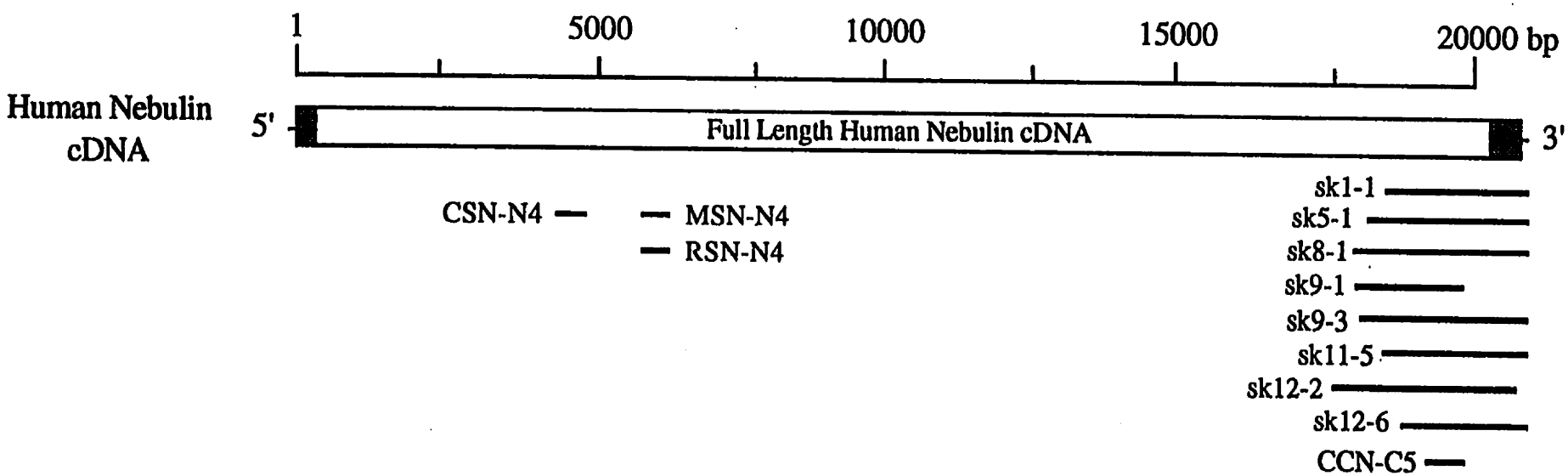
1
5000
10000
15000
20000 bp
Human Nebulin cDNA
5'
Full Length Human Nebulin cDNA
3'
CSN-N4
MSN-N4
RSN-N4
sk1-1
sk5-1
sk8-1
sk9-1
sk9-3
sk11-5
sk12-2
sk12-6
CCN-C5

E. A Green Fluorescent Protein - Nebulin Fusion Protein for Eukaryotic Expression and *In Vivo* Characterization.

The nebulin cDNA sk9-3 was used as template for eukaryotic expression of the nebulin COOH-terminus. The nebulin cDNA was fused to a 5' template encoding the GFP protein to facilitate detection of the expressed fusion protein (Fig. 2.4). Using the pcDNA 3.1 eukaryotic expression vector backbone and a 2.5 kb mouse slow troponin T promoter sequence, a eukaryotic expression construct was made. The advantages of the slow troponin T promoter over the cytomegalovirus promoter are twofold: i) the slow troponin T promoter provides a higher expression level in the C2C12 mouse myoblast cell line as compared to the cytomegalovirus promoter (Jin *et al.*, 1997), and ii) unlike the exogenous viral promoter, regulation of the slow troponin T promoter is differentiation dependent, providing a means of controlling expression in the transfected cells.

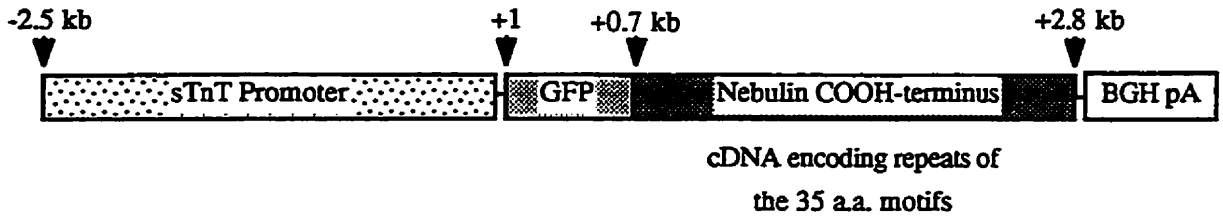

Figure 2.4. A eukaryotic expression vector encoding a nebulin COOH-terminal fragment linked to Green Fluorescent Protein.

Using the nebulin COOH-terminal encoding sk9-3 cDNA and a coding template for Green Fluorescent Protein (GFP), a eukaryotic expression vector was constructed for *in vivo* expression of the nebulin protein in mouse skeletal muscle myoblasts. A 2.5 kb fragment of the slow skeletal muscle troponin T promoter was used to drive expression of the GFP-nebulin fusion protein. A downstream bovine growth hormone polyadenylation signal (BGH pA) ensures proper processing of the mRNA transcript.

DISCUSSION

To provide genetic coding templates, cDNA encoding nebulin and nebulette was cloned. PCR, RT-PCR and radioactive oligonucleotide probe screening of a recombinant cDNA library all provided successful results in cloning the desired nebulin and nebulette sequences to be used for further characterization.

A. Conservation of Nebulin Primary Structure Among Species

Polymerase chain reaction using a single set of oligonucleotide primers (Neb-F and Neb-R) was successful in isolating nebulin cDNA from mouse, rat and chicken, attesting to the conservation of the nebulin primary structure. Sequencing of mouse nebulin cDNA demonstrated high identity between the mouse and human nebulin mRNA transcripts and an even higher identity at the amino acid level (Fig. 2.2). The high conservation noted between nebulin cDNA from various species indicates that nebulin or nebulin-like motifs, like those found in nebulette, are analogous structures with a well conserved function.

B. A Divergent Chicken Nebulin Sequence

Interestingly, the chicken nebulin cDNA isolated had a significantly different primary structure as compared to the mouse and rat nebulin cDNAs isolated with the same set of primers. Sequence comparison showed that the chicken nebulin cDNA showed highest identity with two stretches of human nebulin which were ~500 residues apart. This is an interesting observation regarding the genomic organization as well as the primary structure organization of nebulin. Since the continuous chicken nebulin sequence best matched a discontinuous sequence of human nebulin, this indicates that the position of the repeating nebulin motifs along the thin filament is not fixed, i.e. a certain motif is not specific for a certain region of the thin filament. Instead, their positions are likely to be a result of nebulin's arrangement on the thin filament as a result of initial interactions between the unique NH_2- and/or COOH-terminal regions with specified locations at either the pointed end of the thin filaments, or the Z line, respectively.

CHAPTER THREE:
CLONING OF MOUSE NEBULIN GENOMIC DNA

INTRODUCTION

The primary structure of all eukaryotic proteins is encoded by exons within the gene. In many cases, the exon organization of the gene reflects the function units or domains of the protein encoded. In this fashion, the organization of exons within a gene can provide invaluable information regarding avenues to pursue in characterizing a protein's function. In the case of the large nebulin polypeptide, characterization of the complete protein is not feasible due to difficulties in purifying native nebulin from muscle. For this reason, an understanding of the exon organization will provide a basis to dissect the protein in an attempt to study the structure / function of nebulin units and attempt to extrapolate these results to the entire polypeptide.

Cloning of nebulin genomic DNA also provides a necessary tool for future *in vivo* genetic manipulation, wherein gene targeting technology may be used to create nebulin deficient backgrounds and allow the characterization of the protein through transgenic mice expressing various nebulin fragments of interest. Standard molecular biological methods and specific mouse nebulin cDNA will be used to isolate and clone mouse nebulin genomic DNA. To date, no information is published regarding the genomic organization of the nebulin gene.

MATERIALS AND METHODS

A. Northern Blot of Muscle RNA

To assess the size and expression pattern of the mouse nebulin mRNA transcript, Northern blotting was done. To prepare the Northern blot membrane, total RNA from 129

mouse skeletal and cardiac muscle was prepared using the TRIzol reagent, as described earlier. To 10 μg (in 10 μL) of total RNA, 2 volumes of formamide were added as well as MOPS buffer to 1x (10x MOPS: 0.4 M MOPS, pH 7.0, 0.1 M NaOAc, pH 4.0, 10 mM EDTA) and formaldehyde to 2 M. The mixture was denatured by heating to 80 °C for 15 minutes and then chilled on ice. The total RNA was separated at 3 mV/cm by a 15 cm x 15 cm 1% agarose gel containing 2 M formaldehyde, using 1x MOPS buffer as the running buffer. After separation of the RNA, a replica of the gel was made by transferring the RNA onto nylon membrane by capillary action, according to the protocol described (Ausubel *et al.*, 1995). Briefly, a bridge and a filter paper wick were placed on a dish containing 0.025 N NaOH. The gel was then placed face down on the paper wick, and the nylon membrane, cut to the size of the gel, was placed overtop, followed by three pieces of Whatman filter paper and a 10 cm high stack of paper towels. A glass plate and weights were placed on top of the paper towels to ensure even weight for capillary transfer, which was allowed to proceed overnight. Following overnight transfer, the membrane was rinsed in 6x SSPE and the RNA baked onto the membrane by incubating at 80 °C until dry. In all steps, DEPC-treated water was used to inhibit RNase activity.

B. Southern Blot Analysis of Nebulin

To identify the nebulin gene copy number, Southern blotting using the isolated 129 mouse nebulin cDNA was performed. High molecular weight genomic DNA was prepared from 129 mouse spleen according to the method outlined (Ausubel *et al.*, 1995). Briefly, 100 mg of frozen spleen was minced in 2 mL of SDS Lysis buffer (0.1 M NaCl, 10 mM Tris-HCl, pH 8, 25 mM EDTA, 0.5% SDS, 0.1 mg/mL Proteinase K) and incubated overnight at 50 °C with shaking. The solution was centrifuged (2000rpm/10min/4 °C) in a clinical centrifuge and the supernatant recovered with a wide mouth pipet. This solution was extracted twice with an equal volume of phenol:chloroform and chloroform. To the aqueous phase from the last extraction, 0.5 volume of 10 M ammonium acetate, pH 7.4, and 2.5 volumes of cold 100% ethanol was added to precipitate the high molecular weight

genomic DNA. The stringy precipitate was recovered around a 9" pipet, transferred to a 15 mL tube and washed with 2 mL of 70% ethanol. The precipitated genomic DNA was resuspended in TE buffer to a final concentration of 1 μg/μL. The isolated high molecular weight genomic DNA was digested in separate 40 μg aliquots by 5 restriction endonucleases: BamHI, EcoRI, HinDIII, PstI and XbaI. The digestion reactions were analyzed by agarose gel electrophoresis to verify complete digestion of the high molecular weight DNA. The digested genomic DNA was separated by a 15 cm x 15 cm 1% agarose gel by overnight electrophoresis using a low potential difference (1 mV/cm). Digested DNA was transferred to nylon membrane as per the protocol described for Northern blotting, save for two modifications. The DNA separated by agarose gel electrophoresis was depurinated by shaking the agarose gel in 0.25 N HCl for 10 minutes and rinsed three times in double distilled H_2O prior to transfer. In addition, due to the higher resistance of DNA to NaOH, 0.4 N NaOH was used for efficient transfer.

C. Probe Preparation and Hybridization of Northern and Southern Blot Membranes

For both Southern and Northern blotting, high activity radioactive probes are necessary for clear results. The nebulin DNA fragment (100 ng) was denatured by boiling for 5 minutes in a mixture containing 1 μg of random hexamers, 10 mM Tris-HCl, pH 7.5, 3 mM $MgCl_2$ and a dATP / dGTP / dTTP mixture (0.2 mM concentration of each). The tube was incubated on ice for 2 minutes and 50 μCi of α^{32}P-labelled dCTP and 10 units of the Klenow fragment of DNA polymerase I were added, providing a final 50 μL reaction volume. The reaction was allowed to proceed at room temperature for three hours. The labelled DNA was separated from unincorporated α^{32}P-labelled dCTP by gel filtration using a Bio-Gel P30 column (0.4 cm x 2 cm; Bio-Rad). Only probes labelled to a specific activity of greater than 5 x 10^8 dpm/μg were used, as determined by scintillation counting. The dried Northern and Southern membranes were prehybridized at 55°C for 6 hours in a sodium phosphate hybridization buffer (0.2 M Na_2HPO_4, 14 mM H_3PO_4, 0.8 mM EDTA, 1% BSA, 5% SDS, 0.1 mg/mL salmon sperm DNA, 30% formamide) followed by the

addition of the denatured, radiolabelled DNA probe. Dextran sulfate was added to 5% into the hybridization mixture to decrease the aqueous phase and increase hybridization efficiency. Hybridization was carried out at 55°C for 16 hours. The Northern blot membranes were washed with 0.1x SSPE at room temperature and exposed to x-ray film at -70°C. Southern blot membranes were stringently washed to 0.1x SSPE at 55°C before exposure to x-ray film at -70°C.

D. Isolation of a λDashII Phage Containing 129 Mouse Nebulin Genomic DNA

To isolate nebulin genomic DNA, a 129 mouse genomic DNA library was screened by radioactive probe hybridization. The MSN-N4 mouse nebulin cDNA was cut from the pBL-SK plasmid by BamHI and EcoRI restriction enzyme digestion and separated by agarose gel electrophoresis. The DNA fragment of interest was cut from the agarose gel and purified using the Prep-a-Gene DNA binding matrix (Bio-Rad). The purified DNA fragment was randomly labelled with ^{32}P-labelled dCTP for use as a radioactive probe in screening nylon filter replicas of a genomic library.

A 129 mouse genomic DNA library constructed in the λ Dash II phage was used to screen for a mouse nebulin genomic DNA fragment. Based on the average insert size of the library (12 - 15 kbp), an aliquot of phage harboring inserts which total 1.5x the mouse genome (3 x 10^9 bp) was plated out on 12 150 mm LB-agar plates. Briefly, an aliquot of phage equivalent to 2.5 x 10^5 plaque forming units was incubated with 1.44 mL of O.D.$_{600}$ = 1.0 *E. coli* MRA(P2) at 37°C for 15 minutes. The infected bacteria were then resuspended in 120 mL of 37°C LB-agar (LB-agar, per litre: 10 g tryptone, 5 g yeast extract, 10 g NaCl, 15 g agar). The top agar was spread evenly among the twelve plates, allowed to set and incubated at 37°C for 8 hours. Once the individual phage plaques were visible, filter replicas were made from the plates as described before. The filters were sealed in a bag containing 100 mL of prehybridization solution (30% (v/v) formamide, 5x SSPE, 5x Denhardt's solution, 100 μg/mL denatured salmon sperm DNA) and incubated at 50°C

for 6 hours, after which time the radiolabelled probe, once denatured by boiling, was added to the immersed filters and incubated at 50°C for 16 hours. Following the hybridization period, the filters were washed successively at room temperature with 1x SSPE, 0.5x SSPE, 0.1x SSPE, followed by washing with 0.1x SSPE at 50°C. The filters were exposed to film overnight to reveal hybridization signals. For putative positive signals, a small circular agar window was recovered from the original plate corresponding to the area of the signal. Hybridization screening was repeated until a pure population of the positive phage was isolated.

The isolated phage was prepared in large amounts to recover the mouse genomic DNA insert. Six 150 mm plates were plated out using a phage:bacteria ratio of 1:200 and incubated overnight until complete lysis of the bacterial lawn by the positive phage. The top agar layer was recovered, 10 mL of SM buffer was added and the mixture vortexed to break up the agar and completely elute the phage into the SM buffer medium. The mixture was centrifuged (10000rpm/10min/4°C/JA14 rotor) and the aqueous layer containing the phage was recovered. The phage solution was layered onto a CsCl step gradient (1.3 g/mL (5 mL), 1.5 g/mL (5 mL), 1.7 g/mL (8 mL)) and centrifuged for 2.5 hours at 26000 rpm using a Beckman SW28 rotor. Following centrifugation, the phage DNA, now layered at the 1.5 g/mL / 1.7 g/mL CsCl interface, was recovered using a 9" glass pipet. The recovered phage DNA was condensed into a smaller volume by centrifugation at 46000 rpm for 20 hours at 4°C in a Ti50 rotor by overlaying 1.5 g/mL CsCl on top of the collected phage DNA solution. Following centrifugation, the phage DNA band was collected and dialyzed against 500 volumes of TE buffer with three changes. The phage DNA solution was then extracted twice each with equal volumes of phenol:chloroform and chloroform. To the extracted phage solution, 0.5 volume of 10 M ammonium acetate, pH 7.4, and 2.5 volumes of cold 100% ethanol was added to precipitate the phage DNA. The precipitated DNA was recovered as described earlier.

E. Subcloning and Partial Sequencing of Nebulin Genomic DNA

The isolated phage DNA was digested with EcoRI and BamHI restriction endonucleases to subclone the mouse genomic DNA into smaller overlapping DNA fragments. Following digestion, an aliquot of the digestion reaction was analyzed by agarose gel electrophoresis to visualize the restriction enzyme generated DNA fragment sizes. The digested phage DNA was ligated to a similarly digested pBL-SK vector which had been dephosphorylated by calf intestinal alkaline phosphatase (1 unit / 10 pmol of phosphorylated DNA ends for 1 hour at 37 °C) to minimize non-recombinant self ligation of the vector. The ligation reaction catalyzed by 1 unit of T4 DNA ligase was left overnight at 14 °C and used to transform *E. coli* JM109 competent cells, as previously described.

Recombinant *E. coli* colonies from the initial plating out were seeded and expanded on LB-agar plates to allow overnight growth. The bacterial smear was resuspended in 20 μL of water and extracted with an equal volume of phenol:chloroform. The total DNA extracted into the aqueous layer was resolved by agarose gel electrophoresis to visualize the supercoil size of the recombinant vector. Recombinant vectors in the size range expected were chosen for small scale preparation. The prepared vectors were partially sequenced, followed by a homology search using the NCBI DNA database to ensure that the inserts cloned were not restriction enzyme digests of the *E.coli* genome. Recombinant vectors containing sequences which show homology to nebulin or mouse intron sequences were further sequenced by preparing restriction endonuclease deletion clones or serial nested deletion sets using an Exonuclease III-based nested deletion kit (Promega).

RESULTS

A. Northern Analysis using Nebulin cDNA Indicates a Skeletal Muscle Specific Transcript

The mouse nebulin MSN-N4 cDNA was used as a probe in Northern blotting to verify the transcript size of the mouse nebulin mRNA as well as to further characterize the cloned mouse nebulin MSN-N4 cDNA. Northern blotting using total RNA extracted from 129 mouse skeletal and cardiac muscles indicated a positive transcript in skeletal muscle RNA (Fig. 3.1) migrating in the limiting mobility region of the agarose gel, consistent with the large size of the nebulin mRNA transcript (Labeit and Kolmerer, 1995a). No probe positive transcript was identified in total RNA extracted from cardiac muscle.

B. Southern Blot Analysis of the Nebulin Gene Shows a Single Copy in the Mouse Genome

The mouse nebulin MSN-N4 cDNA probe was used in Southern blots of mouse genomic DNA to verify the nebulin gene copy number. The copy number of a gene is important to ensure accurate cloning of the gene, as duplicate copies or partial duplications of the nebulin gene in the genome may be revealed by Southern blotting. The nebulin cDNA probe identified single bands in all five restriction enzyme digested genomic DNA sets: BamHI, 4.1 kb; EcoRI, 8 kb; HinDIII, 6 kb; PstI, 8 kb; and XbaI, 1.7 kb. This pattern is consistent with the mouse nebulin gene being a single copy gene (Fig. 3.2).

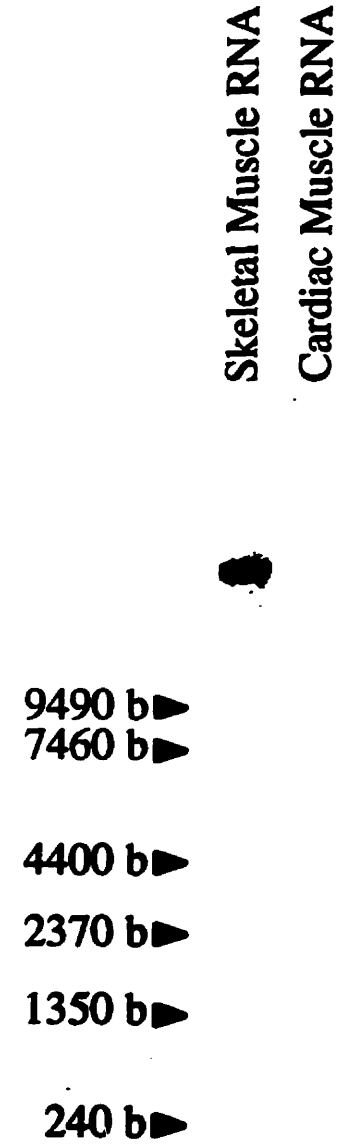

Figure 3.1. The large nebulin mRNA transcript is specific to skeletal muscle.
Northern analysis of 129 mouse skeletal and cardiac muscle total RNA using the 129 mouse MSN-N4 nebulin cDNA probe identified a single RNA transcript significantly greater than 9000 bases and present in the limiting mobility region of the agarose gel. The size of the mRNA species is consistent with the large size of the corresponding nebulin polypeptide. The Northern analysis did not identify a transcript in total RNA from 129 mouse cardiac muscle total RNA, indicating that the mouse nebulin and nebulette transcripts do not share significant identity in this region.

C. Isolation of Nebulin Genomic DNA Indicates a Conserved Exon / Intron Boundary

A λ Dash II phage N6-1 containing a mouse nebulin genomic DNA fragment was isolated. The phage DNA was digested by restriction endonucleases to give the following fragments: BamHI, 6 kb, 3 kb, 0.8 kb; EcoRI, 5.3 kb, 5.1 kb, 3.4 kb, 1.6 kb. The EcoRI fragments of 5.3 kb (E5.3), 5.1 kb (E5.1) and 3.4 kb (E3.4) were subcloned into pBL SK. Restriction enzyme fragments from the subclones E5.3 and E5.1 were sequenced to identify nebulin exons. Subclone E3.4 was sequenced in full by generating Exonuclease III nested deletions to facilitate sequencing of the large fragment. DNA sequencing revealed the structure of representative nebulin exons and their intron/exon junctions (Fig. 3.3). The intron/exon junctions were conserved and occurred in the conserved SxxxY pentapeptide, precisely two amino acids before the tyrosine residue (Sx / xxY). This splicing junction was also conserved in exons identified from partial DNA sequencing of the restriction endonuclease subclones of E5.3 and E5.1 (data not shown). Of the nebulin exons identified, all were found to encode either 1 or 2 full motifs (Fig. 3.3).

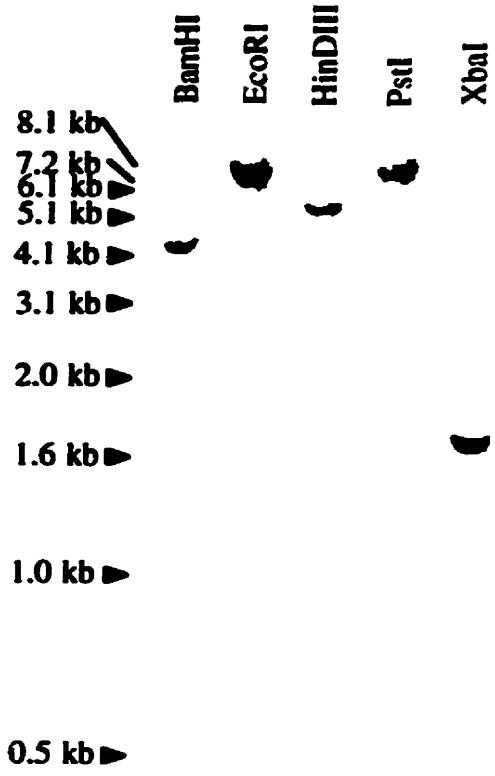

Figure 3.2. A single copy of the nebulin gene in the mouse genome.

The 129 mouse nebulin MSN-N4 cDNA identified single bands in restriction endonuclease digested 129 mouse genomic DNA: BamHI (4.1 kb), EcoRI (8 kb), HinDIII (6 kb), PstI (8 kb) and XbaI (1.7 kb). The restriction fragment lengths are consistent with the nebulin transcript being the product of a single gene.

Figure 3.3. Exon map of a nebulin genomic DNA fragment and comparison of nebulin exons with the proposed nebulin motifs.

From the isolated λN6-1 phage, a 3.2 kb nebulin genomic DNA fragment E3.4 was subcloned and sequenced in full to identify nebulin exons. Two exons were identified, with exon A encoding 72 amino acids and exon B encoding 35 amino acids. The amino acid sequences of the two exons are shown continuously, with the filled arrowheads indicating the exon/intron junctions. Exon B encodes a 35 amino acid exon encoding a single motif, and is proposed to encode the minimum functional unit of nebulin. The white arrowheads point to dissection points of the nebulin motifs based on previous assumptions of nebulin's functional unit (Jin and Wang, 1991a,b). The results show that nebulin exons encode multiples of a ~35 amino acid motif which is shifted when compared to the previously proposed nebulin functional unit.

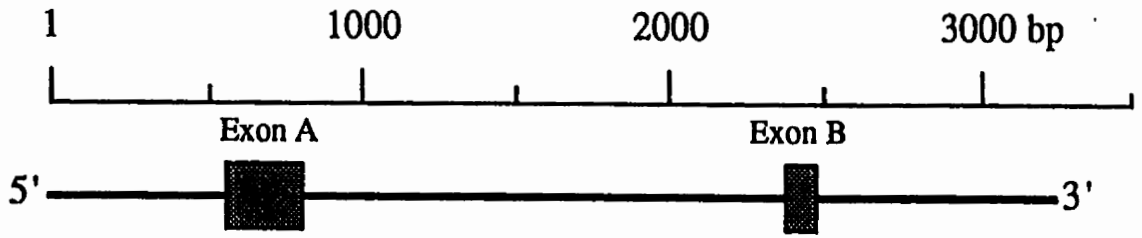
1
1000
2000
3000 bp
Exon A
Exon B
5'
3'


Proposed Single Motif
Exon A (2 Motifs)
Exon B (1 Motif)
NVYKDEYNSFFKGIGWIPIGSLEVEKAKKAGEALNERKYRQHPDTIKFTSVPDSMGMVLAQQNTKQLSDLNYKVEGEKMKHKYTMDPELPQFIQAKVNAINMSD
Previous Single Motif

DISCUSSION

In this chapter, mouse nebulin genomic DNA was cloned to investigate the exon organization of the gene, the copy number of the gene, and also to provide genetic materials for future *in vivo* genetic manipulations of the mouse nebulin gene.

A. The Single Copy Nebulin Gene Generates a Single mRNA Transcript

Northern analysis of total RNA extracted from skeletal and cardiac muscles of 129 mouse indicated a nebulin MSN-N4 cDNA specific transcript to be present only in skeletal muscles. This, combined with Northern analysis of cardiac muscle total RNA with nebulin cDNA probes covering the 5' and 3' untranslated regions of the human nebulin transcript (Labeit and Kolmerer, 1995a) indicates that the nebulin gene encodes a single mRNA species, specific to skeletal muscle. Further analysis of the nebulin gene by genomic DNA Southern blotting demonstrated that nebulin is a single copy gene in the mouse genome.

B. The Exon / Intron Junctions of Nebulin Exons are Conserved

A ~15 kb mouse nebulin genomic DNA fragment was isolated by screening a 129 mouse genomic library with the radiolabelled MSN-N4 mouse cDNA. Partial sequencing of restriction endonuclease subclones, as well as full sequencing of a limited segment of this genomic DNA, identified mouse nebulin exons encoding a segment of the repeating region of the nebulin mRNA transcript. All exons identified had a conserved splicing site two amino acids prior to the tyrosine residues in the conserved SxxxY pentapeptide motif (Fig. 3.3). The high conservation of this splicing site likely indicates that the conserved pentapeptide marks the beginning of the nebulin functional unit. Further, the identification of an exon encoding a single ~35 amino acid motif is a likely indication that this is the minimum required peptide for nebulin's function. This is an important factor for a protein

like nebulin, which is comprised almost exclusively of the repeating ~35 amino acid motifs, and provides a logical dissection point for the polypeptide.

CHAPTER FOUR:
EXPRESSION AND PURIFICATION OF NEBULIN AND NEBULETTE FRAGMENTS

INTRODUCTION

Recombinant DNA technology allows the use of cDNA in expressing cloned proteins in prokaryotic or eukaryotic hosts. Because of the large size, insolubility and difficulty in purifying native, intact nebulin, studies characterizing the protein must work through protein fragments. The use of cDNA engineering allows the researcher to set and design the protein for expression, allowing direct testing of experimental models and hypotheses.

Previous work in expressing cloned nebulin fragments has documented their tendency to be insoluble when expressed, being found in the inclusion bodies of the bacterial lysate (Jin and Wang, 1991a,b). Although relatively easy to purify, the insolubility of the proteins creates difficulties in further characterization. It is especially difficult to obtain high resolution structure determination by techniques such as x-ray crystallography and nuclear magnetic resonance spectroscopy, which primarily require protein solutions of ~1 mM concentration. No data are yet available regarding the expression of cloned nebulette proteins.

The cDNA encoding mouse nebulin MSN-N4 as well as the chicken nebulin CSN-N4 and nebulette CCN-C5 will be used to advantage in expressing cloned protein in the *E.coli* prokaryotic host. Effective purification of the cloned proteins will provide sufficient material for *in vitro* characterization assays, as well as for use in generating an antiserum against the nebulette protein.

MATERIALS AND METHODS

A. Expression and Purification Protocol for Cloned Mouse Nebulin MSN-N4

The full length MSN-N4 cDNA was ligated in-frame into the T7 RNA polymerase-based pAED4 vector for expression in BL21(DE3)pLysS *E. coli* (Studier *et al.*, 1990). The mouse MSN-N4 cDNA encodes a four motif nebulin polypeptide. To ensure correct expression of the nebulin protein, a small trial induction was done using the constructs prior to a large scale protein purification. A 2 mL aliquot of NZ medium (NZ media: per litre, 10 g casein hydrolysate, 5 g NaCl) containing 100 μg/mL ampicillin and 25 μg/mL was inoculated with BL21(DE3)pLysS *E. coli* transformed with the expression construct. The culture was incubated with shaking at 37°C until $O.D._{600}$ = 0.4, half the culture was induced by the addition of 0.3 mM IPTG, and allowed to grow an additional 3 hours. After induction, the cells were pelleted and lysed in 3x SDS gel sample buffer (3x Buffer: 150 mM Tris-HCl, pH 6.8, 6% SDS, 0.3% bromophenol blue, 30% glycerol, 15 mM β-mercaptoethanol) and resolved by sodium dodecyl sulfate polyacrylamide gel electrophoresis (SDS-PAGE) (Laemmli, 1970) by a 12% gel with an acrylamide to bisacrylamide ratio of 29:1 and a stacking gel of 4%. Induced and uninduced samples were resolved by SDS-PAGE and compared to determine if a protein in the expected size range was overexpressed.

The expression plasmid construct MSN-N4 encodes a 4 unit nebulin protein toward to the NH_2-terminus of the full length polypeptide. Following confirmation of the sequence and trial expression of the protein, the expression plasmid was freshly transformed into chloramphenicol resistant *E. coli* BL21 pLyS cells, and 4 individual colonies were used to inoculate 4 L of NZ medium containing 100 μg/mL ampicillin and 25 μg/mL. After overnight incubation at 37°C with shaking, the culture was induced with 0.3 mM IPTG at $O.D._{600}$ = 0.65 and grown for a further 3 hours. The bacteria were harvested by centrifugation (9000rpm/15 min/JA10/4°C) and lysed by three passes through a French

press cell at >700 p.s.i. The cell lysate was centrifuged (10000rpm/15 min/JA14/4 °C) and the supernatant separated from the inclusion body pellet. The inclusion body pellet was solubilized by stirring in 80 mL of 6 M urea, 20 mM imidazole, pH 7, 1 mM EDTA at 4 °C for 30 minutes. This fraction was loaded onto a 10 cm x 2.5 cm CM52 column equilibrated in the same buffer. Elution from the column was by a linear gradient of 0 - 400 mM KCl in the equilibration buffer. The A_{280nm} peaks of the eluate were analyzed by 12% SDS-PAGE, and those containing the protein of interest were collected, dialyzed to equilibrium against 4 L of 0.1% formic acid for three changes and lyophilized.

B. Immunological Reactivity of the Purified MSN-N4 Mouse Nebulin Protein Fragment

The nebulin nature of the purified mouse nebulin protein was verified by enzyme linked immunosorbant assay (ELISA) using an antibody specific to nebulin. The mouse nebulin MSN-N4, chicken nebulin CSN-N4 and chicken nebulette CCN-C5 proteins were diluted to 5 μg/mL in ELISA coating buffer (40 mM Na_2CO_3, 60 mM $NaHCO_3$, pH 9.8) and 100 μL of this solution were aliquoted into triplicate wells of a 96 well ELISA plate and allowed to coat overnight at 4 °C. The wells were washed once with PBS containing 0.05% Tween-20 (PBS-T) and blocked by incubation at room temperature for two hours with 150 μL of PBS plus 1% BSA and 0.05% Tween-20 (PBS-B). The wells were then washed twice with PBS-T and incubated at 37 °C for two hours with 100 μL/well of serial dilutions of the nebulin specific monoclonal antibody Ne105 (unpublished results) made in phosphate buffered saline (PBS; 137 mM NaCl, 2.7 mM KH_2PO_4, 8.0 mM Na_2HPO_4, pH 7.4) plus 0.1% BSA and 0.05% Tween-20 (PBS-P). Following primary antibody incubation, the plates were washed three times with PBS-T and incubated at 37 °C for 50 minutes with 100 μL of a 1/1500 dilution of horseradish peroxidase conjugated goat anti-mouse IgG second antibody (Sigma). Following washing with PBS-T, 100 μL per well of 0.04 % (w/v) H_2O_2 - 2,2'-azinobis-(3-ethylbenzthiazolinesulfonic acid) (ABTS) substrate in 0.1 M citrate buffer, pH 4.0, were added to develop the horseradish peroxidase mediated

color reaction monitored by recording A_{405nm} using a Benchplate Microplate reader (Bio-Rad). Microtitre wells coated with 5 μg/mL BSA were used to verify the specificity of the monoclonal antibody and provide a negative control. Student's T test was used to determine the statistical significance of the curves versus the negative control BSA curve.

C. Purification of the Cloned Chicken Nebulin CSN-N4 and Chicken Nebulette CCN-C5 Proteins

Using either the pAED4-CCN-C5 chicken nebulette expression construct or the chicken nebulin pAED4-CSN-N4 expression construct, *E. coli* BL21 pLysS cells were transformed and allowed to grow until the colonies were just visible. Four fresh colonies were chosen to inoculate 4 L of NZ broth containing 100 μg/mL ampicillin and 25 μg/mL chloramphenicol. The cultures were incubated overnight at 37°C with shaking until $O.D._{600} = 0.8$, at which time protein expression was induced by the addition of IPTG to 0.4 mM. Following three hours of growth, the bacteria were harvested and lysed by three passes through a French press at >700 p.s.i. Successive ammonium sulfate cuts from 0 - 30% saturation and from 30-50% saturation were taken from the bacterial lysate. The 30%-50% ammonium sulfate precipitation pellet was resuspended in 30 mL of 20 mM imidazole, pH 7, 1 mM EDTA, 15 mM β-mercaptoethanol and dialyzed against 4 L of 20 mM imidazole, pH 7, 1 mM EDTA, 15 mM β-mercaptoethanol with two changes at 4 hour intervals. To the dialyzed fraction, urea powder was added to 6 M, the pH was adjusted to 7 and the solution was clarified by centrifugation (12000rpm/15min/4°C/JA14). The supernatant was loaded onto a 100 mL (2.5 cm x 20 cm) CM52 column equilibrated with 6 M urea, 20 mM imidazole, pH 7, 1 mM EDTA, 15 mM β-mercaptoethanol. A KCl gradient of 0 - 400 mM in the equilibration buffer was used to elute the nebulin or nebulette protein from the column. Fractions containing the protein of interest, as analyzed by 12% SDS-PAGE, were collected, dialyzed against 4 L of 0.1% formic acid (three changes) and lyophilized. Pure chicken nebulette or nebulin was obtained from the cation exchange column.

D. Purification of Thin Filament Proteins

D.1. Purification of F-actin

For use in *in vitro* binding assays, fresh F-actin was prepared from rabbit psoas muscle acetone powder. Two grams of acetone powder were extracted at 4°C for 30 minutes with 60 mL of extraction buffer containing 2 mM Tris base, 2 mM $CaCl_2$, 0.2 mM ATP and 0.5 mM dithiothreitol. Following extraction, the suspension was centrifuged (10250rpm/25min/4°C/JA17) and the supernatant filtered through Whatman #5 filter paper. To the filtered supernatant, KCl was added to 50 mM and $MgCl_2$ added to 2 mM and the solution was stirred at room temperature to precipitate F-actin. After one hour, the KCl concentration of the solution was increased to 0.9 M and stirred for a further two hours at room temperature. The suspension was centrifuged for 16 hours (29000rpm/4°C/Ti55) and the supernatant discarded. The pellet was rinsed with a minimal volume of extraction buffer and then solubilized in 4.5 mL of extraction buffer. The actin suspension was dialyzed overnight with two changes against 2 L of extraction buffer and then centrifuged for two hours (45000rpm/4°C/Ti55) to pellet insoluble materials. The supernatant containing G-actin was recovered and four 1/20 dilutions were used to quantify the G-actin by measuring A_{280nm}, using a 1 mg/mL extinction coefficient of 1.1. The G-actin was polymerized to F-actin by dialysis overnight at 4°C with two changes against 4 L of 20 mM imidazole, pH 7, 3.5 mM $MgCl_2$, 6.5 mM KCl, 0.5 mM EGTA, 0.5 mM dithiothreitol and 0.01% NaN_3. For long term storage at -20°C, the F-actin was dialyzed against an equal volume of 100% glycerol. Purity of the F-actin preparation was determined by 12% SDS-PAGE.

D.2. Preparation of the Troponin Complex

Troponin was reconstituted from its individual subunits by a modification of the method described in Tobacman and Lee (1987). Chicken breast troponin T, troponin I and

troponin C were mixed in a 1:1:1.4 molar ratio in a minimal volume of 4.6 M urea, 50 mM Tris-HCl, pH 8.0, 1 M KCl, 1 mM dithiothreitol, 0.01% NaN_3, 50 μM $CaCl_2$. A greater molar ratio of troponin C is included to compensate for loss of the small protein during dialysis. The mixture was transferred to dialysis tubing and dialyzed for 8 hours at 4°C against 100 volumes of the same buffer. The subunits were then dialyzed against 100 volumes of 2 M urea, 50 mM Tris-HCl, pH 8.0, 1 M KCl, 1 mM DTT, 0.01% NaN_3, 50 μM $CaCl_2$. The denatured troponin subunits were gradually renatured by decreasing the salt concentration of the dialysis buffers, promoting troponin complex formation. The subsequent two dialyses were against 100 volumes of 20 mM imidazole, pH 7.0, 1 mM dithiothreitol, 0.01% NaN_3, 50 μM $CaCl_2$ containing 1 M and 0.1 M KCl, respectively. The troponin complex was then dialyzed against the ATPase buffer (20 mM imidazole, pH 7.0, 6.5 mM KCl, 3.5 mM $MgCl_2$, 1 mM DTT, 0.01% NaN_3) containing 50 μM $CaCl_2$. The renatured troponin complex was separated from any free subunits by gel filtration using a 100 cm x 2.5 cm G75 column (Pharmacia) running at 0.5 mL/min with the ATPase buffer plus 50 μM $CaCl_2$ as the running buffer. Fractions containing the stoichiometric troponin subunits were identified by SDS-PAGE analysis of the single A_{280nm} peak which revealed the troponin complex to be stoichiometric in its subunits. The dilute troponin solution was concentrated using Millipore Ultrafree 30 kDa molecular weight cut off centrifugal filters. The concentration of the troponin complex solution was determined by absorbance (E_{280} 1mg/mL = 0.45; Mr = 70 000) and the stoichiometry of the subunits was confirmed by 12% SDS-PAGE.

RESULTS

A. Rapid Purification of Mouse Nebulin MSN-N4

The mouse nebulin MSN-N4 cDNA encoded a 150 amino acid protein with a theoretical Mr of 17268 and a pI of 9.195. Following harvesting and breaking of bacteria with a French press, the lysate was centrifuged and a significant amount of inclusion bodies were observed as they separated from the lysate supernatant. The inclusion body pellet was

solubilized in urea and the basic mouse nebulin protein effectively fractionated from other contaminant proteins by a cation exchange column running at pH 7. Owing to the high expression level and rapid purification procedure, 36 mg of MSN-N4 protein was purified from 4 L of bacterial culture (Fig. 4.1).

B. Purification of Chicken Nebulin and Nebulette Fragments

A four motif chicken nebulin protein and a five motif chicken nebulette protein were expressed in *E.coli* BL21 pLysS. After lysing the harvested bacteria, the overexpressed proteins were present in the soluble fraction and initially separated from bacterial proteins by precipitation in the 30-50% ammonium sulfate saturation pellet. The cloned nebulin and nebulette proteins were effectively separated from the remaining bacterial contaminants by CM52 chromatography at pH 7.0. Both proteins showed high level expression (Fig. 4.1) and effective purification protocols provided 24 mg of CSN-N4 and 18 mg of CCN-C5 protein from 4 L of culture for further structure / function studies.

C. Authenticity of the Expressed Nebulin and Nebulette Proteins to be used for Characterization

The authenticity of the mouse nebulin MSN-N4 and chicken nebulette CCN-C5 proteins were verified to ensure accurate cloning and expression of the proteins. Immunological techniques and amino acid analysis was used to verify the authenticity of the cloned proteins. This is an important step as the mouse nebulin MSN-N4 and chicken nebulette CCN-C5 cloned proteins will be used in subsequent functional assays.

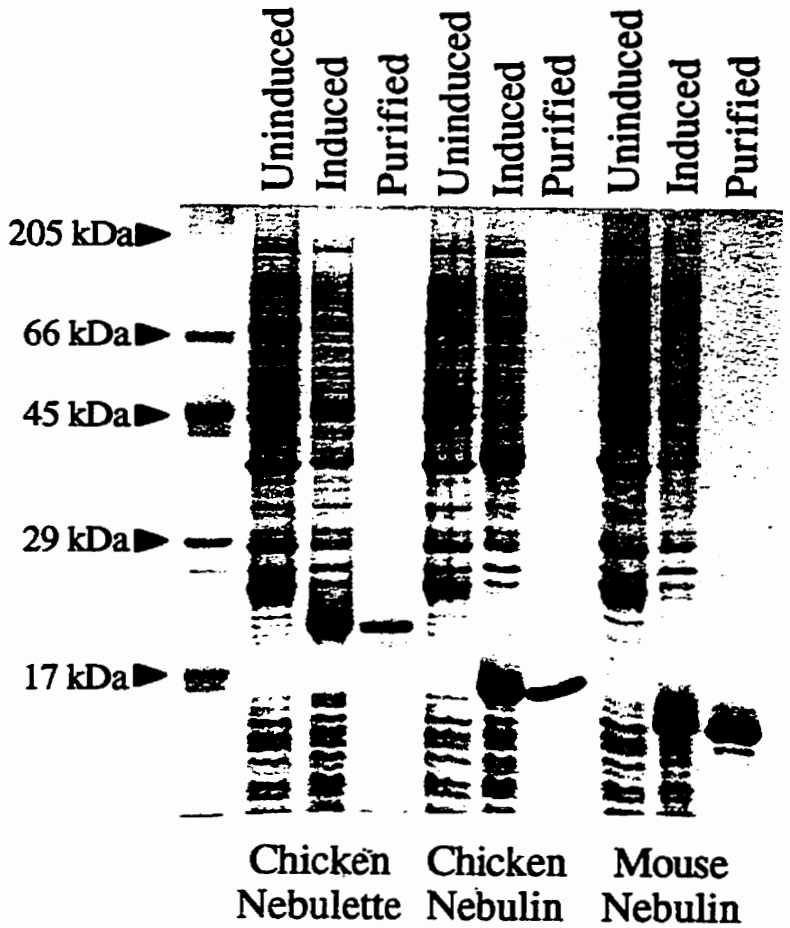

Figure 4.1. Expression levels and purified nebulin and nebulette fragments.

SDS-PAGE analysis of large scale *E.coli* BL21 pLysS cultures transformed with expression vectors encoding the chicken nebulette (CCN-C5), chicken nebulin (CSN-N4) and mouse nebulin (MSN-N4) protein fragments. Upon induction with IPTG, all three bacterial cultures showed overexpression of the distinct proteins encoded by the expression vector. The expressed proteins were effectively purified as described in Materials and Methods to provide abundant protein for structure / function studies.

C.1. A Mouse Nebulin Derived Cloned Protein

The expressed and purified mouse MSN-N4 nebulin protein was characterized for authenticity by ELISA using a nebulin specific monoclonal antibody Ne105 (unpublished results). As compared to the negative BSA control, the monoclonal antibody showed specific reaction with the expressed mouse nebulin protein ($P < 0.05$), indicating correct expression of the cloned cDNA (Fig. 4.2). In the same experiment, the monoclonal antibody did not show a cross-reaction to the cloned chicken nebulin CSN-N4 protein or the chicken nebulette CCN-C5 protein as compared to the system negative control ($P > 0.05$).

C.2. Authenticity of the Cloned Chicken Nebulette Fragment

The cloned chicken nebulette CCN-C5 protein was verified for correct expression of the cDNA by amino acid analysis of the purified protein. As seen in Table 4.1, a very close correlation between the theoretical amino acid composition and that determined by amino acid analysis was demonstrated. This verifies the expression of the correct chicken nebulette protein fragment and the effective purification protocol, providing a true cloned nebulette protein for characterization.

D. Efficient Preparation of F-actin and Troponin

F-actin was prepared from rabbit psoas muscle acetone powder. Actin was separated from tropomyosin and myosin, two major contaminants, by initially extracting the soluble actin from the acetone powder in low ionic strength buffer to prevent extraction of tropomyosin and myosin. The extracted actin was then precipitated in the absence of ATP while solubilizing contaminants in high ionic strength buffer. Purified G-actin was then repolymerized to F-actin in the presence of Mg^{2+} and absence of ATP. From 2 g of acetone

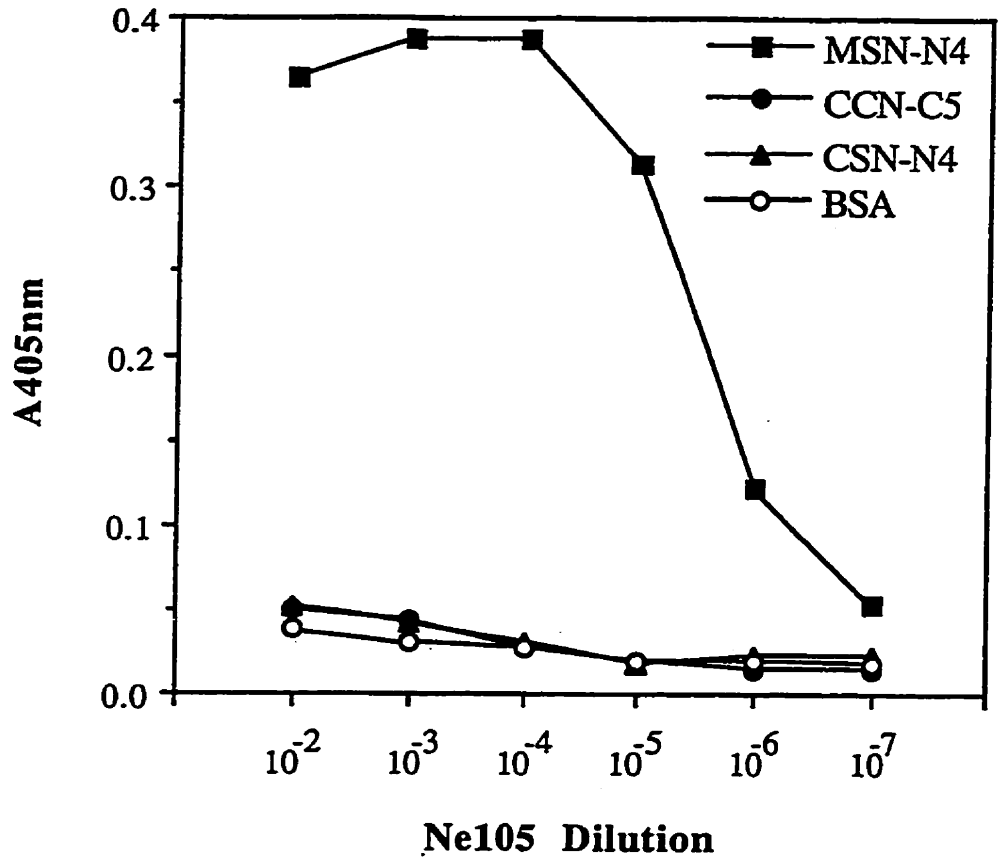

Figure 4.2. A nebulin specific monoclonal antibody specifically identifies the cloned mouse MSN-N4 nebulin protein.

In indirect ELISA experiments using a monoclonal antibody Ne105 raised against a cloned human nebulin protein, the cloned mouse MSN-N4 protein was specifically identified, attesting to the correct expression of the cloned nebulin cDNA. The monoclonal antibody did not identify the cloned CSN-N4 chicken nebulin or CCN-C5 chicken nebulette proteins.

Amino Acid	*Expected Recovery (residues/mol)*	*Experimental Recovery (residues/mol)*
Asparagine + Aspartic Acid	17	15.9
Threonine	10	8.9
Serine	15	12.8
Glutamine + Glutamic Acid	28	27.8
Proline	9	8.6
Glycine	4	9.8
Alanine	6	9.0
Valine	17	15.8
Methionine	4	2.7
Isoleucine	13	11.7
Leucine	4	6.2
Tyrosine	6	6.1
Phenylalanine	2	2.1
Histidine	5	5.1
Lysine	18	17.1
Arginine	12	11.2
Cysteine	1	0

Table 4.1. Amino acid analysis verification of the cloned chicken nebulette CCN-C5 protein.

The amino acid analysis of the purified chicken nebulette CCN-C5 protein showed a high correlation with the theoretical amino acid content as predicted from the cDNA sequence. The results indicate accurate expression of the cloned cDNA and an effective purification protocol to provide a highly pure protein sample.

powder, the protocol yielded 15 mg of pure F-actin, as determined by 12% SDS-PAGE and spectrophotometry.

Troponin complex was reconstituted using the three subunits of chicken skeletal muscle troponin. Although relatively insoluble individually in low salt buffers, troponin I and troponin T were soluble in the low salt ATPase buffer once renatured in the troponin complex. Gel filtration of the dialyzed troponin revealed a single A_{280nm} peak, indicating that all three subunits had reconstituted into the complex. The gel filtration eluate was concentrated by ultrafiltration, providing pure, stoichiometrically correct troponin complex for use in *in vitro* experiments, as determined by 12% SDS-PAGE.

DISCUSSION

Three cloned nebulin or nebulette proteins were expressed in *E. coli* and effectively purified by rapid methods. Of the three cloned proteins, the chicken nebulin (CSN-N4) and chicken nebulette (CCN-C5) proteins were soluble at concentrations as high as 10 mg/mL or roughly 0.5 mM. In contrast, the mouse nebulin fragment (MSN-N4) was soluble only at concentrations below 15 μM, consistent with the human nebulin fragments previously expressed (Jin and Wang, 1991a,b). This difference in solubility between the expressed mouse and chicken proteins is surprising, considering that all are composed of the well conserved ~35 amino acid motifs. Although the solubility of the chicken nebulin and nebulette protein fragments is high, this can not be assumed for the intact proteins since experimental data have shown them to be relatively insoluble and difficult to extract from muscle (Moncman and Wang, 1995; Wang, 1982; Meng *et al.*, 1995). It remains possible that certain stretches of the intact nebulin or nebulette proteins are soluble when cloned and expressed individually.

The authenticity of the mouse nebulin MSN-N4 and chicken nebulette CCN-C5 proteins to be further characterized in this study were verified. Specific antibody interaction and amino acid analysis demonstrated accurate expression of the cloned cDNA, providing authentic, representative nebulin and nebulette proteins for functional characterization. In addition, effective adaptation of published protocols allowed rapid and efficient purification and preparation of F-actin and troponin complex for use in *in vitro* binding assays, as well as for regulated and unregulated acto-myosin S1 ATPase assays.

CHAPTER FIVE:
SPECIFIC ANTIBODY PRODUCTION AND TISSUE CULTURE

Antibodies are important tools in investigating protein - protein interactions, as well as following protein expression through development and demonstrating tissue-specific expression of proteins. To study the expression pattern of the novel nebulette protein, a specific antiserum will be generated, using the chicken nebulette fragment as an immunogen. The chicken antigen has advantages as it is from a distinct phylum and therefore evolutionarily separate from mouse, allowing a greater chance of high titre antibody production.

Immunoelectron microscopy studies of nebulin using specific monoclonal antibodies have shown the protein to be rigid in the framework of the thin filament, with the NH_2-terminus of the protein pointing towards the M line of sarcomeres (Wang and Wright, 1988). The COOH-terminus of nebulin appears to be anchored at the Z line of sarcomeres, but epitope mapping using NH_2-terminus specific antibodies has demonstrated that the true NH_2-terminus of nebulin may surpass the length of the thin filament (Wang and Wright, 1988). Immunoprecipitations using anti-nebulin monoclonal antibodies cross-reacting with nebulette demonstrated a single immunoreactive band of 107 kDa (Moncman and Wang, 1995) in cardiac muscle extracts. Immunofluorescence microscopy with the same antibodies has shown I-Z-I region staining in the cardiac muscle sarcomeres. The immunoreactive proteins were reported to be resistant to extraction conditions which removed the thick filament or both the thin and thick filaments. There are no data available regarding the orientation of the NH_2- and COOH-termini of the nebulette protein with respect to the sarcomere.

In this Chapter, the generation of a specific antiserum against the cloned chicken nebulette CCN-C5 protein is described. The specificity of the antiserum, along with SDS-PAGE conditions to advantageously resolve proteins over 100 kDa, have shown that two

nebulette isoforms can be identified in cardiac muscle extracts. The protein is expressed throughout development and exhibits different expression patterns in the four chambers of the bovine heart. Further, a mouse nebulin eukaryotic expression construct will be transfected into C2C12 mouse myoblast cell line to provide an *in vivo* system for future characterization.

MATERIALS AND METHODS

A. Generation of a Specific Antiserum Against Nebulette

Using the purified chicken nebulette CCN-C5 protein, one female Balb/C mouse was immunized to generate an antiserum specific for nebulette. For the primary immunization, 200 μg of the antigen in 200 μL of PBS was made into a water in oil immersion using an equal volume of Freund's complete adjuvant. Immunizations were administered intraperitoneally. Subsequent boosts using 100 μg of the purified protein were made at three week intervals using Freund's incomplete adjuvant. To determine the serum titer and specificity of the antiserum generated, 20 μL of blood was collected from a small incision in the mouse tail. The blood was allowed to clot overnight at 4°C and the serum separated by centrifugation (2000g/5min). Collected serum was diluted by an equal volume of 100% glycerol for storage at -20°C. The serum was used for indirect ELISA against the chicken nebulette antigen coated on ELISA plates, as previously described in Chapter Four.

To test a possible cross-reaction of the CCN-C5 antiserum against the MSN-N4 and CSN-N4 cloned nebulin proteins, indirect ELISA was done. BSA, MSN-N4, CSN-N4 and CCN-C5 were dissolved in ELISA coating buffer to 5 μg/mL and coated (100 μL/well) in triplicate wells of an ELISA plate overnight at 4°C. After washing and blocking as described before, the wells were incubated for two hours at 37°C with serial dilutions of the CCN-C5 antiserum (100 μL/well) in PBS-P. After incubation with 1/1500 dilution of

horseradish peroxidase labelled goat anti-mouse IgG second antibody iluted in PBS-P, H_2O_2-ABTS substrate was added and the color development monitored as before.

B. Immuno-identification of Nebulette in Species and Through Development

To monitor nebulette expression, Western blots were done using the specific anti-nebulette antiserum on developing or mature cardiac muscle extracts of various species solubilized in 3x SDS gel sample buffer. To better resolve large proteins (>100 kDa) a high porosity 14% SDS-PAGE with an acrylamide to bisacrylamide ratio of 180:1 was used. After resolving total cardiac muscle extracts by 180:1 14% SDS-PAGE, a three buffer system (Granzier and Wang, 1993) of 300 mM Tris, 10% methanol, 0.05% SDS (buffer 1), 25 mM Tris, 10% methanol, 0.05% SDS (buffer 2) and 1x Tris buffered saline (TBS: 150 mM NaCl, 50 mM Tris-HCl, pH 7.5, 0.1% NaN_3), 10% methanol (buffer 3) was used to efficiently transfer resolved proteins. Briefly, two layers of filter paper as well as 0.45 μm nitrocellulose membrane were soaked in buffer 3 and used as the bottom layer of the sandwich, representing the positive end. The resolved SDS-PAGE was rinsed in buffer 2 and placed atop the nitrocellulose filter, overlayed with one piece of filter paper soaked in buffer 2 and one piece of filter paper soaked in buffer 1. Transfer using the Bio-Rad Semi-dry transfer apparatus was at 5 mA/cm^2 of gel for 40 minutes. After transfer, the nitrocellulose replica was blocked by incubation at room temperature for three hours with TBS containing 1% BSA. The blocked membrane was then incubated at 4°C overnight with polyclonal antisera against chicken nebulette diluted 1/2000 in TBS containing 0.1% BSA. Following primary antibody incubation, the blots were washed once with TBS for 10 minutes, three times for 10 minutes each with 1x TBS / 0.05% Tween-20 and then twice for 5 minutes with TBS. The blots were then incubated at room temperature for 50 minutes with alkaline phosphatase-labelled anti mouse IgG second antibody (Sigma) diluted 1/2000 in TBS containing 0.1% BSA. Following second antibody incubation, the blots were washed as before and color development was done using 5-bromo-4-chloro-3-

indolylphosphate (BCIP, 0.00165 % (w/v)) and nitro blue tetrazolium (NBT, 0.0033 % (w/v)) in 10 mL of 100 mM NaCl, 100 mM Tris, 5 mM $MgCl_2$, pH 9.5 buffer.

C. Transfection of the Green Fluorescent Protein - Nebulin Eukaryotic Expression Vector

The eukaryotic expression vector encoding the GFP-nebulin fusion protein under control of the slow troponin T promoter (Chapter 2) was used to transfect the mouse myoblast cell line C2C12 (Bains *et al.*, 1984). C2C12 cells were grown at 37 °C with 10% CO_2 in Dulbecco's modified Eagle's medium (DMEM) containing 10% fetal calf serum (FCS). Once the cells reached near confluency in a 100 mm x 50 mm plate, the medium was aspirated and the plate rinsed with 2 mL of Versene. The cells were digested from the plate using 0.5 mL of trypsin solution (40 mM NaCl, 1 mM KCl, 0.1 mM Na_2HPO_4, 1.1 mM glucose, 5 mM Tris, pH 7.6, 0.5 mg/mL trypsin) and recovered in 4.5 mL of DMEM / 10% FCS. The cells were washed once with 5 mL of DMEM / 10% FCS, pelleted, resuspended in 0.5 mL DMEM / 10% FCS and transferred to a 0.2 cm electroporation cuvette. The expression vector was linearized at a PvuI restriction endonuclease site upstream of the slow troponin T promoter insert to increase transfection efficiency into cells. To the resuspended cells, 5 μg of the PvuI-linearized expression vector were added and the cell / DNA mixture incubated on ice for 12 minutes. Cells were electroporated at 0.45 V and a capacitance of 500 μF. Immediately after electroporation, the cells were added to a plate containing 7 mL of DMEM / 10% FCS and incubated at 37 °C with 10% CO_2. Two days after electroporation, the medium was changed to DMEM / 10% FCS / 500 μg/mL G418 for selection of expression vector bearing colonies. Alternatively, transfection of the linearized expression construct was done by liposome mediated transfection. Briefly, 30 μg of the DOTAP transfection reagent (Boehringer Mannheim) was mixed in 100 μL of 20 mM HEPES, pH 7.2. To this mixture, 5 μg of the PvuI linearized vector in 50 μL of 20 mM HEPES, pH 7.2 was added, mixed, and incubated at room temperature for 15 minutes. Following incubation, 5 mL of fresh DMEM / 10% FCS was added to the DOTAP/DNA

mixture and used as medium for C2C12 cells nearing confluency in a 100 mm x 20 mm culture dish. The C2C12 cells were grown in DOTAP / DNA containing medium for two days, and then changed to DMEM / 10% FCS / 500 μg/mL G418 for selection.

The transfected C2C12 cells were grown in selection medium until cell numbers decreased and individual colonies appeared. The culture dish was cleared of medium and small, circular plastic rings were placed around individual colonies on the plate. A small amount of vacuum grease was used on the bottom of the rings to adhere them to the plate. To release the colony surrounded by the ring, one drop of trypsin solution was added and allowed to digest for one minute. The cells were then resuspended from inside the ring using DMEM / 10% FCS / 500 μg/mL G418 and seeded into individual wells of a 12 well plate. The colonies were allowed to grow to near confluency, at which point the cells were harvested for extraction of genomic DNA to verify incorporation of the linear expression construct into the genome. Collected cells were resuspended in 20 μL of digestion buffer (100 mM NaCl, 10 mM Tris-HCl, pH 8, 25 mM EDTA, 0.5% SDS and 150 μg/mL Proteinase K) and incubated at 55 °C overnight. From this lysed cell / DNA mixture, 1 μL was used as a PCR template using a gene specific NC-F primer (5' - TCAACATATGATCAGCTCGGTTTTGTA - 3') and a vector specific pcDNA 3.1 reverse primer (Invitrogen) in the following PCR cycle : 95 °C 1 min., 55 °C 1 min., 72 °C 1.5 min., for 35 cycles. Colonies showing amplification of the expression construct specific 1.5 kb band were expanded and frozen for storage in DMEM / 30% FCS / 10 % DMSO.

RESULTS

A. A Nebulette Specific Mouse Antiserum

The chicken nebulette protein fragment CCN-C5 was used to immunize a female mouse to produce a nebulette specific antiserum, MACN. The specificity of the antiserum was determined by indirect ELISA using serial dilutions of the antiserum on the CCN-C5

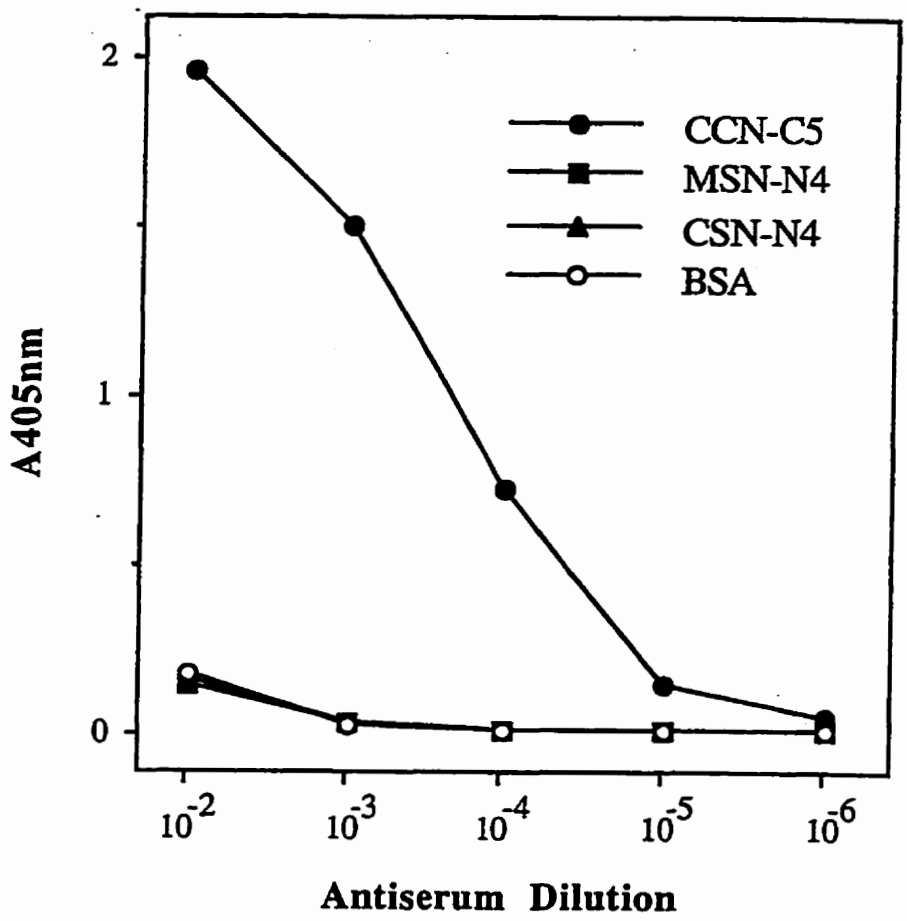

Fig. 5.1 ELISA analysis of the titre and specificity of the anti-nebulette antiserum. Indirect ELISA was done using the mouse anti-CCN-C5 antiserum to determine the specificity of the antigen versus other homologous nebulin proteins. The results demonstrate that the antiserum was specific for the nebulette protein, providing a curve which was statistically different than the curves for MSN-N4 ($P < 0.05$), CSN-N4 ($P < 0.05$) and BSA ($P < 0.05$). The antiserum was not cross-reactive with the mouse MSN-N4 and chicken CSN-N4 proteins, as the two curves are not significantly different when compared to BSA, the system negative control ($P > 0.05$).

antigen as well as the mouse MSN-N4, chicken CSN-N4 and BSA proteins. The results indicate the serum to be specific for the antigen, with specific reactivity even at dilutions of 10^{-5} (Figure 5.1). The specificity of the antiserum is also demonstrated by the background level immunoreactivity versus the cloned nebulin proteins.

B. The Mouse Anti-Nebulette Antiserum Does Not Show Broad Reactivity to Nebulettes Among Species

The mouse anti-nebulette antiserum was tested for specificity and diversity of nebulettes identified by Western blots using cardiac muscle homogenates from various species. The antiserum showed greatest reactivity to chicken, human and bovine nebulettes, limited reactivity to rat nebulette and little or no reactivity to mouse, rabbit and sheep nebulettes (Fig. 5.2). Two very closely migrating bands were identified in chicken cardiac muscle, two bands were identified in bovine cardiac muscle and only single immunoreactive bands were identified in human and rat cardiac muscle extracts.

C. Developmental and Chamber Specific Expression Pattern of Nebulette

To follow the expression pattern of nebulette through development, the specific anti-nebulette antiserum was used on cardiac muscle extracts from day 8 embryo, neonatal and adult chickens. Figure 5.3 demonstrates that both of the closely migrating nebulette isoforms expressed in the chicken heart are expressed throughout development. Also, to determine whether the expression level of nebulette was different among the chambers of the mammalian heart, muscle samples were dissected from adult bovine left and right ventricle walls as well as the left and right atria. The antiserum detected two nebulette isoforms in all chambers of the bovine heart (Fig. 5.4). Interestingly, although the total expression of nebulette remained constant throughout the chambers, a visible increased proportion of the lower Mr isoform is expressed in the bovine left ventricle.

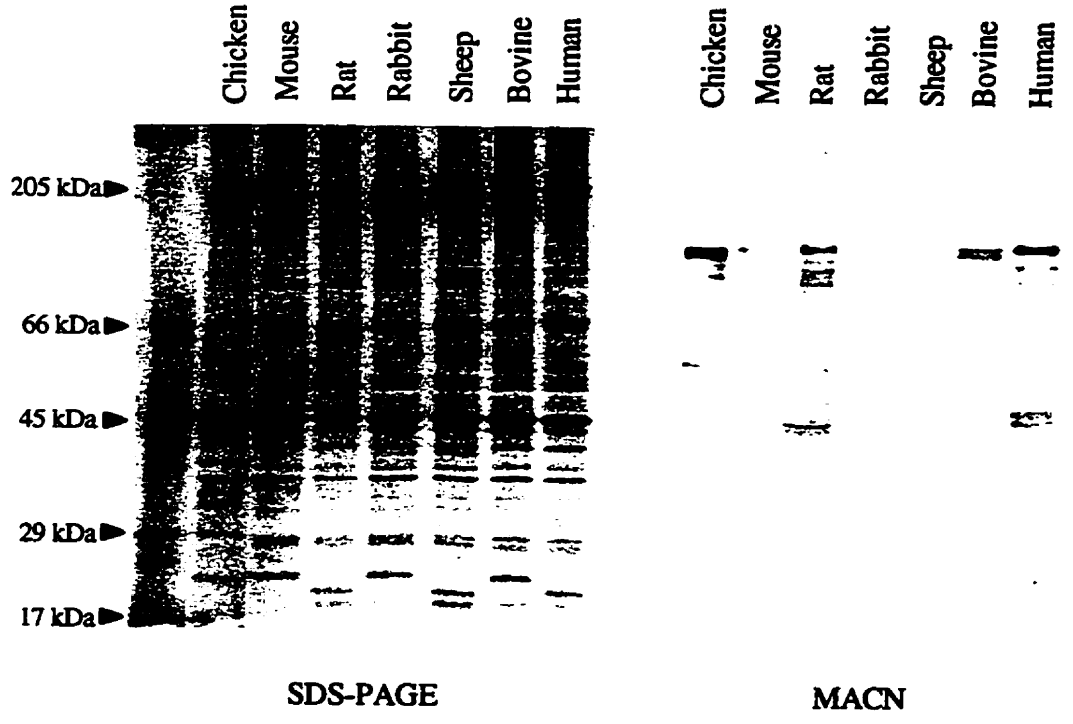

Figure 5.2. Species specificity of the anti-nebulette antiserum.

The anti-nebulette mouse antiserum was used to survey the species specificity of the antibody versus various nebulettes. The results demonstrate that the antiserum showed strongest reaction to nebulettes in cardiac muscle extracts of chicken, rat, bovine and human. The antiserum was not reactive with nebulette in cardiac muscle extracts from mouse, rabbit or sheep. The results also demonstrate that two nebulette isoforms may be expressed, seen as two very closely migrating bands in chicken and two distinctly migrating bands in bovine cardiac muscle extracts.

D. C2C12 Myoblast Colonies Transfected with a Green Fluorescent Protein - Nebulin Expression Construct

Mouse myoblast C2C12 cells were grown to near confluency and transfected with the linearized eukaryotic expression vector encoding a GFP-nebulin fusion protein under the direction of a 2.5 kb fragment of the mouse slow skeletal muscle troponin T promoter. Following selection of recombinant cell colonies by G418, individual colonies were picked, reseeded, and grown to near confluency. PCR screening of DNA extracted from the recombinant C2C12 colonies showed that six out of twelve recombinant colonies had incorporated the linearized vector into the genome (results not shown). Frozen stocks were made of these recombinant C2C12 colonies for future characterization.

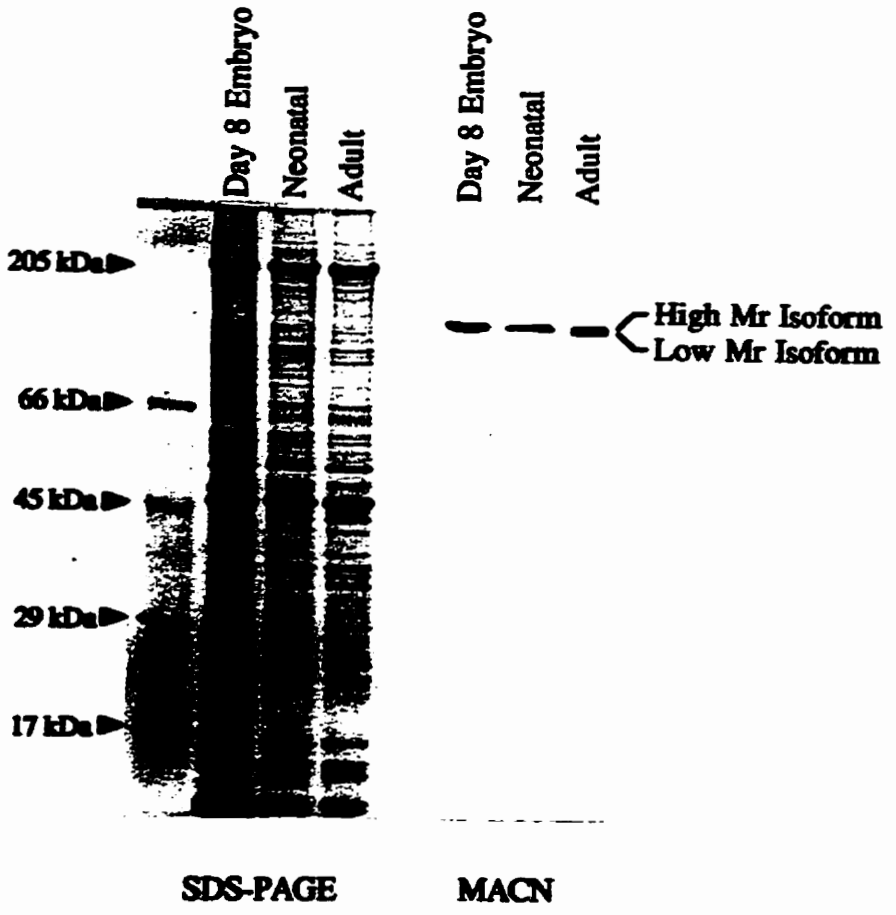

Figure 5.3. Nebulette is expressed throughout development.

Comparable amounts of cardiac muscle extracts from day 8 embryo, neonatal and adult Leghorn chicken heart were resolved by 14% SDS-PAGE and immunoblotted with the anti-nebulette antiserum MACN. Two closely migrating nebulette isoforms are expressed throughout development of the chicken heart, indicating that nebulette is a protein present and required through development of the heart.

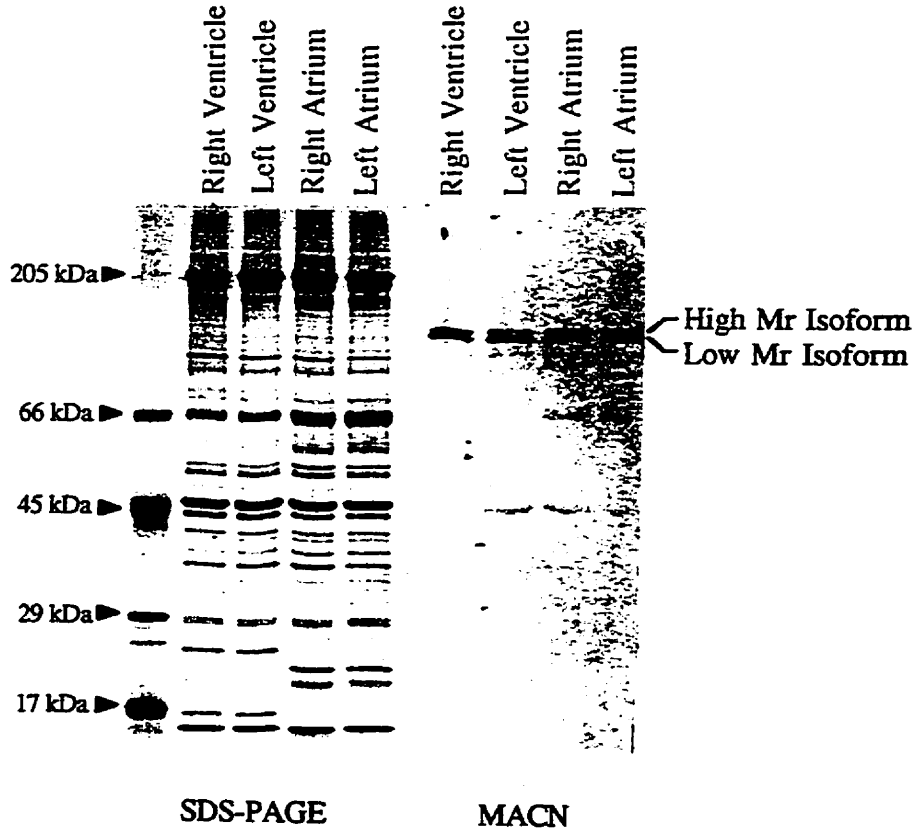

Fig. 5.4. Nebulette isoforms and different expression levels in the adult bovine heart. Total protein homogenates from the right and left ventricles as well as the right and left atria of an adult bovine were resolved by 14% SDS-PAGE and transferred to nitrocellulose membrane. Western blotting with the mouse anti-nebulette antiserum (MACN) identified two nebulette isoforms in the bovine heart. Although total nebulette expression between the chambers of the heart appears comparable, the proportion of the expressed isoforms is significantly different in the left ventricle where the lower Mr nebulette isoform is dominant.

DISCUSSION

This chapter described the generation of an antiserum against a cloned chicken nebulette protein, as well as the expression pattern of native nebulette. The antiserum raised against the chicken nebulette CCN-C5 fragment showed specificity for the cloned chicken CCN-C5 nebulette protein and did not recognize the cloned mouse MSN-N4 or chicken CSN-N4 nebulin proteins. This indicates that, although nebulin-like domains appear well conserved in both nebulin and nebulette, the antigenic character of the individual domains still remains distinctive. Therefore, no broad range antibodies were generated with this immunization.

Variety of Nebulette Epitopes Among Species

A survey of the heart homogenates of various species showed that the anti-nebulette antiserum was immunoreactive to nebulette proteins in chicken, rat, bovine and human cardiac extracts whereas nebulette proteins from other species tested such as mouse, rabbit and sheep were not identified (Fig. 4.2). This is an interesting observation regarding the antigenic character of nebulettes from various species. With respect to species, the antiserum specifically recognized both bovine nebulette isoforms but no isoforms were recognized in sheep. Although a close evolutionary species to bovine, sheep nebulette was not identified, indicating a significant antigenic difference between the bovine and sheep nebulette proteins. It is possible that alternative splicing of exons may account for this difference in reactivity, and in turn differences in nebulette primary structure among species.

Nebulette Isoforms are Expressed at Different Levels in the Chambers of the Bovine Heart

The expression pattern of native nebulette using the nebulette antiserum demonstrated that the protein is expressed throughout development in the chicken heart. This indicates that the protein is required or plays a role in the morphogenesis of cardiac muscle. More interestingly, a survey of the expression pattern of nebulette in the chambers of the bovine heart identified a difference in the proportion of the two nebulette isoforms expressed, specifically an increase in the proportion of the lower Mr isoform in the left ventricle. It is well documented that the left and right ventricles are phenotypically different, with the former being significantly larger in size. Furthermore, pressures in the left ventricle during ventricular systole may reach ~110-120 mm Hg whereas pressures developed in the right ventricle are significantly lower at ~30 mm Hg. In this aspect, the left ventricle is well suited for its role in supplying the energy for the flow of blood through the high pressure, high resistance systemic circulation (Rushmer, 1976). The observation that nebulette isoform expression levels are different in the left and right ventricles is an interesting observation as few sarcomeric proteins show such differences, although myosin is a major example (Swynghedauw, 1986). As the major motor of muscle, the differences in the ATPase activities of myosin isoforms can be correlated with performance of various muscles (reviewed in Schiaffino and Reggiani, 1996). Such a correlation is reliable since the ATPase activity of myosin is the major determinant in muscle contraction. Nonetheless, the possibility exists that other regulatory and/or structural proteins may also contribute to this process, providing a rationale for the alternative splicing generated isoforms of proteins such as nebulette, troponin T (Cooper and Ordahl, 1984; 1985; Jin and Lin, 1988), tropomyosin (Lees-Miller *et al.*, 1990) and titin (Labeit and Kolmerer, 1995b).

CHAPTER SIX:
FUNCTIONAL ASSAYS CHARACTERIZING CLONED NEBULIN AND NEBULETTE PROTEINS

INTRODUCTION

The function of nebulin in the skeletal muscle sarcomere is proposed to be as a length regulating and organizational template for thin filament assembly (Trinick, 1992). This hypothesis was due to the protein's interaction with F-actin, as well as the correlation between nebulin polypeptide size and thin filament length from skeletal muscle sarcomeres of various species (Locker and Wild, 1986). Nonetheless, the discovery of the homologous, but significantly smaller nebulette protein in cardiac muscle does not support the role of nebulin like motifs as templates, particularly since the 107 kDa nebulette protein is not large enough to span the lengths of the cardiac muscle thin filaments (Moncman and Wang, 1995). Therefore, the function of the well conserved nebulin proteins remains under investigation.

In this Chapter, the cloned nebulin MSN-N4 and nebulette CCN-C5 proteins will be used to probe the functional properties of nebulin and nebulette. Solid phase binding assays will provide a survey of the interactions of the novel cloned nebulette protein with other constituents of the thin filament, allowing a comparison to previous data for cloned nebulin proteins. These experiments will be important in proposing a structural basis of nebulette's interaction within the sarcomere. Further, the role of nebulin/nebulette will be further explored by regulated and unregulated acto-myosin S1 ATPase assays to determine what effect, if any, these cloned proteins will have on the actin activated ATPase activity of myosin subfragment 1.

The results indicate that the cloned nebulette protein is an actin binding protein, similar to nebulin. A survey of sarcomeric proteins showed no specific binding between the

CCN-C5 nebulette protein and tropomyosin, troponin T, C or I. Tropomyosin and tropomyosin / troponin decreased the nebulette protein's binding to immobilized F-actin, indicating a competition for binding sites. Further, both nebulin MSN-N4 and nebulette CCN-C5 proteins had inhibitory effects on unregulated acto-S1 ATPase activity, with this inhibition removed by Ca^{2+} - troponin - tropomyosin in regulated acto-myosin S1 ATPase assays.

MATERIALS AND METHODS

A. Protocol for ELISA-Mediated Solid Phase Protein Binding Assays

The binding of the nebulin fragments to other proteins was analyzed by an ELISA-mediated protein-binding assay (Ogut and Jin, 1996). Proteins were coated on microtitre plates overnight at 4 °C (100 μL/well) after dissolving in 0.1 M KCl, 10 mM Tris-HCl, pH 7.5, 3 mM $MgCl_2$ (Buffer A) to a concentration of 5 μg/mL, with the exceptions of F-actin, which was coated at 30 μg/mL, and myosin, coated at 50 μg/mL. The plates were then washed once with Buffer A plus 0.05% Tween-20 (Buffer T) and blocked for two hours at room temperature with 150 μL/well of Buffer A plus 1% BSA and 0.05% Tween-20 (Buffer B). Following blocking, the plates were washed three times with Buffer T and incubated with serial dilutions of a second protein or a fixed dilution of a specific antibody. Subsequent protein coatings (100 μL/well) were done by dissolving the protein in Buffer A and incubating at room temperature for two hours with the immobilized proteins. Otherwise, a fixed dilution of a specific antibody was made in Buffer A plus 0.1% BSA and 0.05% Tween-20 (Buffer P) and incubated (100 μL/well) at room temperature for 1.5 hours. Following primary antibody incubation, the plates were washed three times with Buffer T and incubated at room temperature for 45 minutes with horseradish peroxidase conjugated second antibody (Sigma) diluted 1/1000 in Buffer P. The plates were washed three times with Buffer T and incubated with H_2O_2-ABTS substrate for color development and

monitored for absorbance at 405 nm, as described earlier. The significance of differences between binding curves was determined Student's T test.

B. Binding of CCN-C5 to Myofibril Proteins

To monitor possible binding of the cloned CCN-C5 nebulette protein to thin filament proteins, triplicate wells of microtitre plates were coated overnight at 4°C with 100 µL/well of 5 µg/mL troponin C, troponin I, troponin T, tropomyosin, cloned Ti I, Ti II, Ti I-II, PEVK protein (Jin, 1995 and unpublished results), a cardiac muscle specific N2 line titin protein (N2B, a gift of Dr. Seigfried Labeit), 30 µg/mL F-actin or 50 µg/mL myosin diluted in Buffer A. Following washing and blocking as described, the wells were incubated at room temperature for two hours with 1 in 10 serial dilutions of 10 µM CCN-C5 diluted in Buffer A, providing a wide concentration range to monitor high and low affinity binding. Following incubation with the CCN-C5 protein, the plates were washed as described and incubated at room temperature for 1.5 hours with a 1/10000 dilution of the mouse anti-nebulette antiserum in Buffer P. The plates were washed, and second antibody incubation and H_2O_2-ABTS color development were done as described in A.

C. Interaction of CCN-C5 with Decorated F-actin

F-actin was decorated with tropomyosin or troponin - tropomyosin to determine the effect on CCN-C5 nebulette protein's binding to F-actin. Triplicate wells of microtitre plates were coated with 30 µg/mL of F-actin dissolved in Buffer A, as before. The plates were washed, blocked, and then incubated with either 2 µM tropomyosin or 2 µM tropomyosin pre-incubated for 20 minutes with 1 µM troponin. The protein incubation was done at room temperature for 2 hours, following which 1 in 5 serial dilutions of 2 µM CCN-C5 were incubated with the immobilized, decorated F-actin for 2 hours at room

temperature. The following washings, primary and secondary antibody incubations and color development were done as before.

D. Unregulated Actin-Activated Myosin S1 ATPase Assays

To determine the effects of the MSN-N4 nebulin and CCN-C5 nebulette proteins on the actin activated S1 myosin ATPase activity, a novel microtitre plate-based procedure was developed. The phosphate released from cleavage of ATP due to the ATPase activity of the S1 fragment of myosin can be quantified using ammonium molybdate and malachite green color reagent (Baykov *et al.*, 1988). This allows a non-radioactive method to measure the amount and rate of Pi release in ATPase assays.

To determine the effect of varying concentrations of MSN-N4 nebulin or CCN-C5 nebulette proteins on the unregulated actin-activated activity of myosin S1, MSN-N4 nebulin (Mr 17268), CCN-C5 nebulette (Mr 19251) and tropomyosin (Mr 33000) were titrated under conditions of 1.25 μM F-actin (Mr 42000) and 50 nM S1 (Mr 115000), providing an F-actin:S1 molar ratio of 25:1. The cloned protein fragments were used in 1 in 2 serial dilutions from 5 μM to 0.31 μM, providing protein : F-actin ratios of 4, 2, 1, 0.5 and 0.25 to 1. The F-actin filaments for the ATPase assays were constituted in a conserved order by adding ATPase buffer, followed by F-actin to 1.56 μM, and the second protein of interest to 6.24 μM, ensuring a final volume of 700 μL. After mixing, 350 μL of this mixture was added to 350 μL of 1.56 μM F-actin in the ATPase buffer, providing a 1 in 2 serial dilution of the protein to be tested while maintaining a constant F-actin concentration. The serial dilutions were incubated at room temperature for 10 minutes, at which point myosin S1 was added to 71 nM. The mixtures were aliquoted into triplicate wells (35 μL/well) of a microtitre plate and reactions initiated by the addition of 15 μL of 0.33 mM ATP in the ATPase buffer. Following addition of ATP, final concentrations of the protein constituents were: F-actin: 1.25 μM; MSN-N4, CCN-C5 and tropomyosin: 1 in 2 dilutions from 5 μM to 0.31 μM; myosin S1: 50 nM. The reactions were incubated at 25°C for

various times and terminated by addition of 12.5 μL of inorganic phosphate color reagent prepared as described (Baykov *et al.*, 1988). The reactions were allowed to stand at room temperature for 10 minutes and the amount of inorganic phosphate released was quantified by comparison with a standard A_{655nm} curve of known phosphate concentrations. For calculation of ATPase activities, simultaneous control reactions without the addition of ATP were done to record the basal ATPase activity, which was subtracted from all samples.

E. Effect of Nebulin and Nebulette Proteins on Ca^{2+}-Dependent Activation of a Reconstituted Acto-myosin System

To determine the effect of the cloned nebulin and nebulette fragments on the Ca^{2+}-dependent activation of actin-activated myosin S1 ATPase, the thin filament was reconstituted in the ATPase buffer using F-actin, tropomyosin, troponin complex and the nebulin or nebulette protein of interest. To a solution containing 3.57 μM F-actin, 5.72 μM tropomyosin was added, as well as 2.86 μM of either the mouse nebulin MSN-N4 fragment or the chicken nebulette CCN-C5 fragment. The mixture was incubated at room temperature for five minutes, at which point 2.86 μM troponin (Mr 70000) was added, and the mixture incubated for an additional 10 minutes at room temperature. For control experiments, no nebulin or nebulette fragment was added. The myosin S1 ATPase was measured at pCa 8 and 4, representing resting and activating concentrations of Ca^{2+}. Following equilibration of the thin filament complex, myosin S1 was added to 71 nM and $CaCl_2$ added to the samples to adjust the necessary calcium concentration, as determined by the program of Fabiato (1988). The mixture was aliquoted (35 μL/well) into triplicate wells for three time points. The reactions were incubated at room temperature and initiated by the addition of 15 μL of 0.33 mM ATP in the ATPase buffer. Following addition of ATP, the final concentrations of proteins were: 2.5 μM F-actin, 4 μM tropomyosin, 2 μM troponin, 50 nM myosin S1 and 2 μM of either the mouse nebulin MSN-N4 or chicken nebulette CCN-C5 fragments. Triplicate reactions were stopped by the addition of 12.5 μL of Pi color solution at various time intervals. The absorbance values at 655 nm were compared with a

standard curve of known phosphate concentrations (serial dilutions of KH_2PO_4) to calculate the Pi released through hydrolysis of ATP and allow calculation of myosin S1 activity. The significance of the differences between ATPase values under various conditions were determined by the Student's T test.

RESULTS

A. Interaction of the Cloned Nebulette Protein with Individual Thin Filament Proteins

The cloned chicken nebulette fragment CCN-C5 was used for solid-phase protein binding assays against various sarcomeric proteins. A wide concentration range of the nebulette fragment was used to monitor both high and low affinity binding. The results indicate that the nebulette fragment showed greatest binding to immobilized F-actin and less, but significant, binding to myosin (Figure 6.1; $P < 0.05$ for actin and myosin as compared to BSA). Tropomyosin or the individual troponin subunits did not show significant interaction with the cloned nebulette protein ($P > 0.05$ in all cases versus BSA), consistent with results obtained for cloned human nebulin proteins (Jin and Wang, 1991a,b). A survey of the cloned immunoglobulin-like (class II) and fibronectin-type (class I) motifs showed low binding to the cloned single motif Ti I and Ti II proteins, although differences between these two curves and the BSA control curve were not statistically significant ($P > 0.05$). On the other hand, the effect of binding the titin motifs appeared cumulative, as a cloned protein of a linked type I and type II motifs showed increased and significant binding ($P < 0.05$; Figure 6.2). No binding was seen to a cloned protein fragment of the PEVK domain of titin ($P > 0.05$), consistent with the hypothesis that this region may be free to fold and unfold to aid in titin elasticity (Rief *et al.*, 1997; Kellermayer *et al.*, 1997). The cloned nebulette protein interacted with the cloned ~20 kDa protein protein corresponding to the N2-line region of titin unique to cardiac muscle ($P < 0.05$).

B. Troponin and Tropomyosin Inhibit Binding of Chicken Nebulette CCN-C5 Fragment to F-actin

To determine the effect of tropomyosin and troponin on chicken nebulette fragment CCN-C5's binding to F-actin, solid phase binding assays using purified F-actin, troponin and tropomyosin were done (Figure 6.3). In the absence of tropomyosin or troponin, the chicken nebulette protein showed greatest binding to coated F-actin. When immobilized F-actin was decorated with tropomyosin or tropomyosin / troponin, the chicken nebulette protein showed decreased binding to F-actin, with the tropomyosin / troponin complex showing greatest inhibition of CCN-C5 binding to F-actin. Both F-actin / Tm and F-actin / Tm / Tn curves were statistically different as compared to the F-actin curve ($P < 0.05$).This indicates a competition for F-actin binding sites between the chicken nebulette protein and troponin / tropomyosin in this *in vitro* binding assay. Competition for F-actin binding sites would therefore imply that the interaction of nebulette with F-actin may be regulated. This competition between nebulette and troponin / tropomyosin for F-actin binding is similar to that observed for cloned human nebulin fragments (Jin and Wang, 1991a,b), indicating a possible common function.

C. An Inhibitory Effect of Nebulin and Nebulette Fragments on the ATPase Activity of Unregulated Acto-myosin S1

Given that cloned nebulin and nebulette fragments may compete for F-actin binding sites with tropomyosin / troponin, the effect of the mouse nebulin MSN-N4 and chicken nebulette CCN-C5 proteins on the ATPase activity of unregulated acto-myosin S1 was determined. Figure 6.4 shows the effect of the nebulin and nebulette protein fragments on the actin activated myosin S1 ATPase (Pi / S1 head / sec). Using a fixed 25:1 molar ratio of F-actin to myosin S1, various concentrations of the mouse nebulin, chicken nebulette or tropomyosin were titrated for their effect on the actin activated myosin S1 ATPase activity. The results demonstrate that both cloned nebulin and nebulette fragments inhibited the

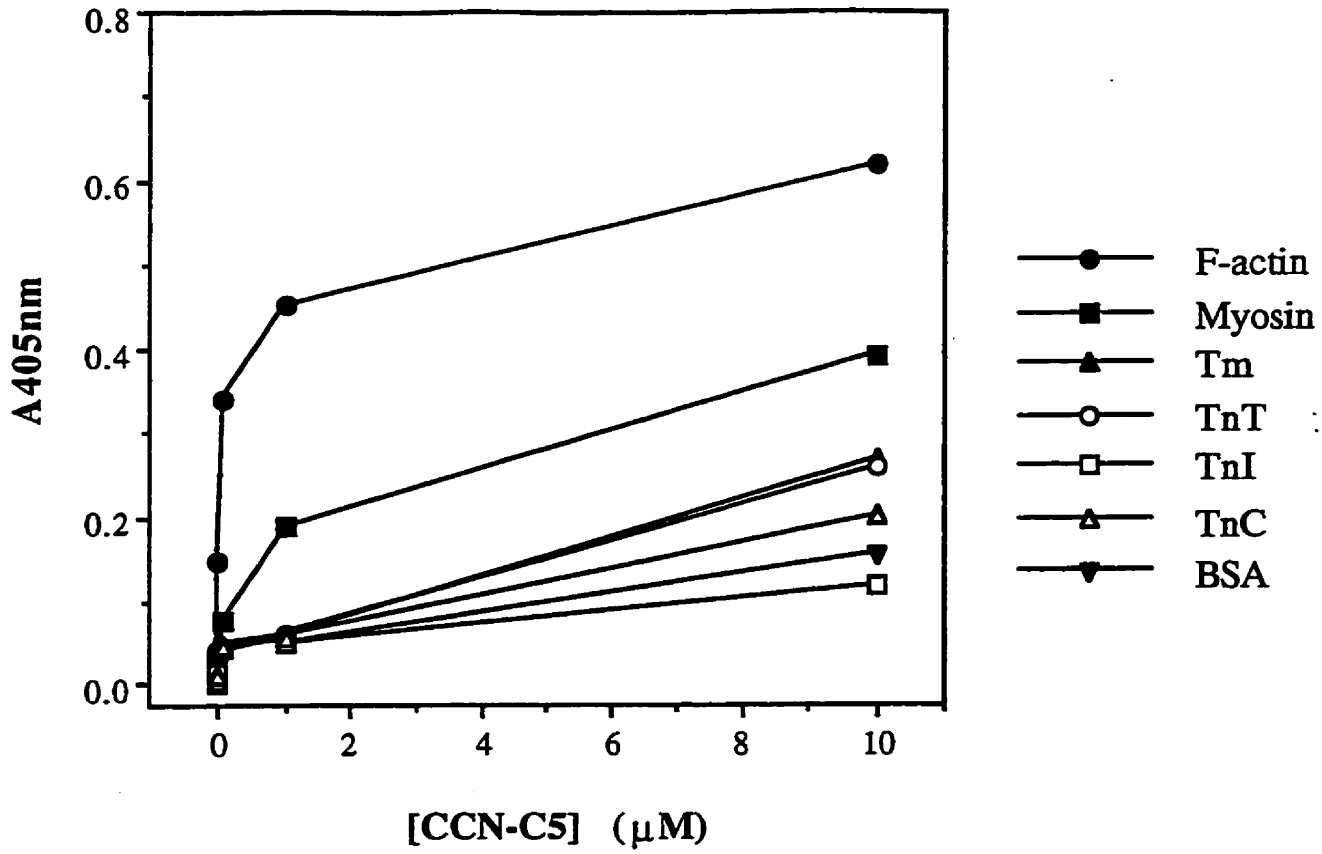

Figure 6.1. Solid phase binding of the cloned chicken CCN-C5 nebulette protein to thin filament proteins and myosin.

To determine the interactions that the cloned chicken nebulette protein has with the thin filament, solid phase binding assays were done using individual thin filament components, as well as myosin, coated on microtitre plates. Following coating of the proteins, serial dilutions of the cloned chicken nebulette CCN-C5 protein were overlayed, and the amount of protein bound to the immobilized thin filament proteins was quantified by detection using the anti-CCN-C5 mouse antiserum. The results indicate significant binding of the chicken nebulette protein to immobilized F-actin ($P < 0.05$), as well as lower, but significant, binding to myosin ($P < 0.05$). No interaction was seen with individual troponin subunit components or tropomyosin ($P > 0.05$ in all cases). The results demonstrate that the cloned chicken nebulette protein is an actin-binding protein, similar to nebulin.

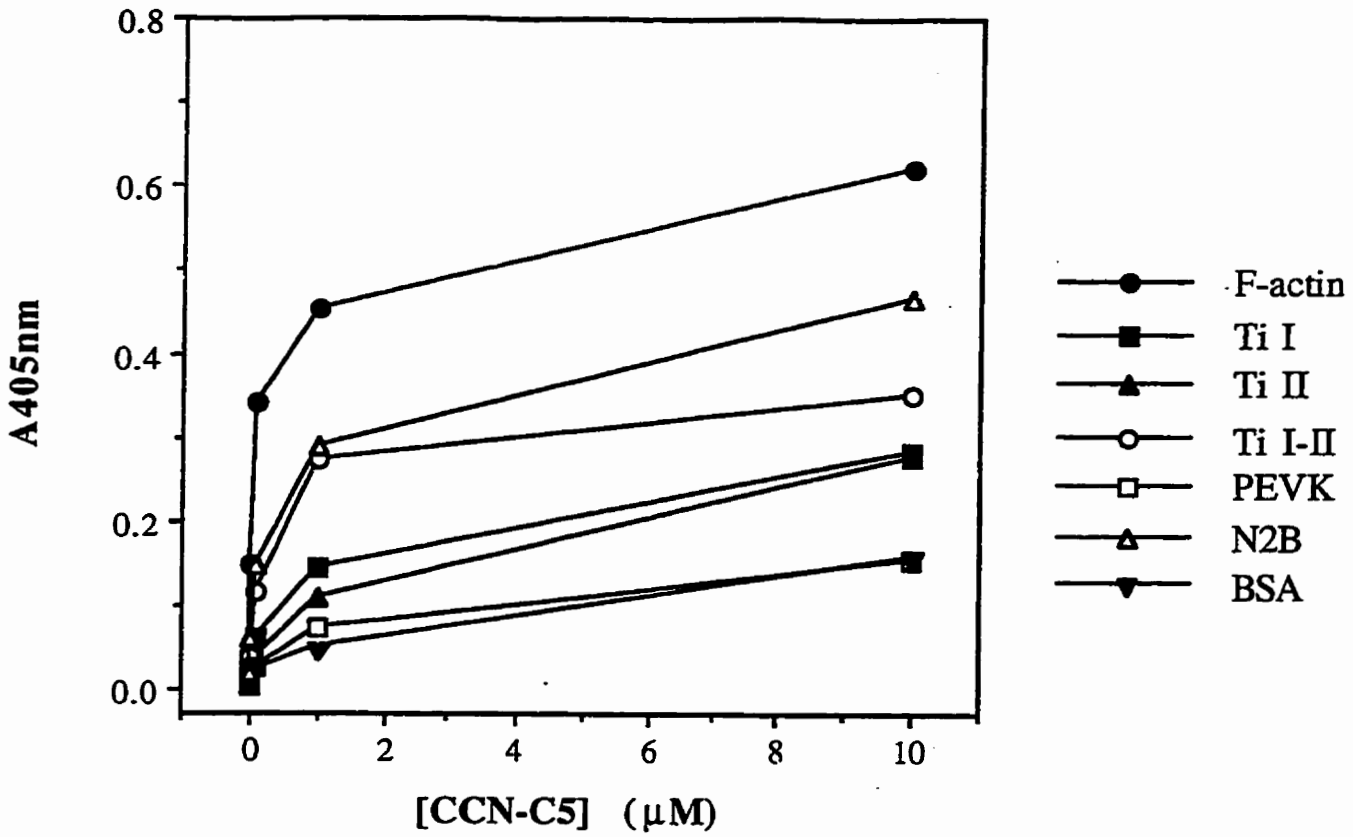

Figure 6.2. The cloned chicken nebulette CCN-C5 protein interacts with cloned titin proteins.

The binding of the chicken nebulette CCN-C5 protein to various cloned titin protein fragments was monitored by solid phase binding assays. Coated titin proteins were overlayed with serial dilutions of the cloned chicken nebulette protein, and bound protein was detected by the specific anti-nebulette antiserum. The binding curve of the cloned chicken nebulette protein to F-actin, done in the same experiment (Figure 6.1), is included for comparison of CCN-C5 binding to the titin proteins. The cloned protein showed significant binding only to the linked Ti I-II protein and the cardiac muscle N2 line specific cloned titin protein ($P < 0.05$). The cloned nebulette protein did not show significant binding to cloned Ti I and Ti II proteins or the PEVK protein, as compared to the BSA negative control curve ($P > 0.05$ in all cases).

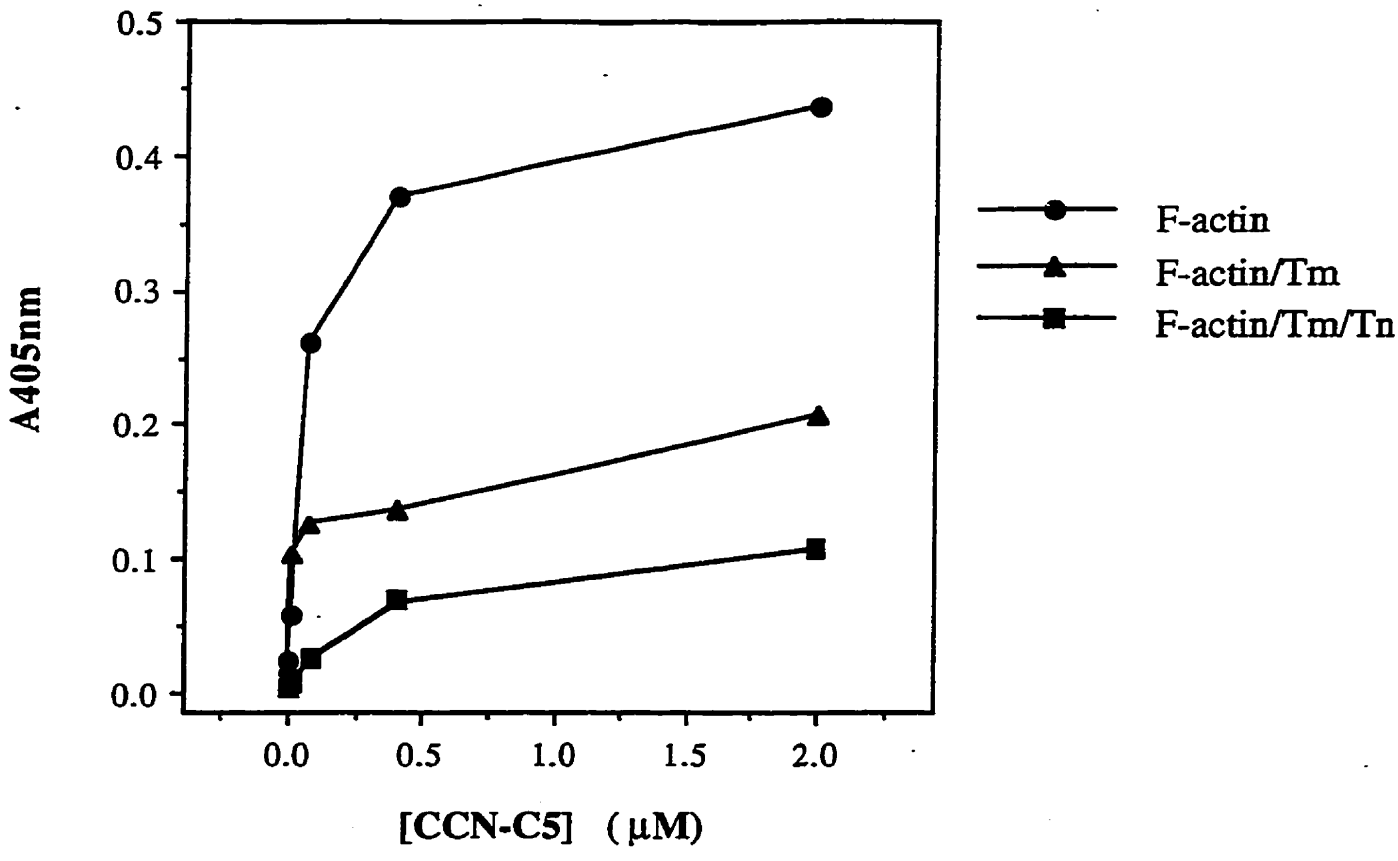

Figure 6.3. Tropomyosin and troponin - tropomyosin decoration of immobilized F-actin decreases CCN-C5 binding.

The interaction of the cloned nebulette protein with tropomyosin or troponin - tropomyosin decorated F-actin was monitored by solid phase protein binding assay. Immobilized F-actin was incubated with tropomyosin or troponin - tropomyosin and then incubated with the cloned CCN-C5 chicken nebulette protein. The bound nebulette protein was quantified by the specific anti-nebulette antiserum. Although the cloned protein showed binding to F-actin, decoration of F-actin with tropomyosin or troponin - tropomyosin decreased the cloned nebulette protein's interaction with F-actin. Assuming that binding to undecorated F-actin was 100%, binding to tropomyosin and troponin-tropomyosin decorated F-actin decreased by 53% and 76%, respectively. The results indicate that these thin filament associated proteins may compete for similar binding sites on F-actin. Readings for the BSA negative control were subtracted from all values.

actin-activated ATPase activity of myosin S1. Inhibition in the presence of tropomyosin was most effective, as evidenced by a sharp decrease in ATPase activity at low tropomyosin concentrations (Lehrer and Morris, 1982). Low concentrations of MSN-N4 or CCN-C5 did not show as sharp a decrease in the ATPase activity as compared to tropomyosin, consistent with the understanding that tropomyosin is the major factor contributing to the inhibition of actin-activated myosin ATPase activity. No statistically significant difference was observed between the maximum ATPase values when no MSN-N4, CCN-C5 or tropomyosin were added ($P > 0.05$).

D. Nebulin and Nebulette Do Not Inhibit the Acto-Myosin S1 ATPase in a Ca^{2+}-Regulated System

To test the effect of the cloned mouse nebulin or chicken nebulette fragments on the maximum and minimum activity of Ca^{2+} regulated acto-myosin S1 ATPase, thin filaments were reconstituted in the presence and absence of the cloned mouse nebulin or chicken nebulette fragments. The results from Figure 6.4 demonstrated that unregulated acto-myosin S1 ATPase was inhibited in the presence of the cloned nebulin and nebulette proteins. Therefore, the effect of the cloned proteins on the activity of Ca^{2+} regulated acto-myosin S1 ATPase assays would demonstrate whether or not this inhibition was regulated by Ca^{2+}-troponin-tropomyosin. The data (Figure 6.5) demonstrated no significant difference between the activity of myosin S1 in either low Ca^{2+} (pCa 8) or activating Ca^{2+} (pCa 4) concentrations in thin filaments reconstituted with or without nebulin or nebulette proteins ($P > 0.05$ in all cases). At pCa 8, ATPase rates (Pi / S1 head / sec) were: control, 0.12 +/- 0.005; MSN-N4, 0.14 +/- 0.04; CCN-C5, 0.15 +/- 0.018. At pCa 4, the ATPase rates were: control, 1.42 +/- 0.35; MSN-N4, 1.28 +/- 0.24; CCN-C5, 1.22 +/- 0.24. This indicates that the inhibition of the acto-myosin S1 ATPase by the cloned nebulin and nebulette fragments may be relieved by the major Ca^{2+} regulatory mechanism of striated muscle.

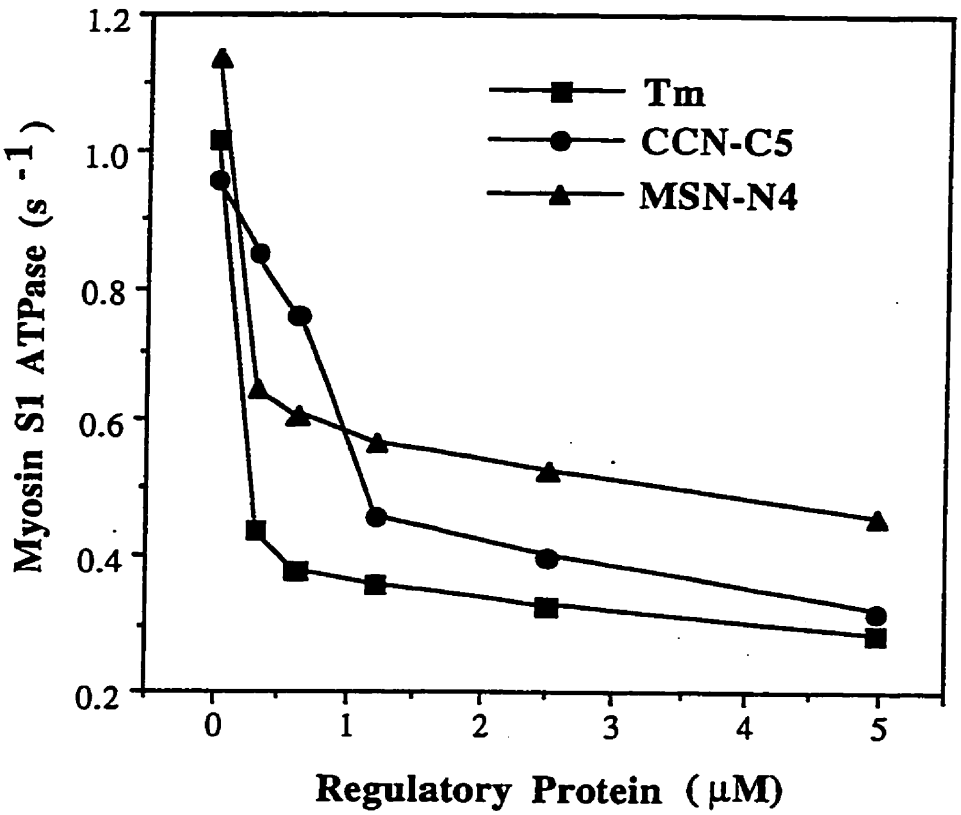

Figure 6.4. Tropomyosin, nebulin MSN-N4 and nebulette CCN-C5 proteins inhibit the ATPase activity of unregulated acto-myosin S1.

Using a fixed molar ratio of 25:1 F-actin to myosin S1, the effects of tropomyosin, nebulin MSN-N4 and nebulette CCN-C5 proteins on the actin-activated ATPase activity were determined by measuring the released phosphate by a Malachite green - ammonium molybdate color reaction. All three proteins showed inhibition of the actin-activated myosin S1 ATPase activity, with tropomyosin being most effective. The concentration of tropomyosin was determined using the monomer Mr of 33000.

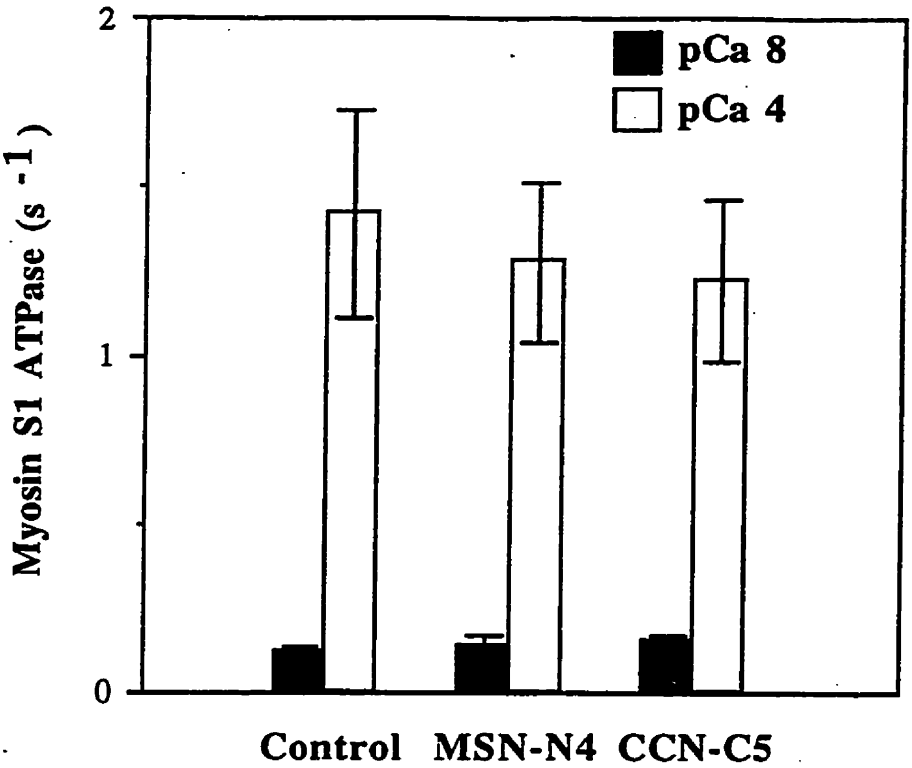

Figure 6.5. Ca^{2+} regulated actin-activated myosin S1 ATPase activities of an acto-myosin system reconstituted in the presence and absence of the nebulin MSN-N4 and nebulette CCN-C5 proteins.

Thin filaments were reconstituted with F-actin, tropomyosin and troponin in the presence and absence of the cloned nebulin MSN-N4 and nebulette CCN-C5 proteins. Actin activated myosin S1 ATPase activity was measured at pCa 8 and pCa 4 , representing resting and activating Ca^{2+} concentrations. Measured ATPase values (Pi / S1 head / sec) at pCa 8 were: control, 0.12 +/- 0.005; MSN-N4, 0.14 +/- 0.04; CCN-C5, 0.15 +/- 0.018. At pCa 4, the ATPase rates were: control, 1.42 +/- 0.35; MSN-N4, 1.28 +/- 0.24; CCN-C5, 1.22 +/- 0.24. The results demonstrate no significant difference ($P > 0.05$) between the ATPase activities at pCa 8 or 4 in the presence or absence of the cloned nebulin and nebulette proteins.

class I or class II motifs. More experiments are required to further explore this possible interaction.

B. The Cloned Nebulin and Nebulette Proteins Inhibit the Activity of Unregulated Acto-Myosin ATPase

The inhibition of the unregulated actin-activated myosin S1 ATPase activity by the cloned nebulin and nebulette fragments demonstrates that the intact proteins would have the capability to inhibit the sliding of actin and myosin relative to each other. Therefore, the interaction of nebulin and nebulette with the thin filament would require regulation. It has been demonstrated that nebulin and nebulette proteins have the ability to bind F-actin, and to a lower extent, myosin. The possibility remained that the inhibition demonstrated by the cloned proteins is as a result of nebulin binding to myosin and inhibiting myosin activity rather than covering F-actin active sites. This concern was addressed by the Ca^{2+} - troponin - tropomyosin regulated acto-myosin S1 ATPase assays.

C. Ca^{2+} - Troponin - Tropomyosin Regulates Nebulin Interaction with the Thin Filament

Experiments on the effect of the cloned nebulin and nebulette fragments on the maximum and minimum activity of Ca^{2+}-regulated acto-myosin S1 ATPase demonstrated no significant changes introduced by the cloned proteins at either low (pCa 8) or high (pCa 4) Ca^{2+} concentrations. Two conclusions may be drawn from these experiments: 1) the activity of regulated acto-myosin is not affected by the presence of cloned nebulin or nebulette fragments and the inhibition of acto-myosin S1 ATPase by the cloned nebulin or nebulette fragments may be relieved by Ca^{2+} - troponin - tropomyosin, and 2) the inhibition of the ATPase activity of unregulated acto-myosin S1 by the nebulin or nebulette proteins was due to specific interactions with the F-actin filament and not as a result of the cloned proteins binding to myosin S1 and interfering with its ATPase activity. Contrary to previous data (Root and Wang, 1994), no extra regulatory apparatus, such as Ca^{2+}-

calmodulin, was required to relieve nebulin or nebulette inhibition of the acto-myosin ATPase. This finding is consistent with the fact that, to date, Ca^{2+} - troponin - tropomyosin has been found to be the major regulatory determinant for contraction of striated muscles. The data suggest that contacts between nebulin or nebulette and F-actin are regulateable by Ca^{2+}-troponin- tropomyosin, further supported by the finding that nebulin and nebulette may compete with troponin - tropomyosin for binding sites on F-actin.

CHAPTER SEVEN:
SUMMARY

The data in this thesis are summarized as follows:

1. Nebulin and nebulette are two homologous proteins composed mainly of conserved ~35 amino acid motifs. Complementary DNAs encoding nebulin demonstrate a high degree of conservation at both the amino acid and nucleotide level.

2. A study of nebulin genomic DNA has demonstrated the exons to be composed of multiples of the ~35 amino acid motif, indicating these to be the functional units of the repeating nebulin protein. The functional units of nebulin are proposed to begin and end with the conserved SxxxY pentapeptide sequence. Further, Southern and Northern blotting also revealed the nebulin gene to be a single gene and did not indicate nebulette to be the product of the same gene.

3. Nebulette is present as two isoforms and is expressed throughout development. The expression pattern of nebulette in the chambers of the bovine heart has revealed a difference in the expression level of the two isoforms, possibly indicating a difference in expression level in response to functional demands of the cardiac chambers.

4. A cloned nebulette protein fragment demonstrated its ability to bind F-actin, similar to findings for the homologous nebulin, indicating that these two proteins share an analogous function. Similar to previous results for nebulin, the interaction of the cloned nebulette protein with F-actin was decreased by tropomyosin, and further by tropomyosin-troponin, indicating a competition for F-actin binding sites.

5. Cloned nebulin and nebulette proteins had inhibitory effects on the unregulated actin-activated myosin S1 ATPase activity, indicating that the interaction of nebulin and

nebulette with the F-actin thin filament should be regulated. In this aspect, it was observed that the Ca^{2+}-regulated acto-myosin S1 ATPase activity in the presence or absence of the nebulin or nebulette proteins was not significantly different, indicating that Ca^{2+} - troponin - tropomyosin is able to regulate the interaction of the cloned nebulin and nebulette proteins with F-actin.

Further experiments characterizing nebulin and nebulette would take advantage of well established eukaryotic expression and genetic engineering techniques. For example, a nebulin knock out mouse line could be produced and allow a direct measurement of the contribution of nebulin to the physical properties of skeletal muscles. This mouse line could be used as a host for transgenes expressing either of the full length nebulette protein isoforms in the nebulin deficient skeletal muscles, providing a direct comparison of the effects of longer and shorter nebulin-like modules on the contraction and performance of skeletal muscles. Also, transgenes encoding shorter forms of nebulin could be expressed in the skeletal muscles of the knock out mice, providing another model to study the effect of nebulin lengths on thin filament assembly and regulation. It is known that a significant difference exists between the speed of shortening in cardiac and skeletal muscle sarcomeres. In this respect, nebulin and nebulin-like proteins may work to increase the rate of dissociation of myosin head from the actin filament, known to be a major factor in determining the speed of contraction. Therefore, along the length of the skeletal muscle thin filament, nebulin may work to increase the rate of dissociation of myosin from actin, aiding to increase the speed of shortening of the sarcomere. Both nebulin and nebulette are composed of the ~35 amino acid motifs, and initial characterization of cloned protein fragments from both proteins have not shown significant functional differences, as expected for such well conserved proteins. Therefore, the application of further *in vitro* experiments is limited, and *in vivo* models, such as the knock out / knock in method proposed here, provide excellent working models which provide definitive answers regarding the contribution of nebulin and nebulette to the structure and function of striated muscle sarcomeres.

Benian, G.M., Kiff, J.E., Neckelmann, N., Moerman, D.G. and Waterston, R.H. 1989. Sequence of an unusually large protein implicated in the regulation of myosin activity in *C. elegans*. Nature **342**, 45-50.

Bennet, P., Craig, R., Starr, R. and Offer, G. 1986. The ultrastructure and location of C-protein, X-protein and H-protein in rabbit muscle. J. Muscle Res. Cell Motil. **7**, 550-567.

Breitbart, R.E. and Nadal-Ginard, B. 1986. Complete nucleotide sequence of the fast skeletal troponin T gene. Alternatively spliced exons exhibit unusual interspecies divergence. J. Mol. Biol. **188**, 313-324.

Briggs, M.M. and Schachat, F. 1993. Origin of fetal troponin T: developmentally regulated splicing of a new exon in the fast troponin T gene. Dev. Biol. **158**, 503-509.

Brisson, J.R., Golosinska, K., Smillie, L.B. and Sykes, B.D. 1986. Interaction of tropomyosin and troponin T: a proton nuclear magnetic resonance study. Biochemistry **25**, 4548-4555.

Campbell, A.P. and Sykes, B.D. 1991. Interaction of troponin I and troponin C. Use of the two dimensional NMR transferred nuclear Overhauser effect to determine the structure of the inhibitory troponin I peptide when bound to skeletal muscle TnC. J. Mol. Biol. **222**, 405-421.

Chalfie, M. 1994. Green fluorescent protein as a marker for gene expression. Science **263**, 802-805.

Cooke, R., Crowder, M.S. and Thomas, D.D. 1982. Orientation of spin labels attached to cross-bridges in contracting muscle fibres. Nature **30**, 776-778.

Cooper, T.A. and Ordahl, C.P. 1984. A single troponin T gene regulated by different programs in cardiac and skeletal muscle development. Science **226**, 979-982.

Cooper, T.A. and Ordahl, C.P. 1985. A single cardiac troponin T gene generates embryonic and adult isoforms via developmentally regulated alternative splicing. J. Biol. Chem. **260**, 11140-11148.

Cummins, P. and Perry, S.V. 1974. Chemical and immunochemical characteristics of tropomyosins from striated and smooth muscle. Biochem. J. **141**, 43-49.

Darnell, H., Lodish, H. and Baltimore, D. 1986. Molecular Cell Biology. W.H. Freeman and Company, New York.

Fabiato, A. 1988. Computer programs for calculating total from specified free or free from specified total ionic concentrations in aqueous solutions containing multiple metals and ligands. Methods Enzymol. **157**, 378-417.

Fairbanks, G., Steck, T.L. and Wallach, D.F. 1971. Electrophoretic analysis of the major polypeptides of the human erythrocyte membrane. Biochemistry **10**, 2606-2617.

Farah, C.S., Miyamoto, C.A., Ramos, C.H., daSilva, A.C., Quaggio, R.B. Fujimori, K., Smillie, L.B. and Reinach, F.C. 1994. Structural and regulatory functions of the NH_2- and COOH-terminal regions of skeletal muscle troponin I. J. Biol. Chem. **269**, 5230-5240.

Farah, C.S. and Reinach, F.C. 1995. The troponin complex and regulation of muscle contraction. FASEB J. **9**, 755-767.

Faulstich, H., Schafer, A.J. and Weckauf, M. 1977. Hoppe Seyler. Z. Physiol. Chem. **358**, 181-184.

Faulstich, H., Zobeley, S., Heintz, D. and Drewes, G. 1993. Probing the phalloidin binding site of actin. FEBS Lett. **318**, 218-222.

Fisher, D., Wang, G. and Tobacman, L.S. 1995. NH_2-terminal truncation of skeletal muscle troponin T does not alter the Ca^{2+} sensitivity of thin filament assembly. J. Biol. Chem. **270**, 25455-25460.

Forry-Schaudies, S., Maihle, N.J. and Hughes, S.H. 1990. Generation of skeletal, smooth and low molecular weight non-muscle tropomyosin isoforms from the chicken tropomyosin 1 gene. J. Mol. Biol. **211**, 321-330.

Frohman, M.A., Dush, M.K. and Martin, G.R. 1988. Rapid production of full length cDNAs from rare transcripts by amplification using a single gene specific oligonucleotide primer. Proc. Natl. Acad. Sci. U.S.A. **85**, 8998-9002.

Furst, D.O., Osborn, M. and Weber, K. 1989. Myogenesis in the mouse embryo: Differential onset of expression of myogenic proteins and the involvement of titin in myofibril assembly. J. Cell Biol. **109**, 517-527.

Furst, D.O., Osborn, M., Nave, R. and Weber, K. 1988. The organization of titin filaments in the half-sarcomere revealed by monoclonal antibodies in immunoelectron microscopy: a map of ten nonrepetitive epitopes starting at the Z line extends close to the M line. J. Cell Biol. **106**, 1563-1572.

Garvey, J.L., Kranias, E.G. and Solaro, R.J. 1988. Phosphorylation of C-protein, troponin I and phospholamban in isolated rabbit hearts. Biochem. J. **249**, 709-714.

Heeley, D.H. and Smillie, L.B. 1988. Interaction of rabbit skeletal muscle troponin T and F-actin at physiological ionic strength. Biochemistry **27**, 8227-8232.

Heeley, D.H., Golosinska, K. and Smillie, L.B. 1987. The effects of troponin T fragments T1 and T2 on the binding of nonpolymerizable tropomyosin to F-actin in the presence and absence of troponin I and troponin C. J. Biol. Chem. **262**, 9971-9978.

Herzberg, O. and James, M.N.G. 1988. Refined crystal structure of troponin C from turkey skeletal muscle at 2.0 A resolution. J. Mol. Biol. **203**, 761-779.

Herzberg, O., Moult, J. and James, M.N.G. 1986. A model for the Ca^{2+}-induced conformational transition of troponin C. A trigger for muscle contraction. J. Biol. Chem. **261**, 2638-2644.

Holmes, K.C., Popp, D., Gebhard, W. and Kabsch, W. 1990. Atomic model of the actin filament. Nature **347**, 44-49.

Horowitz, R., Klempner, E.S., Bisher, M.E. and Podolsky, R.J. 1986. A physiological role for titin and nebulin in skeletal muscle. Nature **323**, 160-164.

Hu, D.H., Kimura, S. and Maruyama, K. 1986. Sodium dodecyl sulfate gel electrophoretic studies of connectin-like high molecular weight proteins of various types of vertebrate and invertebrate muscles. J. Biochem. (Tokyo) **99**, 1485-1492.

Huang, Q.-Q. 1993. Monoclonal antibodies against cloned nebulin fragments. Master of Arts thesis. The University of Texas at Austin, Austin, Texas.

Huxley, H.E. 1969. The mechanism of muscular contraction. Science **164**, 1356-1366.

Huxley, H.E. 1990. Sliding filaments and molecular motile systems. J. Biol. Chem. **265**, 8347-8350.

Ikebe, M. and Reardon, S. 1988. Binding of caldesmon to smooth muscle myosin. J. Biol. Chem. **263**, 3055-3058.

Ikura, M., Clore, G.M., Gronenborn, A.M., Zhu, G., Klee, C.B. and Bax, A. 1992. Solution structure of a calmodulin-target peptide complex by multi-dimensional NMR. Science **256**, 632-638.

Jin, J.-P. and Lin, J.J.-C. 1988. Rapid purification of mammalian cardiac troponin T and its isoform switching in rat hearts during development. J. Biol. Chem. **263**, 7309-7315.

Jin, J.-P. and Wang, K. 1991a. Nebulin as a giant actin-binding template protein in skeletal muscle sarcomere. Interaction of actin and cloned human nebulin fragments. FEBS Lett. **281**, 93-96.

Jin, J.-P. and Wang, K. 1991b. Cloning, expression, and protein interaction of human nebulin fragments composed of varying numbers of sequence modules. J. Biol. Chem. **266**, 21215-21223.

Jin, J.-P. 1995. Cloned rat cardiac titin class I and class II motifs: Expression, purification, characterization and interaction with F-actin. J. Biol. Chem. **270**, 6908-6916.

Jin, J.-P., Chen, A. and Huang, Q.-Q. 1997. Genomic structure of mouse slow skeletal muscle troponin T gene implies a prototype primary structure of troponin T, a muscle regulatory protein with multiple muscle type-specific and developmental isoforms. Biophys. J. **72**, A58.

Johnson, J.D., Nakkula, R.J., Vasulka, C. and Smillie, L.B. 1994. Modulation of Ca^{2+} exchange with the Ca^{2+} specific regulatory sites of troponin C. J. Biol. Chem. **269**, 8019-8023.

Kabsch, W., Mannherz, H.G., Suck, D., Pai, E.F. and Holmes, K.C. 1990. Atomic structure of the actin:DnaseI complex. Nature **347**, 37-44.

Katoh, T. and Fujisawa, H. 1991. Calmodulin dependent protein kinase II. Kinetic studies on the interaction with substrates and calmodulin. Biochim. Biophys. Acta **1091**, 205-212.

Kellermayer, M.S.Z., Smith, S.B., Granzier, H.L. and Bustamante, C. 1997. Folding-unfolding transitions in single titin molecules characterized with laser tweezers. Science **276**, 1112-1116.

Kitazawa, T. and Somlyo, A.P. 1990. Desensitization and muscarinic re-sensatization of force and myosin light chain phosphorylation to cytoplasmic Ca^{2+} in smooth muscle. Biochem. Biophys. Res. Commun. **172**, 1291-1297.

Kron, S.J. and Spudich, J.A. 1986. Fluorescent actin filaments move on myosin fixed to a glass surface. Proc. Natl. Acad. Sci. U.S.A. **83**, 6272-6276.

Krudy, G.A., Kleerekoper, Q., Guo, X., Howarth, J.W., Solaro, R.J. and Rosevear, P.R.C. 1994. NMR studies delineating spatial relationships within the cardiac troponin I - troponin C complex. J. Biol. Chem. **269**, 23731-23735.

Labeit, S., Barlow, D.P., Gautel, M., Gibson, T., Holt, J., Hsieh, C.-L., Francke, U., Leonard, K., Wardale, J., Whiting, A. and Trinick, J. 1990. A regular pattern of two types of 100-residue motif in the sequence of titin. Nature **345**, 273-276.

Labeit, S., Gibson, T., Lakey, A., Leonard, K., Zeviani, M., Knight, P., Wardale, J. and Trinick, J. 1991. Evidence that nebulin is a protein-ruler in muscle thin filaments. FEBS Lett. **282**, 313-316.

Labeit, S., Gautel, M., Lackey, A. and Trinick, J. 1992. Towards a molecular understanding of titin. EMBO J. **11**, 1711-1716.

Labeit, S. and Kolmerer, B. 1995a. The complete primary structure of human nebulin and its correlation to muscle structure. J. Mol. Biol. **248**, 308-315.

Labeit, S. and Kolmerer, B. 1995b. Titins: Giant proteins in charge of muscle ultrastructure and elasticity. Science **270**, 293-296.

Laemmli, U.K. 1970. Cleavage of structural proteins during the assembly of the head of bacteriophage T4. Nature **227**, 680-685.

Leavis, P.C. and Gergely, J. 1984. Thin filament proteins and thin filament-linked regulation of vertebrate muscle contraction. CRC Crit. Rev. Biochem. **16**, 235-305.

Lees-Miller, J.P., Goodwin, L.O. and Helfman, D.M. 1990. Three novel brain tropomyosin isoforms are expressed from the rat α-tropomyosin gene through the use of alternative promoters and alternative RNA processing. Mol. Cell. Biol. **10**, 1729-1742.

Lehman, W., Craig, R. and Vibert, P. 1994. Ca^{2+} induced tropomyosin movement in Limulus thin filaments revealed by three dimensional reconstruction. Nature **368**, 65-67.

Lehrer, S.S. and Morris, E.P. 1982. Dual effects of tropomyosin and troponin-tropomyosin on actomyosin subfragment 1 ATPase. J. Biol. Chem. **257**, 8073-8080.

Liao, R., Wang, C.-K. and Cheung, H.C. 1994. Coupling of calcium to the interaction of troponin I with troponin C from cardiac muscle. Biochemistry **33**, 12729-12734.

Lin, Z., Mei-Hua, L., Schultheiss, T., Choi, J., Holtzer, S., DiLullo, C., Fischman, D.A. and Holtzer, H. 1994. Sequential appearance of muscle-specific proteins in myoblasts as a function of time after cell division: Evidence for a conserved myoblast differentiation program in skeletal muscle. Cell Motil. Cytoskel. **29**, 1-19.

Locker, R.H. and Wild, D.J.C. 1986. A comparative study of high molecular weight proteins in various types of muscle across the animal kingdom. J. Biochem. (Tokyo) **99**, 1473-1484.

Lowey, S., Waller, G.S. and Trybus, K.M. 1993. Skeletal muscle myosin light chains are essential for physiological speeds of shortening. Nature **365**, 454-456.

Meng, Y., Yasunaga, T. and Wakabayashi, T. 1995. Determination of the protein components of native thin filaments isolated from natural actomyosin: Nebulin and α-actinin are associated with actin filaments. J. Biochem. (Tokyo) **118**, 422-427.

Messing, J., Gronenborn, B., Muller-Hill, B. and Hofschnieder, P.H. 1977. Filamentous coliphage M13 as a cloning vehicle: Insertion of a HindIII fragment of the Lac regulatory region n M13 replicative form *in vitro*. Proc. Natl. Acad. Sci. U.S.A. **74**, 3642-3646.

Milligan, R.A., Whittaker, M. and Safer, D. 1990. Molecular structure of F-actin and location of surface binding sites. Nature **348**, 217-221.

Mittmann, K., Jaquet, K. and Heilmeyer, L.M.G. 1990. A common motif of two adjacent phosphoserines in bovine, rabbit and human cardiac troponin I. FEBS Lett. **273**, 41-45.

Moncman, C.L. and Wang, K. 1995. Nebulette: A 107 kDa nebulin-like protein in cardiac muscle. Cell. Motil. Cytoskel. **32**, 205-225.

Muller-Seitz, M., Kaupmann, K., Labeit, S. and Jockusch, H. 1993. Chromosomal localization of the mouse titin gene and its relation to muscular dystrophy with myositis and nebulin genes on chromosome 2. Genomics **18**, 559-561.

Nave, R., Furst, D.O. and Weber, K. 1990. Interaction of α-actinin and nebulin *in vitro*. Support for the existence of a fourth filament system in skeletal muscle. FEBS Lett. **269**, 163-166.

Negele, J.C., Dotson, D.G., Liu, W., Sweeney, H.L. and Putkey, J.A. 1992. Mutation of the high affinity Ca^{2+} binding sites of cardiac troponin C. J. Biol. Chem. **267**, 825-831.

Ngai, P.K. and Walsh, M.P. 1984. Inhibition of smooth muscle actin-activated myosin Mg^{2+}-ATPase activity by caldesmon. J. Biol. Chem. **259**, 13566-13569.

Nurse, P. 1990. Universal control mechanism regulating onset of M-phase. Nature **344**, 503-508.

Ogut, O. and Jin, J.-P. 1996. Expression, zinc-affinity purification and characterization of a novel metal-binding cluster in troponin T: Metal-stabilized α-helical structure and effects of the NH_2-terminal variable region on the conformation of intact troponin T and its association with tropomyosin. Biochemistry **35**, 16581-16590.

Ohtsuki, I. 1979. Molecular arrangement of troponin T in the thin filament. J. Biochem. (Tokyo) **86**, 491-497.

Pearlstone, J.R. and Smillie, L.B. 1982. Binding of troponin T fragments to several types of tropomyosins. Sensitivity to Ca^{2+} in the presence of troponin C. J. Biol. Chem. **257**, 10587-10592.

Pfuhl, M., Winder, S.J. and Pastore, A. 1994. Nebulin, a helical actin binding protein. EMBO J. **13**, 1782-1789.

Pfuhl, M., Winder, S.J., Castiglione Morelli, M.A., Labeit, S. and Pastore, A. 1996. Correlation between conformational and binding properties of nebulin repeats. J. Mol. Biol. **257**, 367-384.

Pollard, T.D., Goldberg, I. and Schwarz, W.H. 1992. Nucleotide exchange, structure, and mechanical properties of filaments assembled from ATP-activated ADP-actin. J. Biol. Chem. **267**, 20339-20345.

Potter, J.D. and Gergely, J. 1974. Troponin, tropomyosin, and actin interactions in the Ca^{2+} regulation of muscle contraction. Biochemistry **13**, 2697-2703.

Potter, J.D. and Gergely, J. 1975. The Ca^{2+} and Mg^{2+} binding sites on troponin and their role in the regulation of myofibrillar adenosine triphosphatase. J. Biol. Chem. **250**, 4628-4633.

Rayment, I., Rypniewski, W.R., Schmidt-Base, K., Smith, R., Tomchick, D.R., Benning, M.M., Winkelmann, D.A., Wesenberg, G. and Holden, H.M. 1993. Three dimensional structure of myosin subfragment 1: a molecular motor. Science **261**, 50-58.

Rief, M., Gautel, M., Oesterhelt, F., Fernandez, J.M. and Gaub, H.E. 1997. Reversible unfolding of individual titin immunoglobulin domains by AFM. Science **276**, 1109-1112.

Robertson, S.P., Johnson, J.D., Holroyde, M.J., Kranias, E.G., Potter, J.D. and Solaro, R.J. 1982. The effect of troponin I phosphorylation on the Ca^{2+} binding properties of the Ca^{2+} regulatory site of bovine cardiac troponin C. J. Biol. Chem. **257**, 260-263.

Robinson, T.F. and Winegrad, S. 1979. The measurement and dynamic implications of thin filament lengths in heart muscle. J. Physiol. **286**, 607-619.

Root, D.D. and Wang, K. 1994. Calmodulin-sensitive interaction of human nebulin fragments with actin and myosin. Biochemistry **33**, 12581-12591.

Ruegg, J.C., Pfitzer, G., Zimmer, M. and Hofmann, F. 1984. The calmodulin fraction responsible for contraction in intestinal smooth muscle. FEBS Lett. **170**, 383-386.

Rushmer, R.F. 1976. Cardiovascular Dynamics (4 th Ed.). W.B. Saunders Company, Toronto.

Samaha, F.J., Guth, L. and Albers, R.W. 1970. Differences between slow and fast muscle myosin. Adenosine triphosphatase activity and release of associated proteins. J. Biol. Chem. **245**, 219-224.

Samuel, J.L., Perrault, M.A., Bercovici, J., Swynghedauw, B. and Feldman, G. 1981. Histoenzymological study of myocardial ATPase activity in experimental infarction in the rat. Basic. Res. Cardiol. **76**, 602-611.

Sanger, F., Nicklen, S. and Coulson, A.R. 1977. DNA sequencing with chain terminating inhibitors. Proc. Natl. Acad. Sci. U.S.A. **74**, 5463-5470.

Schachat, F., Schmidt, J.M., Maready, M. and Briggs, M.M. 1995. Chicken perinatal troponin Ts are generated by a combination of novel and phylogenetically conserved alternative splicing pathways. Dev. Biol. **171**, 233-239.

Schaertl, S., Lehman, S.S. and Geeves, M.A. 1995. Separation and characterization of the two functional regions of troponin involved in muscle thin filament regulation. Biochemistry **34**, 15890-15894.

Schiaffino, S. and Reggiani, C. 1996. Molecular diversity of myofibrillar proteins: Gene regulation and functional significance. Physiol. Rev. **76**, 371-423.

Seamon, K.B. 1980. Ca^{2+} and Mg^{2+} dependent conformational states of calmodulin as determined by NMR. Biochemistry **19**, 207-215.

Sheng, Z., Pan, B.S., Miller, T.E. and Potter, J.D. 1992. Isolation, expression, and mutation of a rabbit skeletal muscle cDNA clone for troponin I. The role of the NH_2-terminal of fast skeletal muscle troponin I in its biological activity. J. Biol. Chem. **267**, 25407-25413.

Shih, C.-L., Chen, M.-J. G., Linse, K. and Wang, K. 1997. Molecular contacts between nebulin and actin: Cross-linking

Short, J.M., Fernandez, J.M., Sorge, J.A. and Huse, W.D. 1988. λ ZAP: a bacteriophage λ expression vector with in vivo excision properties. Nucl. Acid Res. **16**, 7583-7600.

Smillie, L.B. 1979. Structure and functions of tropomyosins from muscle and non-muscle sources. Trends Biochem. Sci. **4**, 151-155.

Smillie, L.B., Golosinska, K. and Reinach, F.C. 1988. Sequences of complete cDNAs encoding four variants of chicken skeletal troponin T. J. Biol. Chem. **263**, 18816-18820.

Sobue, K., Muramoto, Y., Fujita, M. and Kakiuchi, S. 1981. Purification of a calmodulin-binding protein from chicken gizzard that interacts with F-actin. Proc. Natl. Acad. Sci. U.S.A. **78**, 5652-5655.

Sorenson, M.M., DaSilva, A.C.R., Gouveira, C.S., Sousa, V.P., Oshima, W., Ferro, J.A. and Reinach, F.C. 1995. Concerted action of the high affinity Ca^{2+} binding sites in skeletal muscle troponin C. J. Biol. Chem. **270**, 9770-9777.

Soteriou, A., Clarke, A., Martin, S. and Trinick, J. 1993a. Titin folding energy and elasticity. Proc. R.Soc. London B Biol. Sci. **254**, 83-86.

Soteriou, A., Gamage, M. and Trinick, J. 1993b. A survey of interactions made by the giant protein titin. J. Cell. Sci. **104**, 119-123.

Southern, E. 1979. Gel electrophoresis of restriction fragments. Methods Enzymol. **68**, 152-176.

Spudich, J.A., Kron, S.J. and Sheetz, M.P. 1985. Movement of myosin-coated beads on oriented filaments reconstituted from purified actin. Nature **315**, 584-586.

Spudich, J.A. 1994. How molecular motors work. Nature **372**, 515-518.

Squire, J. 1981. The Structural Basis of Muscle Contraction. Plenum Press, New York.

Starr, R. and Offer, G. 1983. H protein and X protein. Two new components of the thick filament of vertebrate skeletal muscle. J. Mol. Biol. **170**, 675-698.

Strasser, P., Gimona, M., Moessler, H., Herzog, M. and Small, J.V. 1993. Mammalian calponin. Identification and expression of genetic variants. FEBS Lett. **330**, 13-18.

Studier, F.W., Rosenberg, A.H., Dunn, J.J. and Dubendorff, J.W. 1990. Use of T7 RNA polymerase to direct expression of cloned genes. Methods Enzymol. **185**, 60-89.

Sutherland, C. and Walsh, M.P. 1989. Phosphorylation of caldesmon prevents its interaction with smooth muscle myosin. J. Biol. Chem. **264**, 578-583.

Sweeney, H.L., Bowman, B.F. and Stull, J.T. 1993. Myosin light chain phosphorylation in vertebrate striated muscle: regulation and function. Am. J. Physiol. **264**, C1085-1095.

Swynghedauw, B. 1986. Developmental and functional adaptation of contractile proteins in cardiac and skeletal muscles. Physiol. Rev. **66**, 711-769.

Syska, H., Wilkinson, J.M., Grand, R.J.A. and Perry, S.V. 1976. The relationship between biological activity and primary structure of troponin I from white skeletal muscle of the rabbit. Biochem. J. **153**, 375-387.

Szent-Gyorgyi, A.G. and Prior, G. 1966. Exchange of ADP bound to actin in superprecipitated actomyosin and contracted myofibrils. J. Mol. Biol. **15**, 515-538.

Takahashi, K., Hiwada, K. and Kokubu, T. 1986. Isolation and characterization of 34 000 dalton calmodulin and F-actin binding protein from chicken gizzard smooth muscle. Biochem. Biophys. Res. Commun. **141**, 20-26.

Takahashi, K., Abe, M., Hiwada, K. and Kokubu, T. 1988. Vascular smooth muscle calponin: a novel troponin T like protein. J. Hypertension **6**, S40-S43.

Talosi, L., Eds, I. and Kranias, E.G. 1993. Intracellular mechanisms mediating reversal of beta-adrenergic stimulation in intact beating hearts. Am. J. Physiol. **264**, H791-H797.

Tanaka, T., Ohta, H., Kanda, K., Tanaka, T., Hidaka, H. and Sobue, K. 1990. Phosphorylation of high Mr caldesmon by protein kinase C modulates the regulatory function of this protein on the interaction between actin and myosin. Eur. J. Biochem. **188**, 495-500.

Tang, D.-C., Stull, J.T., Kubota, Y. and Kamm, K.E. 1992. Regulation of the Ca^{2+} dependence of smooth muscle contraction. J. Biol. Chem. **267**, 11839-11845.

Tao, T., Gong, B.J. and Leavis, P.C. 1990. Ca^{2+} induced movement of troponin I relative to actin in skeletal muscle thin filaments. Science **247**, 1339-1441.

Thierfelder, L., Watkins, H.C. and MacRae, C. 1994. α-tropomyosin and cardiac troponin T mutations cause familial hypertrophic cardiomyopathy: a disease of the sarcomere. Cell **77**, 701-712.

Trinick, J. 1992. Understanding the functions of titin and nebulin. FEBS Lett. **307**, 44-48.

Trombitas, K., Jin, J.-P. and Granzier, H. 1995. The mechanically active domain of titin in cardiac muscle. Circ. Res. **77**, 856-861.

VanBuren, P., Work, S.S. and Warshaw, D.M. 1994. Enhanced force generation by smooth muscle myosin *in vitro*. Proc. Natl. Acad. Sci. U.S.A. **91**, 202-205.

Vieira, J. and Messing, J. 1982. The pUC plasmids, an M13mp7-derived system for insertion mutagenesis and sequencing with synthetic universal primers. Gene **19**, 259-268.

Walsh, M.P., Bridenbaugh, R., Hartshorne, D.J. and Kerrick, W.G.L. 1982. Phosphorylation-dependent activated tension in skinned gizzard muscle fibres in the absence of Ca^{2+}. J. Biol. Chem. **257**, 5987-5990.

Walsh, M.P. 1991. Calcium dependent mechanisms of regulation of smooth muscle contraction. Biochem. Cell Biol. **69**, 771-800.

Walsh, M.P., Carmichael, J.D. and Kargacin, G.J. 1993. Characterization and confocal imaging of calponin in gastrointestinal smooth muscle. Am. J. Physiol. **265**, 1371-1378.

Wang, K., McClure, J. and Tu, A. 1979. Titin: major myofibrillar components of striated muscle. Proc. Natl. Acad. Sci. U.S.A. **76**, 3698-3702.

Wang, K. 1982. Purification of titin and nebulin. Methods Enzymol. **85**, 264-274.

Wang, K. and Williamson, C. 1980. Identification of an N2 line protein of striated muscle. Proc. Natl. Acad. Sci. U.S.A. **77**, 3254-3258.

Wang, K. and Wright, J. 1988. Architecture of the sarcomere matrix of skeletal muscle: Immunoelectron microscopic evidence that suggests a set of parallel inextensible nebulin filaments anchored at the Z line. J. Cell Biol. **107**, 2199-2212.

Wang, K., Knipfer, M., Huang, Q.-Q., van Heerden, A., Hsu, L., Gutierrez, G., Quian, X.-L. and Stedman, H. 1996. Human skeletal muscle nebulin sequence encodes a blueprint for thin filament architecture. J. Biol. Chem. **271**, 4304-4314.

Warrick, H.M. and Spudich, J.A. 1987. Myosin structure and function in cell motility. Annu. Rev. Cell Biol. **3**,379-421.

Watkins, H., McKenna, W.J., Thierfelder, L., Suk, H.J., Anan, R., O'Donoghue, A., Spirito, P., Matsumori, A., Moravec, C.S., Seidman, J.G. and Seidman, C.E. 1995. Mutations in the genes for cardiac troponin T and α-tropomyosin in hypertrophic cardiomyopathy. N. Engl. J. Med. **332**, 1058-1064.

Whiting, A., Wardale, J. and Trinick, J. 1989. Does titin regulate the length of muscle thick filaments? J. Mol. Biol. **205**, 163-169.

Wieczorek, D.F., Smith, C.W.J. and Nadal-Ginard, B. 1988. The rat α-tropomyosin gene generates a minimum of six different mRNAs coding for striated, smooth, and nonmuscle isoforms by alternative splicing. Mol. Cell. Biol. **8**, 679-694.

Winder, S.J., Pato, M.D. and Walsh, M.P. 1992. Purification and characterization of calponin phosphatase from smooth muscle. Effect of dephosphorylation on calponin function. Biochem. J. **286**, 197-203.

Winder, S.J., Sutherland, D. and Walsh, M.P. 1991. in Regulation of smooth muscle contraction (R.S.S. Moreland, ed) pp. 37-52. Plenum Press, New York.

Winder, S.J. and Walsh, M.P. 1990. Smooth muscle calponin. Inhibition of actomyosin MgATPase and regulation by phosphorylation. J. Biol. Chem. **265**, 10148-10155.

Yazawa, M., Ikura, M., Hikichi, K., Ying, L. and Yagi, K. 1987. Communication between two globular domains of calmodulin in the presence of mastoparan or caldesmon fragment. Ca^{2+} binding and 1H NMR. J. Biol. Chem. **262**, 10951-10954.

Zhang, R., Zhao, J. and Potter, J.D. 1995a. Cardiac troponin I phosphorylation increases the rate of cardiac muscle relaxation. Circ. Res. **76**, 1028-1035.

Zhang, R., Zhao, J. and Potter, J.D. 1995b. Phosphorylation of both serine residues in cardiac troponin I is required to decrease the Ca^{2+} affinity of cardiac troponin C. J. Biol. Chem. **270**, 30773-30780.

Zhao, X., Kobayashi, T., Malak, H., Gryczynski, I., Lakowicz, J., Wade, R. and Collins, J.H. 1995. Ca^{2+} induced troponin flexibility revealed by distance distribution measurement between engineered sites. J. Biol. Chem. **270**, 15507-15514.

Zot, A.S. and Potter, J.D. 1987. Structural aspects of troponin-tropomyosin regulation of skeletal muscle contraction. Annu. Rev. Biophys. Chem. **16**, 535-559.

TEST TARGET (QA-3)

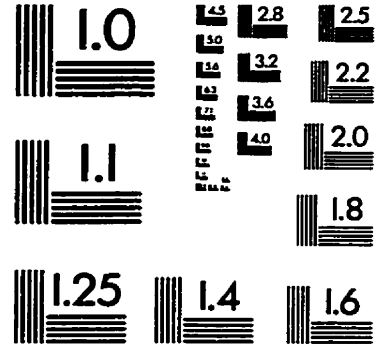

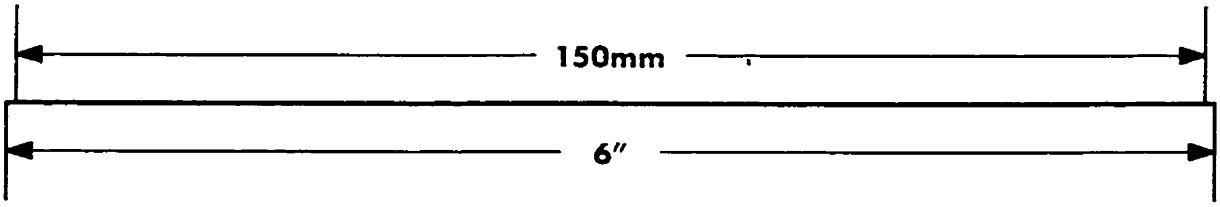

APPLIED IMAGE, Inc
1653 East Main Street
Rochester, NY 14609 USA
Phone: 716/482-0300
Fax: 716/288-5989